THE VEPCO FLAME MODEL

BY

W. C. BECK

NUCLEAR FUEL ENGINEERING GROUP
FUEL RESOURCES DEPARTMENT

VIRGINIA ELECTRIC AND POWER COMPANY
RICHMOND, VIRGINIA

OCTOBER, 1978

Recommended for Approval:

M. L. Smith
Nuclear Fuel Engineer

Approved:

M. L. Bowling, Director
Nuclear Fuel Engineering

CLASSIFICATION/DISCLAIMER

The data and analytical techniques described in this report have been prepared specifically for application by the Virginia Electric and Power Company. The Virginia Electric and Power Company makes no claim as to the accuracy of the data or techniques contained in this report if used by other organizations. Any use of this report or any part thereof must have the prior written approval of the Virginia Electric and Power Company.

ABSTRACT

The Virginia Electric and Power Company (VEPCO) has developed a three-dimensional (x, y, z), one energy group, modified diffusion theory calculational model designated as the Vepco FLAME Model.

The model utilizes the NULIF, PDQ07, FLAFIT, and FLAME3 computer Codes which are part of the Fuel Utilization and Performance Analysis Code (FUPAC) system obtained from the Babcock and Wilcox Company. In addition, the EDITQAR, PICCOLO, and FLMSHUFL codes have been written by Vepco for use in the FLAME Model. The model is used to perform three-dimensional reactor physics analysis in support of reactor startup and cycle operation of the Vepco Surry and North Anna nuclear reactors. The accuracy of the FLAME model is demonstrated through comparisons with measurements taken at Surry Units No. 1 and 2.

ACKNOWLEDGEMENTS

The author would like to thank Messrs. C. B. Franklin, J. R. Rodes and M. L. Smith for their technical assistance during the development of the FLAME model and to Ms. Cathy Langston, Ms. Ivy Wilkerson, and Ms. Miranda Cooper for their typing of the draft and final manuscripts. The author would also like to express his appreciation to a number of people who reviewed and provided comments on this report.

TABLE OF CONTENTS

LIST OF FIGURES

LIST OF FIGURES (Continued)

LIST OF FIGURES (Continued)

LIST OF FIGURES (Continued)

LIST OF TABLES

SECTION 1 - INTRODUCTION

The purposes of this report are to describe one of the computational models developed at Virginia Electric and Power Company (Vepco) and to demonstrate the accuracy of this model by comparing analytical results generated by the model to applicable measurements from Surry Units No. 1 and 2. The capabilities obtained with this model will be directly applicable to Surry Units 1 and 2 and generally applicable to all of the units at the North Anna Nuclear Power Station.

The model described herein is a three-dimensional (x, y, z), one energy group, modified diffusion theory (with thermal feedback) calculational package and is designated as the Vepco FLAME Model. The Vepco FLAME Model uses the NULIF[1], PDQ07[2], FLAME3[3], and FLAFIT[3] computer codes which are part of the Fuel Utilization and Performance Analysis Code[4] (FUPAC) system obtained from the Babcock and Wilcox Company. In addition, the EDITQAR[5], PICCOLO[5], and FLMSHUFL[6] computer codes have been written by Vepco for use in the Vepco FLAME Model. A detailed description of the input requirements, functioning, physical models and output capabilities of the above codes can be obtained from the referenced code manuals.

The types of reactor physics calculations which can be performed within the general capabilities of the Vepco FLAME Model include:

1. Assembly and core average axial power distribution
2. Differential control rod bank worths
3. Integral control rod bank worths as a function of rod bank position
4. Control rod bank insertion limits
5. Axial burnup distribution
6. Axial offset
7. Peaking factors (F_Q^T, $F_{xy}(Z)$, F_Z)

This report is concerned primarily with the documentation of the capability of the Vepco FLAME Model to accurately compute axial power distributions, axial offset, and differential and integral control rod bank worths.

The remainder of this report describes the Surry Units No. 1 and 2 reactor cores to be modeled, the purposes and interrelationships of the various computer codes which comprise the Vepco FLAME Model, the specific modeling of a reactor core with these codes, and comparison of calculated results with appropriate results obtained with the Vepco PDQ07 Discrete Model[7] and with core measurements obtained from Surry Units No. 1 and 2.

SECTION 2 - CORE DESCRIPTION

2.1 Introduction

The Surry Nuclear Power Station, which consists of two operating units, has been selected as the operating system to be modeled for verification of the Vepco FLAME Model. The Surry Units No. 1 and 2 are identical Westinghouse designed three coolant loop pressurized water reactors with thermal ratings of 2441 Mwt. The operating history of the Surry Power Station is summarized in Table 2-1.

2.2 Core Design

The Surry cores consist of 157 fuel assemblies surrounded by a core baffle, barrel, and thermal shield and enclosed in a steel pressure vessel. The pressure inside the vessel is maintained at a nominal 2250 psia. The coolant (and moderator) is pressurized water which enters the bottom of the core at a nominal 532°F and undergoes a nominal average rise in temperature of 65.5°F before exiting the core. The average coolant temperature is 566°F and the average linear power density of the core is 6.2 kw/ft.

Each of the 157 fuel assemblies consists of 204 fuel rods arranged in a 15 by 15 square array. The fuel used in the Surry cores consists of slightly enriched uranium dioxide fuel pellets contained within a Zircaloy-4 clad. A small gap containing pressurized helium exists between the pellets and the inner diameter of the clad. For the positions in the 15 by 15 array not occupied by fuel rods, there are 20 guide tube locations for either solid burnable poison rods or control rods and one centrally located instrumentation tube. (See Figure 2-1). The fuel rods in each fuel assembly are supported by seven Inconel-718 grids located along the length of the assembly. These grids are mechanically attached to the guide tubes, which are, in turn, fastened to the upper and lower nozzles, and thus provide for assembly structural support.

There are 48 full-length Rod Cluster Control Assemblies (referred to as control rods) used to control core reactivity as well as five part-length rods for axial power shaping. (It should be noted that the part-length control rods are physically present but are not currently allowed to be inserted into the core). The absorber material of the control rods is an alloy consisting of 80% silver, 15% indium, and 5% cadmium. The various control rods are arranged in and move in symmetrically located groups, or banks, as depicted in Figure 2-2. Banks D, C, B, and A are denoted as the control banks and are moved in a fixed sequential pattern to control the reactor over the power range of operation. The remaining rods, Banks SA and SB, are denoted as shutdown banks and are used to provide shutdown margin.

In addition to the control rods, a chemical (boric acid) shim is used to control excess core reactivity and to facilitate operational flexibility. Above certain concentrations of chemical shim, burnable poison rods are also used to control excess reactivity. Fresh and/or depleted burnable poison rods can also be used to shape (i.e., improve) the core power distribution. The burnable poison rods contain borosilicate in the form of Pyrex glass clad in a stainless steel tube. Burnable poison rods, which may be used in any fuel assembly not under a control rod bank location, consist of clusters of either 8, 12, 16, or 20 rods which are inserted into the Zircaloy-4 control rod guide tubes.

Specific values of the principal mechanical and thermal-hydraulic parameters for the Surry core are provided in Table 2-2. A complete description of the Surry units is given in Reference 8.

2.3 Fuel Loadings

The initial and reload quarter core fuel loadings (i.e., initial enrichments and density, previous cycle location if appropriate, beginning of cycle burnup predicted by the Vepco PDQ07 Discrete Model and number of

fresh or depleted burnable poison rods present) for both Surry units are provided in Figures 2-3 through 2-16. It should be noted that the fuel loadings for Cycle 1 of both Surry units are identical. The fuel management strategy employed in the initial cycle of operation of each unit was the checkerboard loading of the two lower enriched fuel batches in the center of the core and the highest enriched fuel batch around the periphery of the core. After the first cycle, the fuel management became more complicated as the result of the need to minimize the impact of fuel densification (which was most severe in the lower initial density, lower prepressurization Batches 1, 2, and 3). Generally, a modified out-in strategy was followed wherein higher enrichment fresh fuel was loaded on the core periphery with lower enrichment fresh fuel (and once-burned fuel and twice-burned fuel) checkerboard loaded in the inner region of the core. An exception to this was in the third cycle of Unit No. 1 where no fresh fuel was loaded on the periphery. The only fresh fuel was 16 lower enrichment assemblies loaded in the inner region of the core. Beginning in Cycle 4 of both units, a change was made from the typical 12 month operating cycle to an 18 month operating cycle. However, the basic fuel management strategy (i. e., modified out-in) was not changed for the Cycle 4 loading patterns.

TABLE 2-1

SURRY NUCLEAR POWER STATION OPERATING HISTORY

Surry Unit	Cycle No.	Beginning of Cycle	End of Cycle	Cycle Burnup (MWD/MTU)
1	1	July 1, 1972	October 24, 1974	13547
1	2	January 30, 1975	September 26, 1975	6915
1	3	December 6, 1975	October 17, 1976	8944
1	4	January 17, 1977	April 21, 1978	13107
2	1	March 7, 1973	April 26, 1975	14870
2	2	June 14, 1975	April 22, 1976	9054
2	3	June 1, 1976	September 10, 1977	9422
2	4	October 8, 1977	1st Qtr 1979*	14000*

*Projected

TABLE 2-2

SURRY CORE DESCRIPTION

THERMAL AND HYDRAULIC DESIGN PARAMETERS

Total core heat output, Mwt	2441
Heat generated in fuel, %	97.4
System operating pressure, psi	2250
Total coolant flow rate, lb/hr (gpm)	100.7×10^6 (265,500)
Coolant Temperatures, °F (@100% power)	
Nominal inlet	532
Average rise in the core	65.5
Average in the core	566
Nominal outlet of hot channel	642
Average linear power density, Kw/ft	6.2

MECHANICAL DESIGN PARAMETERS

Fuel Assemblies		
Design	Canless 15 x 15	
Number	157	
Rod pitch, inches	0.563	
Overall dimensions, inches	8.426 x 8.426	
Number of grids per assembly (material)	7 (Inconel-718)	
Number of instrumentation tubes	1	
Fuel Rods		
Number	32,028	
Number of rods/assembly	204	
	Batch 1,2,4,5,6	Batch 3
Outside diameter, inches	0.422	0.422
Diametrical gap, inches	0.0075	0.0085
Clad thickness, inches	0.0243	0.0243
Clad material	Zircaloy-4	
Fuel Pellets		
Material	Sintered UO_2	
Density (% of theoretical) and Enrichment (w/o U235)	See Figures 2-4 through 2-12	
	Batch 1,2,4,5,6	Batch 3
Outer diameter	0.3659	0.3649
Control Rod Assemblies		
Neutron absorber	5% Cd-15% In-80% Ag	
Cladding Material	Type 304 SS-Cold worked	
Clad thickness, inches	0.019	
Number (full length)	48	
Number of rods per assembly	20	

TABLE 2-2 (Continued)

Burnable Poison Rods	
Material	Pyrex glass
Content B_2O_3 (w/o)	12.5
Core Structure	
Core barrel I.D./O.D., inches	133.875/137.875
Thermal shield I.D./O.D., inches	142.625/148.000
Core diameter, inches (approximate)	119.5
Reflector thickness (approximate) and composition	
Top - Water plus steel, in.	10
Bottom - Water plus steel, in.	10
Side - Water plus steel, in.	15

FIGURE 2-1

CROSS SECTIONAL VIEW OF SURRY FUEL ASSEMBLY

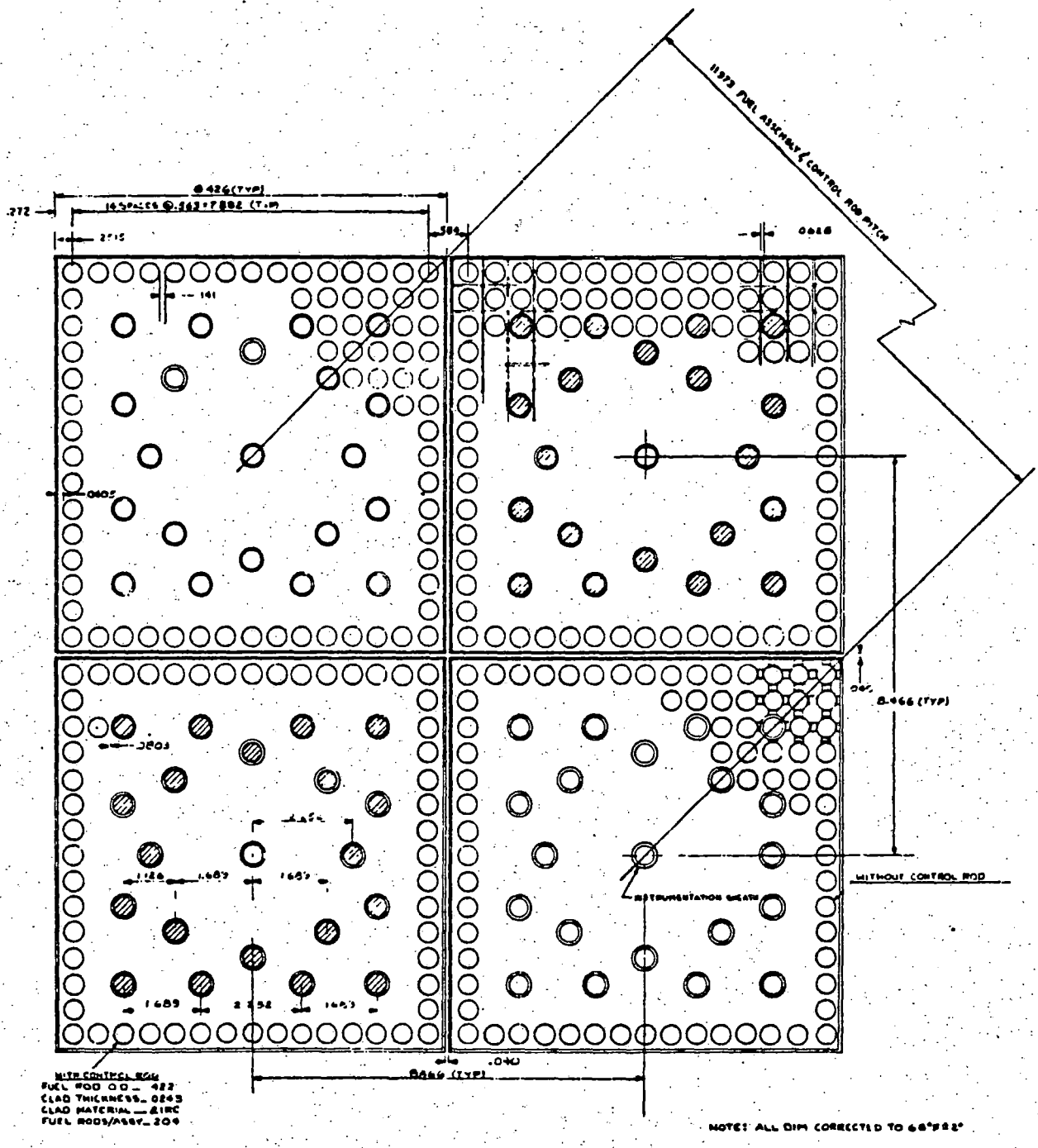

FIGURE 2-2

CONTROL ROD BANK LOCATIONS

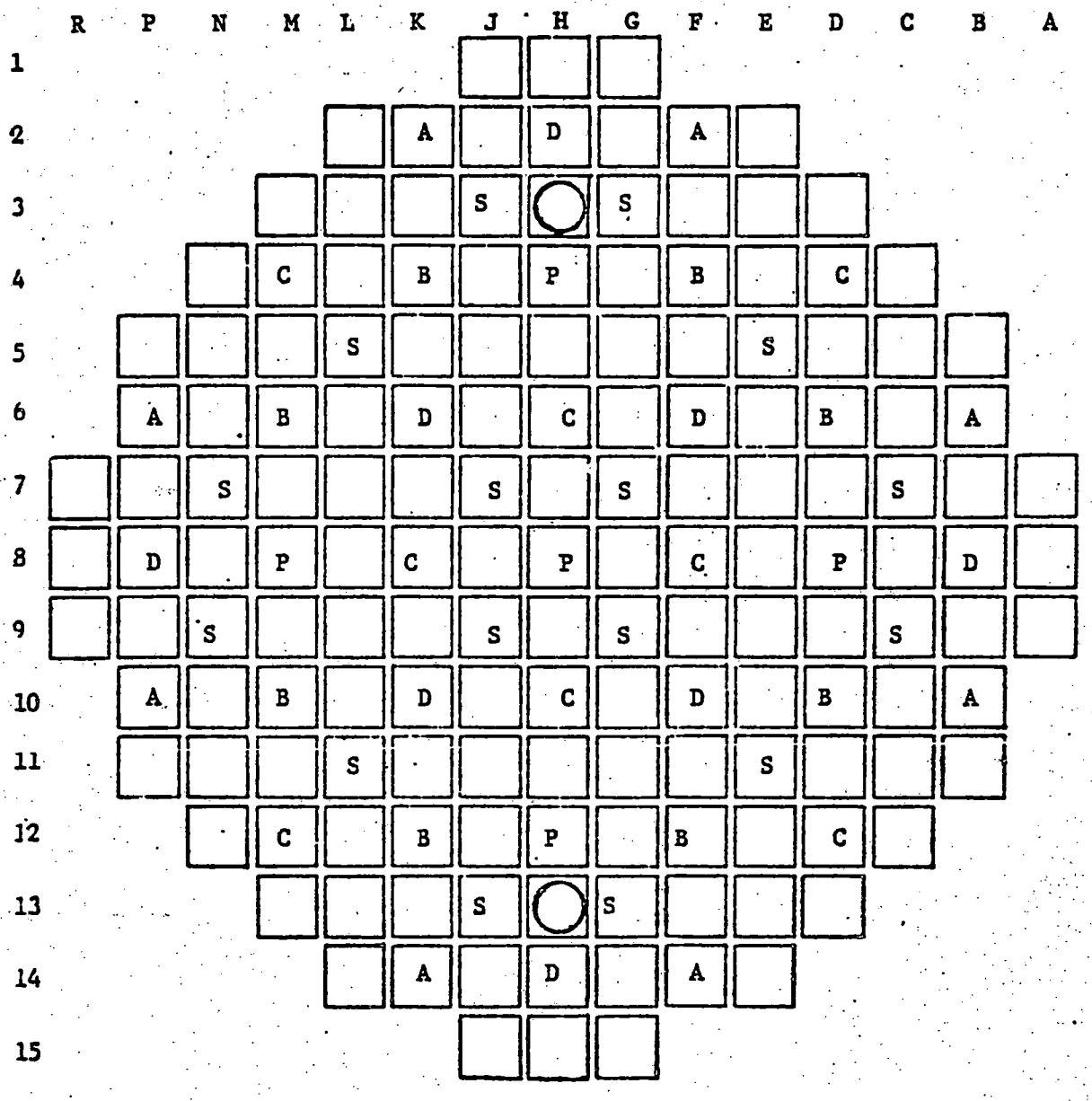

CONTROL ROD ASSEMBLY BANKS

Function	Number of Assemblies
Control Bank D	8
Control Bank C	8
Control Bank B	8
Control Bank A	8
Shutdown (S)	16
Part Length (P)	5
	53

◯ = SOURCE ASSEMBLY LOCATIONS

FIGURE 2-3

SURRY UNITS 1 AND 2 -- CYCLE 1

FUEL LOADING

	08	09	10	11	12	13	14	15
H	1 0 Fresh	2 0 Fresh	1 0 Fresh	2 0 Fresh	1 0 Fresh	2 0 Fresh	1 0 Fresh	3 0 Fresh
J	2 0 Fresh	1 0 Fresh	2 0 Fresh	1 0 Fresh	2 0 Fresh	1 0 Fresh	3 0 Fresh	3 0 Fresh
K	1 0 Fresh	2 0 Fresh	1 0 Fresh	2 0 Fresh	1 0 Fresh	2 0 Fresh	3 0 Fresh	
L	2 0 Fresh	1 0 Fresh	2 0 Fresh	1 0 Fresh	2 0 Fresh	3 0 Fresh	3 0 Fresh	
M	1 0 Fresh	2 0 Fresh	1 0 Fresh	2 0 Fresh	1 0 Fresh	3 0 Fresh		
N	2 0 Fresh	1 0 Fresh	2 0 Fresh	3 0 Fresh	3 0 Fresh			
P	1 0 Fresh	3 0 Fresh	3 0 Fresh	3 0 Fresh				
R	3 0 Fresh	3 0 Fresh						

Batch (#F.A.'s)	Initial Enrichment w/o U235	Density %TD
1 (53)	1.85	94
2 (52)	2.55	93
3 (52)	3.10	92

LEGEND

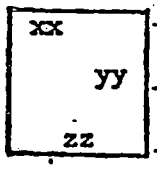

---Batch No.

---Initial Burnup (MWD/MTU)

---Previous Location (If applicable)

FIGURE 2-4

SURRY UNIT 1 - CYCLE 2
FUEL LOADING

	08	09	10	11	12	13	14	15
H	1 15358 H08	4B 0 Fresh	1 12536 H14	4B 0 Fresh	2 15298 H13	4B 0 Fresh	1 14680 H12	4C 0 Fresh
J	4B 0 Fresh	2 16435 L08	4A 0 Fresh	2 14299 K13	2 16075 K11	2 14378 L12	4C 0 Fresh	4C 0 Fresh
K	1 12536 P08	4A 0 Fresh	1 11276 M12	4A 0 Fresh	2 15918 J12	1 14191 K12	4C 0 Fresh	
L	4B 0 Fresh	2 14299 N10	4A 0 Fresh	2 16755 J08	2 16599 J10	4C 0 Fresh	4C 0 Fresh	
M	2 15298 N08	2 16075 L10	2 15918 M09	2 16599 K09	4A 0 Fresh	4C 0 Fresh		
N	4B 0 Fresh	2 14378 M11	1 14191 M10	4C 0 Fresh	4C 0 Fresh			
P	1 14680 M08	4C 0 Fresh	4C 0 Fresh	4C 0 Fresh				
R	4C 0 Fresh	4C 0 Fresh						

Batch (#F.A.'s)	Initial Enrichment w/o U235	Density %TD
1 (21)	1.85	94
2 (52)	2.55	93
4A(20)	1.85	95
4B(12)	2.60	95
4C(52)	3.35	95

LEGEND

xx	---Batch No.
yy	---Initial Burnup (MWD/MTU)
zz	---Previous Location (If applicable)

FIGURE 2-5

SURRY UNIT 2 - CYCLE 2
FUEL LOADING

	08	09	10	11	12	13	14	15
H	1 16693 J09	3 15422 G14	3 11414 H15	2 17992 H11	4A 0 Fresh	2 18295 H09	2 16805 C08	4B 0 Fresh
J	3 15422 P09	4A 0 Fresh	2 17635 K11	4A 0 Fresh	2 15755 K13	3 14725 N11	4B 0 Fresh	4B 0 Fresh
K	3 11414 R08	2 17635 L10	3 15422 J14	2 18151 J10	4A 0 Fresh	2 17470 J12	4B 0 Fresh	
L	2 17992 L08	4A 0 Fresh	2 18151 K09	4A 0 Fresh	2 15860 L12	4B 0 Fresh	4B 0 Fresh	
M	4A 0 Fresh	2 15755 N10	4A 0 Fresh	2 15860 M11	4A 0 Fresh	4B 0 Fresh		
N	2 18295 J08	3 14725 L13	2 17470 M09	4B 0 Fresh	4B 0 Fresh			
P	2 16805 H13	4B 0 Fresh	4B 0 Fresh	4B 0 Fresh				
R	4B 0 Fresh	4B 0 Fresh						

Batch (#F.A.'s)	Initial Enrichment w/o U235	Density %TD
1 (1)	1.85	94
2 (52)	2.55	93
3 (20)	3.10	92
4A(32)	2.60	94
4B(52)	3.10	95

LEGEND

xx	---Batch No.
yy	---Initial Burnup (MWD/MTU)
zz	---Previous Location (If applicable)

FIGURE 2-6

SURRY UNIT 1 - CYCLE 3
FUEL LOADING

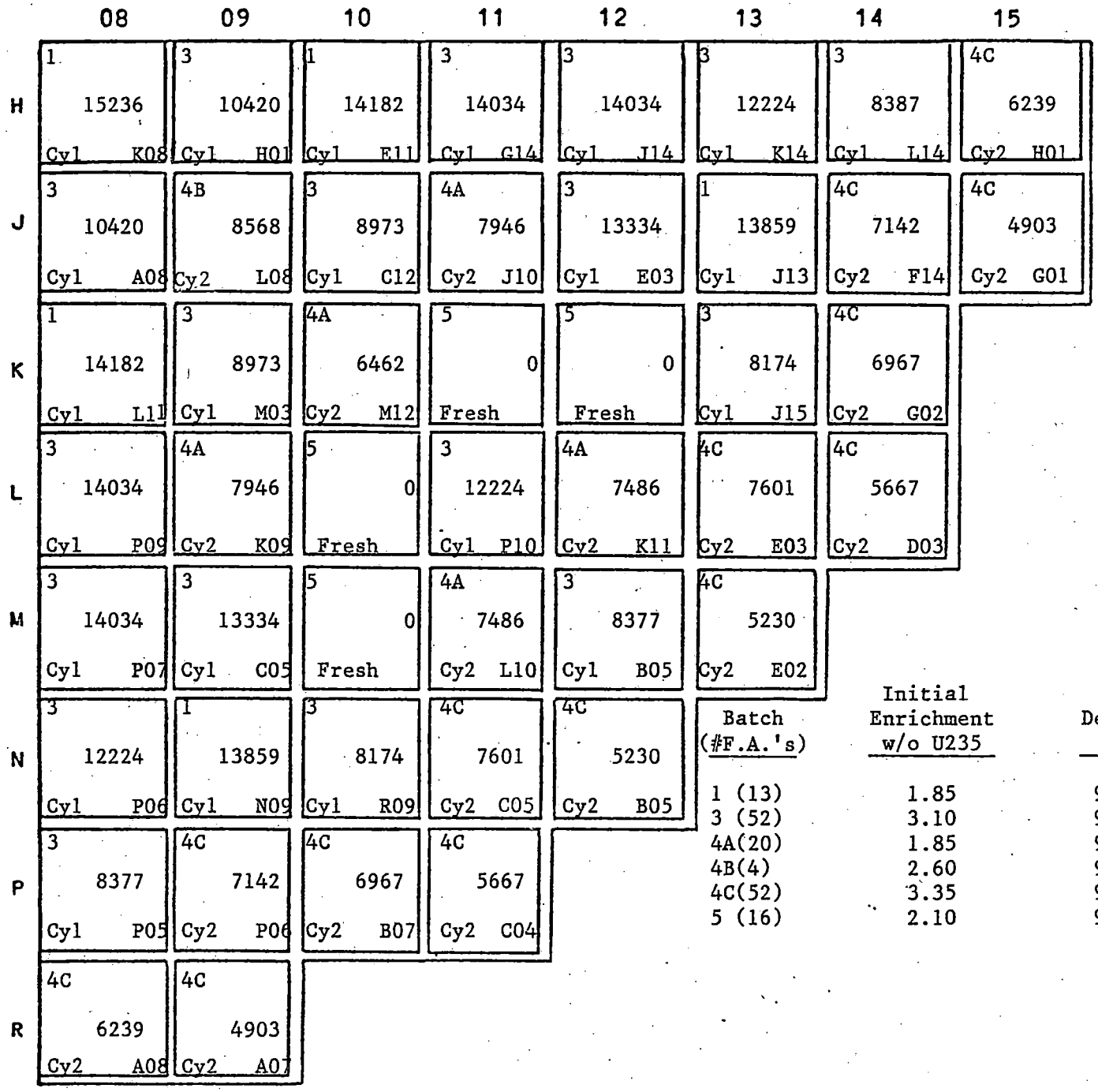

Batch (#F.A.'s)	Initial Enrichment w/o U235	Density %TD
1 (13)	1.85	94
3 (52)	3.10	92
4A(20)	1.85	95
4B(4)	2.60	95
4C(52)	3.35	95
5 (16)	2.10	95

LEGEND

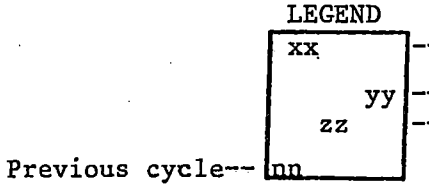

---Batch No.
---Initial Burnup (MWD/MTU)
---Previous Location (If applicable)

FIGURE 2-7

SURRY UNIT 2 - CYCLE 3
FUEL LOADING

	08	09	10	11	12	13	14	15
H	1 16635 Cy1 K08	4B 10342 Cy2 J14	4A 10943 Cy2 G09	3 13414 Cy1 K14	1 15214 Cy1 J13	4B 10342 Cy2 G14	1 13761 Cy2 H14	4B 6985 Cy2 H01
J	4B 10342 Cy2 P07	1 15214 Cy1 N09	4B 10076 Cy2 L13	4A 11093 Cy2 K12	4B 8505 Cy2 K14	4A 11101 Cy2 J11	4B 5739 Cy2 J15	5 0 Fresh
K	4A 10943 Cy2 J09	4B 10076 Cy2 N11	4A 10916 Cy2 M08	3 9228 Cy1 L14	1 15586 Cy1 K12	3 8978 Cy1 J15	4B 5972 Cy2 L14	
L	3 13414 Cy1 P06	4B 11093 Cy2 M10	3 9228 Cy1 P11	1 16377 Cy1 L09	3 9896 Cy1 M13	4B 6806 Cy2 M13	5 0 Fresh	
M	1 15214 Cy1 N07	4B 8505 Cy2 P10	1 15586 Cy1 M10	3 9896 Cy1 N12	3 13414 Cy1 P10	5 0 Fresh		
N	4B 10342 Cy2 P09	4A 11101 Cy2 L09	3 8978 Cy1 R09	4B 6806 Cy2 N12	5 0 Fresh			
P	1 13761 Cy1 P08	4B 5739 Cy2 R09	4B 5972 Cy2 P11	5 0 Fresh				
R	4B 6985 Cy2 A08	5 0 Fresh						

Batch (#F.A.'s)	Initial Enrichment w/o U235	Density %TD
1 (25)	1.85	94
3 (32)	3.10	92
4A(24)	2.60	94
4B(52)	3.10	95
5 (24)	3.10	95

LEGEND

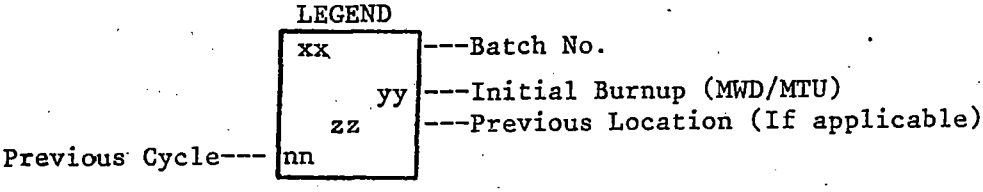

FIGURE 2-8

SURRY UNIT 1 - CYCLE 4
FUEL LOADING

	08	09	10	11	12	13	14	15
H	1 15236 Cy1 H06	6A 0 Fresh	5 10552 Cy3 F11	6A 0 Fresh	4B 8760 Cy2 H09	5 10552 Cy3 E10	4B 8615 CY2 H13	6C 0 Fresh
J	6A 0 Fresh	4C 17296 Cy3 N11	6A 0 Fresh	4C 10529 Cy3 A09	4C 11355 Cy3 N04	4C 14951 Cy3 F02	6C 0 Fresh	6C 0 Fresh
K	5 10552 Cy3 L10	6A 0 Fresh	2/4A 9890 S2C2 M12	6A 0 Fresh	4C 16875 Cy3 J14	6B 0 Fresh	6C 0 Fresh	
L	6A 0 Fresh	4C 10529 Cy3 J01	6A 0 Fresh	4C 17287 Cy3 L13	4C 11267 Cy3 L14	6C 0 Fresh	6C 0 Fresh	
M	4B 8760 Cy2 J08	4C 11355 Cy3 D13	4C 16875 Cy3 P09	4C 11267 Cy3 P11	4C 13240 Cy3 R08	6C 0 Fresh		
N	5 10552 Cy3 K11	4C 14951 Cy3 B06	6B 0 Fresh	6C 0 Fresh	6C 0 Fresh			
P	4B 8615 Cy2 N08	6C 0 Fresh	6C 0 Fresh	6C 0 Fresh				
R	6C 0 Fresh	6C 0 Fresh						

Batch (#F.A.'s)	Initial Enrichment w/o U235	Density %TD
1 (1)	1.85	94
2/4A (4)	2.60	95
4B (8)	2.60	95
4C (52)	3.35	95
5 (8)	2.10	95
6A (24)	2.60	95
6B (8)	2.60	95
6C (52)	2.90	95

LEGEND

xx ----Batch No.
yy ----Initial Burnup (MWD/MTU)
zz ----Previous Location (If applicable)

FIGURE 2-9

SURRY UNIT 2 - CYCLE 4
FUEL LOADING

	08	09	10	11	12	13	14	15
H	1 16635 Cy1 F08	6A 0 Fresh	4B 21458 Cy3 G10	4B 13392 Cy3 H15	4B 21240 Cy3 H09	4B 20813 Cy3 H13	4B 17227 Cy3 E13	6B 0 Fresh
J	6A 0 Fresh	4B 19642 Cy3 M09	6A 0 Fresh	5 5849 Cy3 J15	5 6678 Cy3 L14	4B 14467 Cy3 K14	6B 0 Fresh	6B 0 Fresh
K	4B 21458 Cy3 K09	6A 0 Fresh	4B 19630 J12	5 7340 Cy3 M13	4B 15745 Cy3 J14	6B 0 Fresh	6A 0 Fresh	
L	4B 13392 Cy3 R08	5 5849 Cy3 R09	5 7340 Cy3 N12	4B 21464 Cy3 J10	6A 0 Fresh	6B 0 Fresh	6B 0 Fresh	
M	4B 21240 Cy3 J08	5 6678 Cy3 P11	4B 15745 Cy3 P09	6A 0 Fresh	4B 17255 Cy3 L13	6B 0 Fresh		
N	4B 20813 Cy3 N08	4B 14467 Cy3 P10	6B 0 Fresh	6B 0 Fresh	6B 0 Fresh			
P	4B 17227 Cy3 N11	6B 0 Fresh	6A 0 Fresh	6B 0 Fresh				
R	6B 0 Fresh	6B 0 Fresh						

Batch (#F.A.'s)	Initial Enrichment w/o U235	Density %TD
1 (1)	1.85	94
4B (52)	3.10	95
5 (24)	3.10	95
6A (28)	2.90	95
6B (52)	3.20	95

Legend

xx ----Batch No.
yy ----Initial Burnup (MWD/MTU)
zz ----Previous Location (If applicable)

FIGURE 2-10

SURRY UNITS 1 AND 2 -- CYCLE 1
Burnable Poison Rod Loading

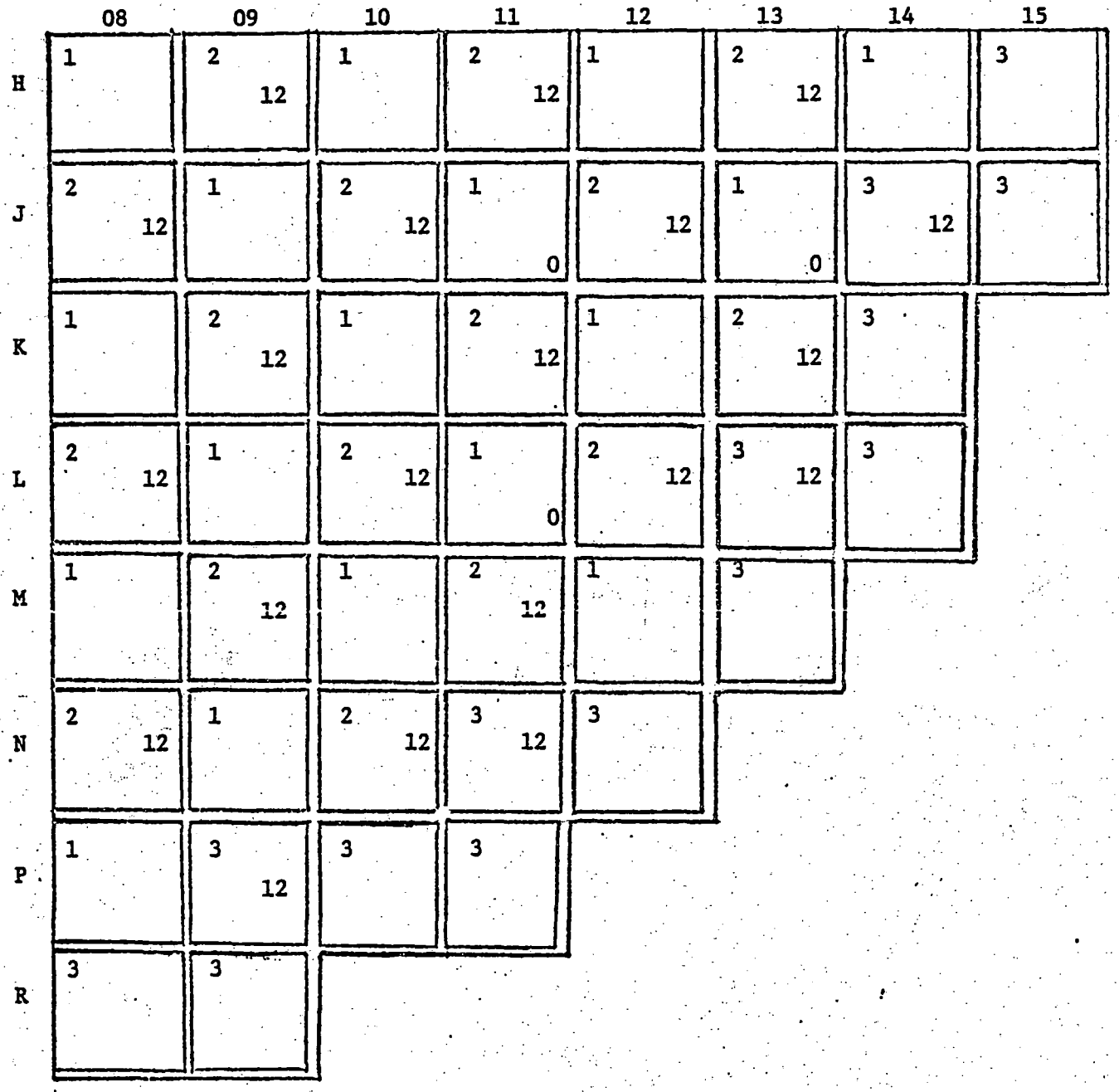

LEGEND

xx ---Batch No.

yy ---No. of Fresh Burnable Poison Rods

FIGURE 2-11

SURRY UNIT 1 -- CYCLE 2
BURNABLE POISON ROD LOADING

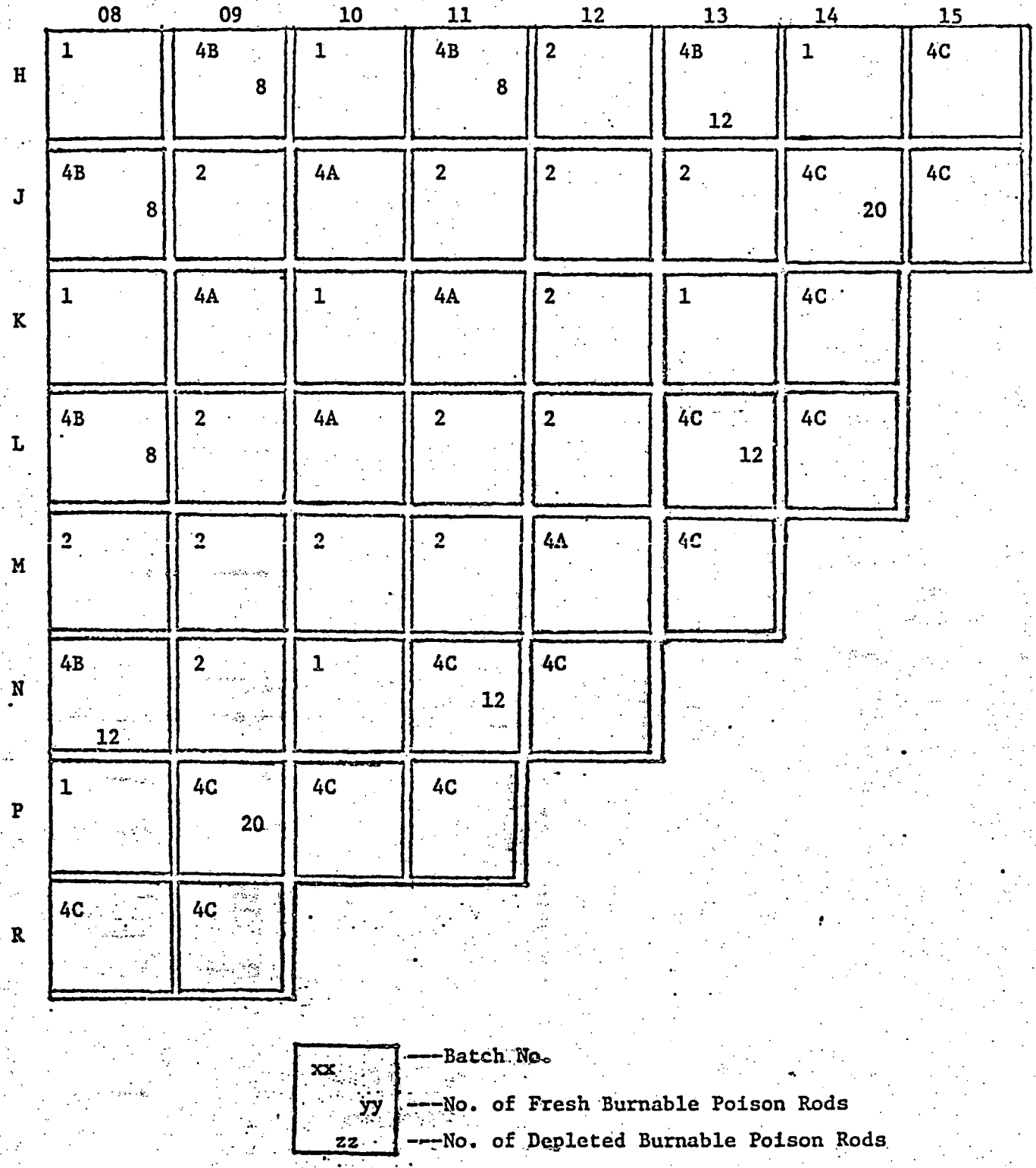

FIGURE 2-12

SURRY UNIT 2 - CYCLE 2
BURNABLE POISON ROD LOADING

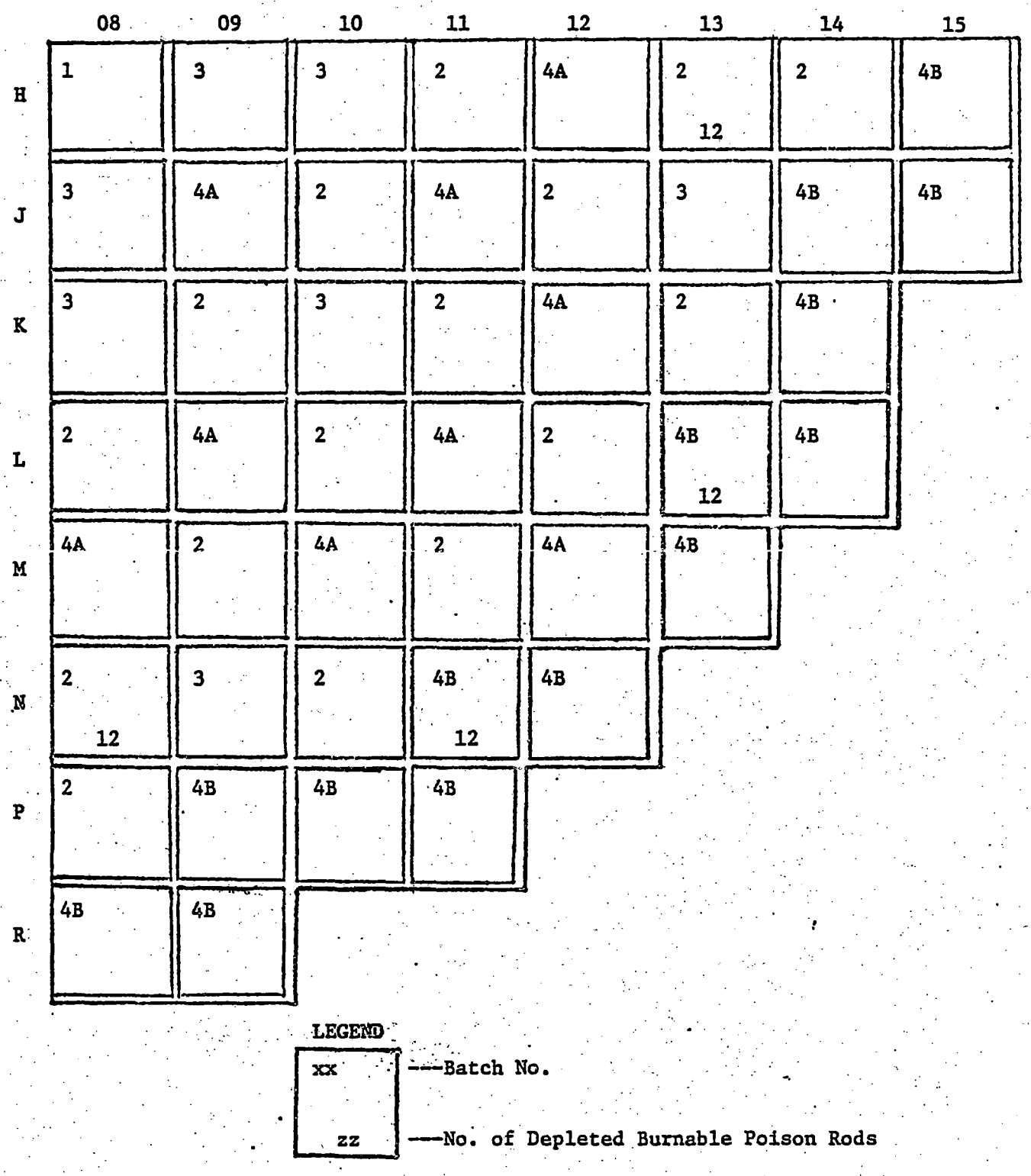

FIGURE 2-13

SURRY UNIT 1 - CYCLE 3
BURNABLE POISON ROD LOADING

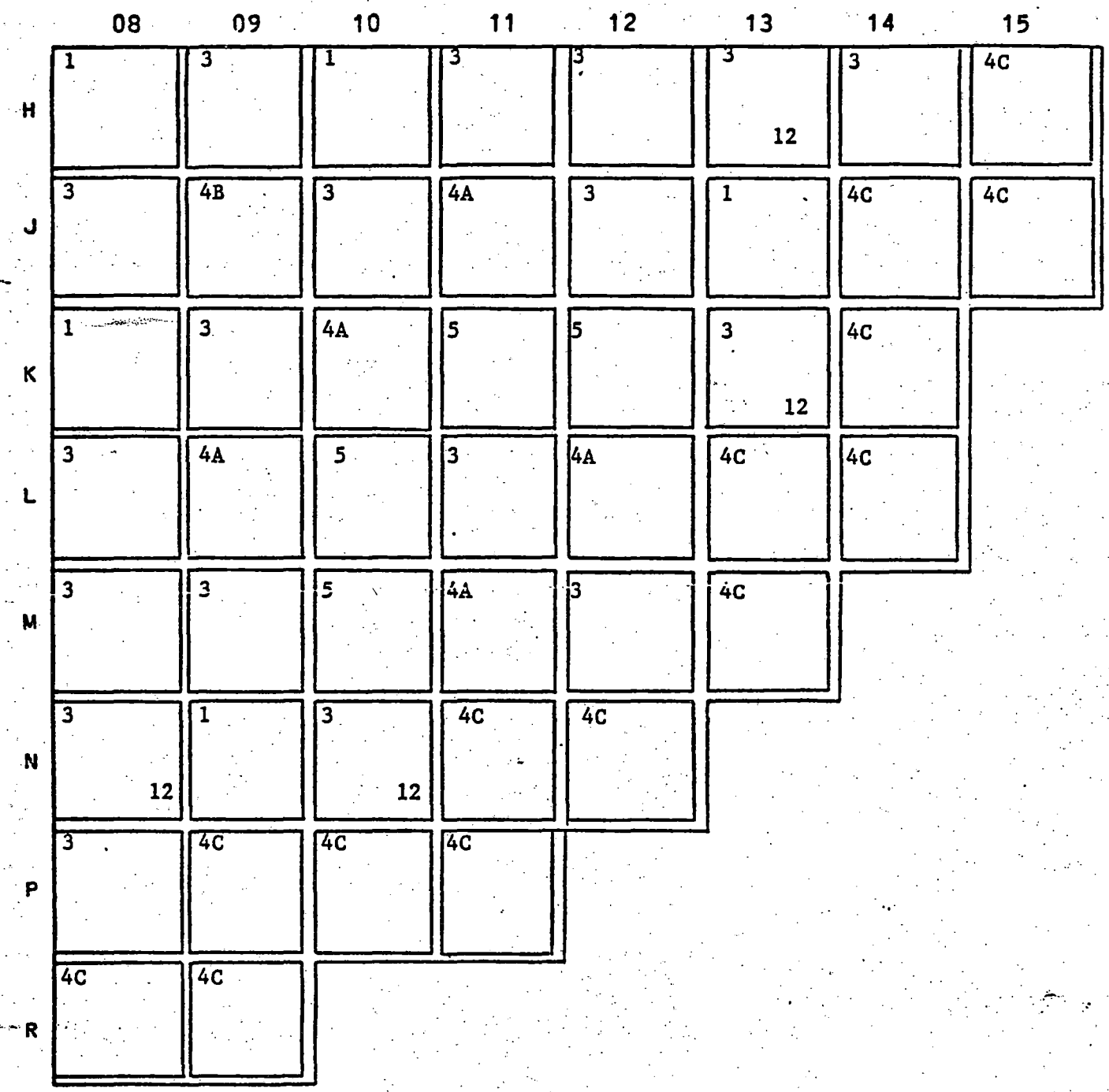

FIGURE 2-14

SURRY UNIT 2 - CYCLE 3
BURNABLE POISON ROD LOADING

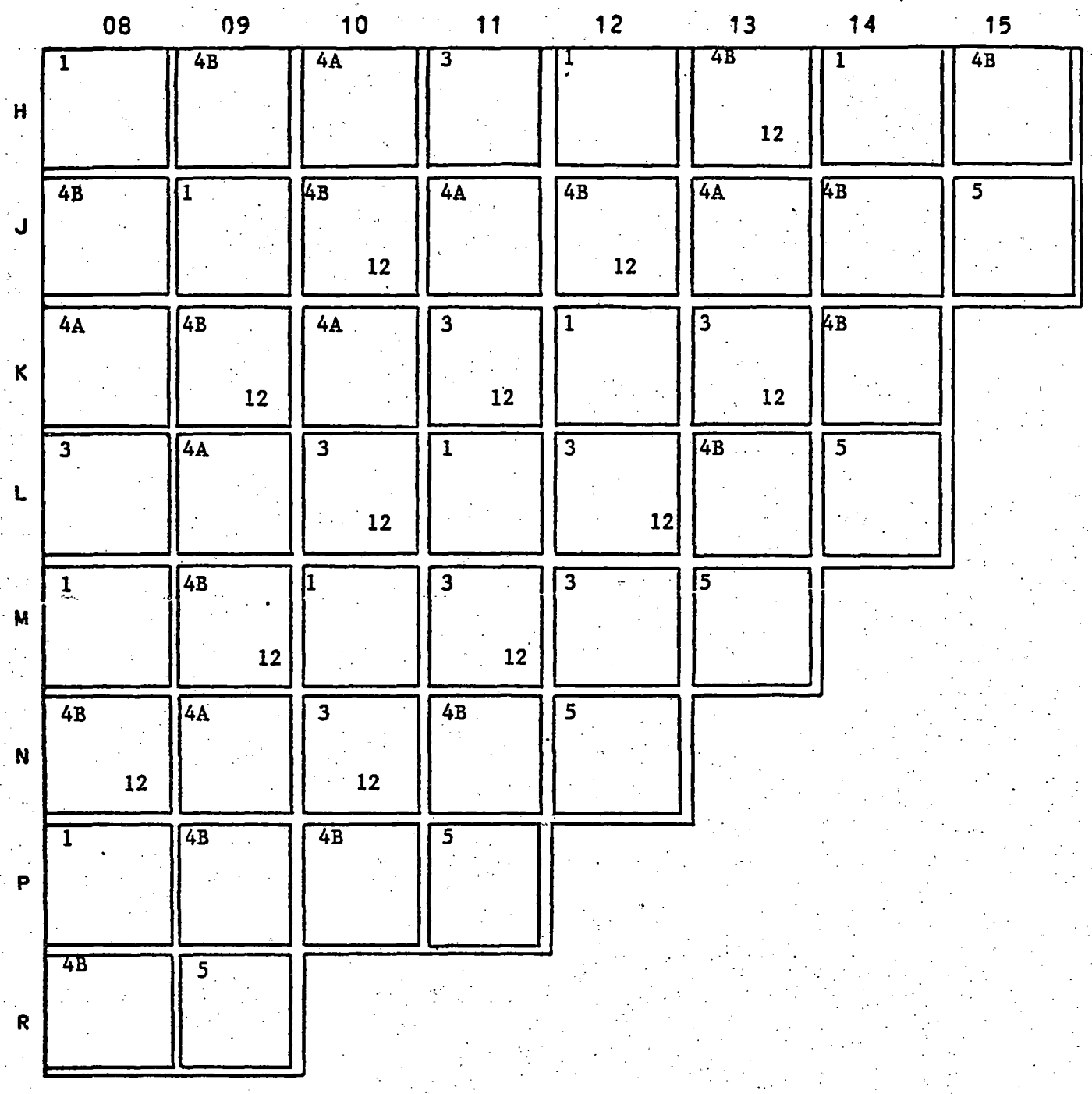

LEGEND

xx ---Batch No.

zz ---No. of Depleted Burnable Poison Rods

FIGURE 2-15

SURRY UNIT 1 - CYCLE 4
BURNABLE POISON ROD LOADING

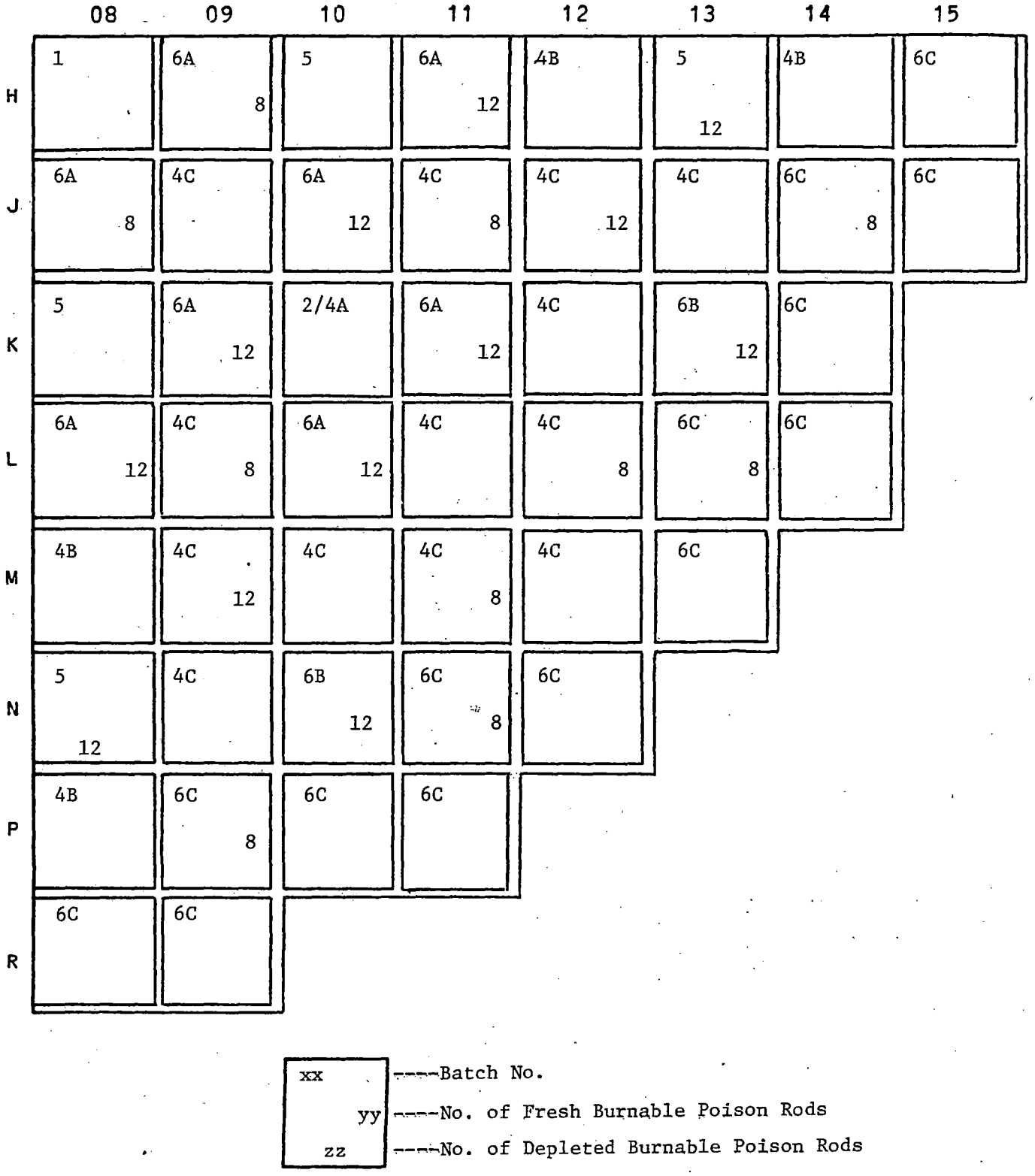

FIGURE 2-16

SURRY UNIT 2 - CYCLE 4
BURNABLE POISON ROD LOADING

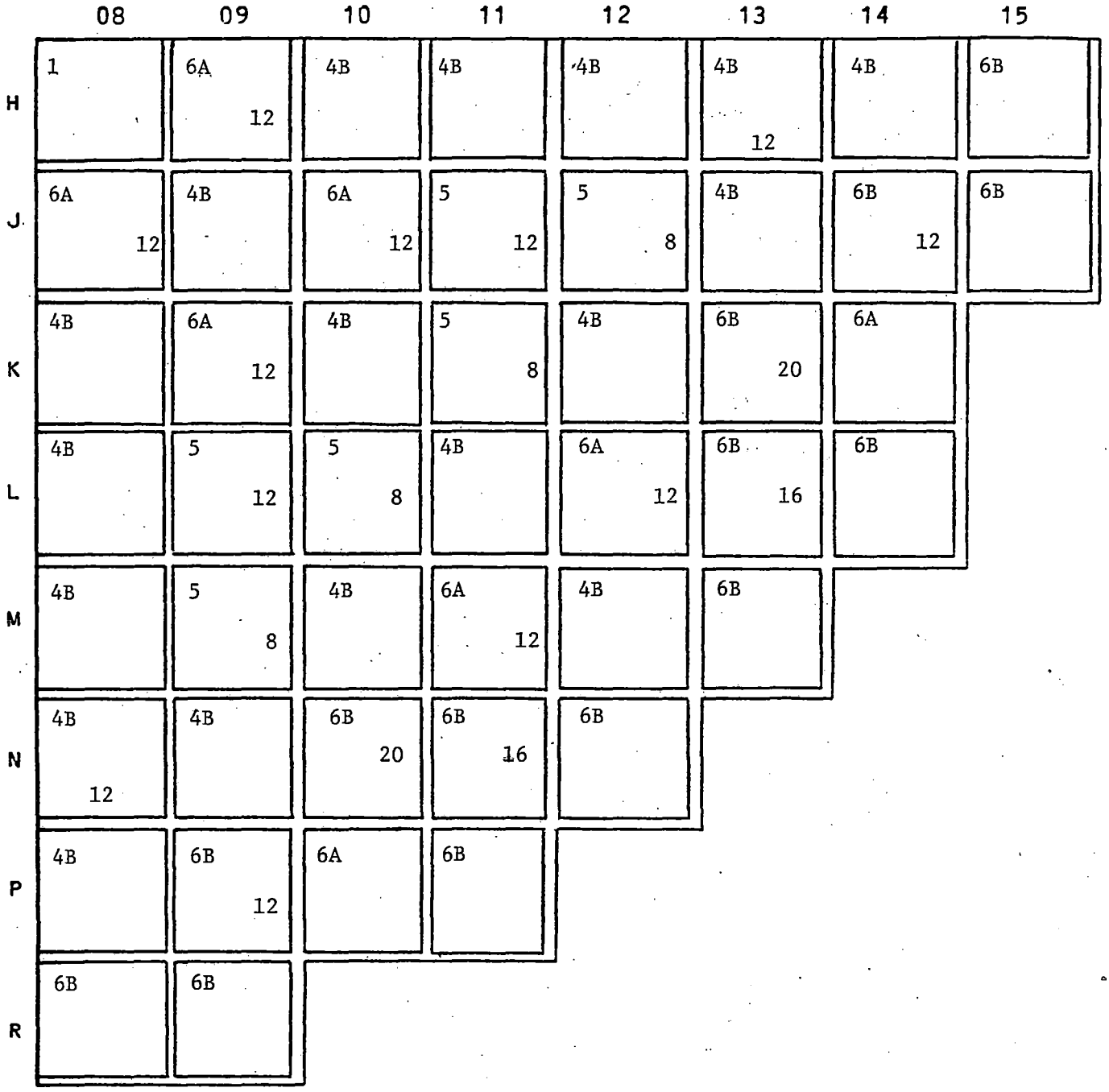

SECTION 3 - MODEL DESCRIPTION

3.1 Introduction

The Vepco FLAME Model is used to calculate nodal power densities and core reactivity for three-dimensional geometries in which each fuel assembly is represented by one radial node and by up to 32 axial nodes. The method used by the Vepco FLAME Model to perform these calculations is based on the FLARE[9] technique which is derived from modified, one energy group diffusion theory. Effects of nonuniform moderator density and fuel temperature are accounted for by thermal-hydraulic feedback.

The Vepco FLAME Model performs calculations in several steps. First, a fine-group neutron flux spectrum and the appropriate cross sections as a function of neutron energy are calculated for each material composition in the fuel assembly by a cross section generating code (i.e., the NULIF[1] computer code). Then the fine-group flux spectrum is used to spectrum weight and collapse the fine-group cross sections into the one energy group parameters required (i.e., K_∞ and M^2) by the FLAME3[3] computer code. These parameters, as well as any appropriate normalization factors, are then used by FLAME3 to perform an iterative, modified diffusion theory calculation for the neutron production rate density as a function of position. The method of solution comprises two levels of iteration: source (or nuclear) and thermal-hydraulic feedback. The source calculation is performed first based on an initial guess for the thermal-hydraulic parameters. Then a new set of thermal-hydraulic parameters are calculated. Using these new thermal-hydraulic parameters, another source calculation is performed. This process is continued until both the source and thermal-hydraulic convergence criteria are satisfied.

Several interrelated computer codes are used to perform the calculations outlined above. The computer codes comprising the Vepco FLAME Model and their interrelationships are presented in the flow chart in Figure 3-1. The FLAME3 computer code is the principal analytical tool in the Vepco FLAME Model. FLAME3 is used to perform the three-dimensional, one group, modified diffusion theory calculations. The other codes provide either input data or data manipulation. As indicated in Figure 3-1, the NULIF code is used to generate the required one group data for the non-rodded fuel assembly. The FLAFIT[3] code formats these data for use by FLAME3. Data for burnable poison and control rods are generated with the Vepco PDQ07 Discrete Model[7] using a quarter assembly discrete representation. The in-house codes EDITQAR[5] and PICCOLO[5] format the data from the quarter assembly PDQ07 calculations for use by FLAME3. The FLMSHUFL[6] code is a data manipulation code that shuffles the appropriate end-of-cycle burnup distributions to duplicate the movement of fuel assemblies during refueling. The shuffled burnup distributions from FLMSHUFL are input to FLAME3 to begin reload cycle analyses.

The remainder of this chapter describes in greater detail the input to and functioning of the computer codes used in the Vepco FLAME Model.

3.2 Input Preparation

The Vepco FLAME Model uses the FLARE neutron source option for all calculations with the FLAME3 code. Two physics parameters are required at each node by the FLARE[9] option: the infinite multiplication factor (K_∞) and the migration area (M^2). At peripheral nodes, it may also be necessary to input a leakage parameter (or albedo).

The infinite multiplication factor, migration area, and albedoes for each node are usually functions of one or more variables. Among these are initial

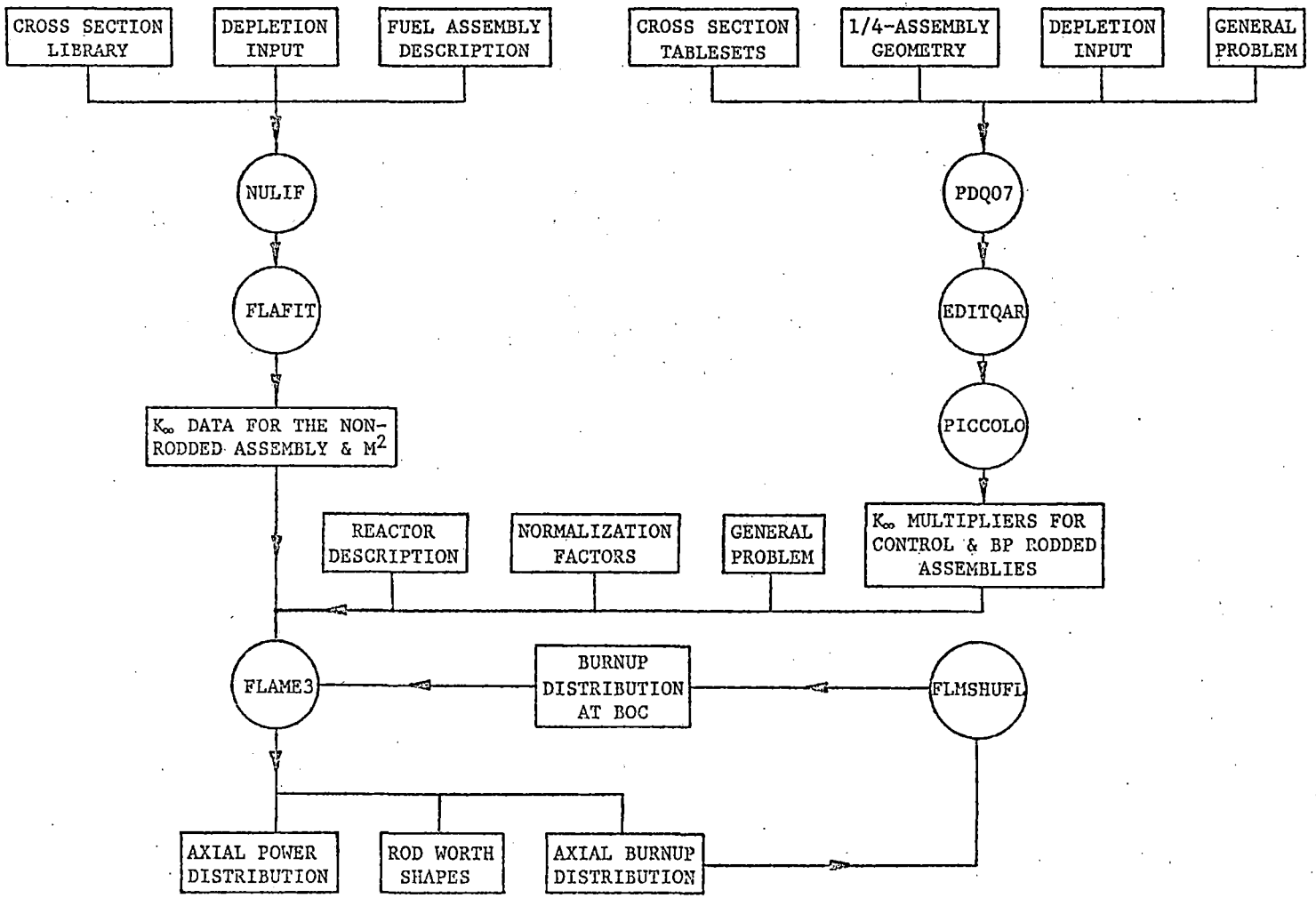

FIGURE 3-1
FLOW CHART FOR VEPCO
FLAME MODEL

enrichment, burnup, soluble boron concentration, xenon concentration, fuel and moderator temperatures, and the presence or absence of burnable poison or control rods. To represent the functional dependencies, K_∞ and M^2 are calculated for various combinations of the appropriate variables. The resulting values of K_∞ (or M^2) are then tabulated for use in the FLAME3 code by using the FLAFIT and PICCOLO codes. The FLAME3 code uses a Lagrangian interpolation routine for selecting the appropriate input data from the tables constructed by FLAFIT and PICCOLO. This routine allows any input variable (e.g., K_∞) to be fit as a function of one, two, or three independent variables. Due to this constraint, it has been necessary to use several tables to properly represent all the functional dependencies of K_∞.

The leakage parameters cannot be input in tabular form. However, the leakage parameters may be changed to reflect changing reactor conditions. This is discussed further in Section 4.1.

The processes by which tabular input for K_∞ and M^2 are developed are described in this section.

3.2.1 Method of Calculating Input Data for the Non-Rodded Fuel Assembly

The NULIF code is used to generate the non-rodded (i.e., no control or burnable poison rods are present) fuel assembly input data for the FLAME3 code. The NULIF calculations are performed using the supercell option. A supercell is defined as a group of unit cells comprising, for example, a fuel assembly. For the supercell group, the fuel rod unit cell is designated as the central cell. Any other unit cell types (e.g., control rod guide tube cell) present in an assembly are designated as subregion cells (subcells). The supercell option is used to represent the fuel assembly in the Vepco FLAME Model because only homogenized groups of unit cells can be represented due the larger-than-discrete mesh description implicit in a nodal representation of the reactor core. The homogenization is performed in a manner that

results in one node representing each fuel assembly.

The calculation of the neutron energy spectrum and the spectrum-weighted two-group cross sections for each supercell is described in detail in Reference 1. Those aspects which involve calculations using the supercell option are described below.

With the supercell option of the NULIF code, the material compositions of the central cell and the various subcells must be homogenized together before the fine-group neutron flux is calculated, since the NULIF code does not perform a spatial calculation for the various subregions. Because of this, a method must be employed to represent the heterogeneous nature of the supercell. This is done by inputting appropriate thermal flux depression factors for each subcell relative to the supercell. These flux depression factors are generated by a detailed spatial calculation (i.e., a quarter assembly discrete PDQ07 calculation where each fuel rod, thimble cell, and water channel associated with the fuel assembly is explicitly represented). From this detailed spatial calculation, the ratios of the thermal flux in the average fuel cell, thimble cell, and water gap relative to the thermal flux in the entire assembly are determined. The above flux depression factors are combined in NULIF with those normally calculated by NULIF for the central cell (i.e., the flux distribution in the fuel pellet, clad, and moderator regions of the central cell) to give the overall flux depression factors to be applied over each of the 80 thermal fine-groups for each nuclide in the supercell.

NULIF calculates the neutron flux in the supercell for each of 31 fast and 80 thermal energy fine groups. The macroscopic, one-energy group parameters needed as input to the FLAME3 code are then determined from the neutron flux and cross sections for each fine group.

Assembly (supercell) calculations of K_∞ and M^2 with the NULIF code are performed as a function of:

1. Initial enrichment
2. Burnup
3. Soluble boron concentration
4. Moderator specific volume
5. Fuel temperature
6. Xenon concentration

An assembly of each enrichment used in the core is depleted with NULIF while maintaining constant soluble boron and xenon concentrations, moderator specific volume and fuel temperature. Recovery cases are then performed at selected burnups where these parameters are varied. Care has been taken to vary each parameter over the range of values expected to occur during the types of operation to be modeled with the Vepco FLAME Model.

3.2.1.I K-Infinity

The Vepco FLAME Model uses for each enrichment a basic K_∞ which is a function of burnup, soluble boron concentration, and xenon concentration. This combination of independent variables was chosen for two reasons. First, these variables have the largest effects on K_∞ for the non-rodded assembly (aside from enrichment which, as stated above, is represented by generating separate tablesets for each initial enrichment). Second, the effects of these variables are relatively insensitive to changes in other parameters. For these reasons, the functional dependencies of K_∞ on burnup, boron, and xenon are represented together in the basic K_∞.

Since K_∞ cannot be adequately represented as a function of only three independent variables (the limit for any table used in the FLAME3 code), other tables (i.e., K_∞ multipliers) are developed to allow the incorporation of additional functional dependencies. The K_∞ multiplier tables contain

factors which are used to modify the values contained in the basic K_∞ tables. These factors are arrived at by taking the ratio of K_∞ at some nominal condition to the K_∞ generated by the NULIF code after a change in one or two independent variables. For the non-rodded fuel assembly, two K_∞ multipliers are used to represent the effects of fuel and moderator temparatures.

The first K_∞ multiplier represents the effects on K_∞ of changing moderator temperature. Changes in moderator temperature result in two important phenomena: 1) change in moderation (neutron spectrum) and 2) change in parasitic absorption in the moderator. For these reasons, the first K_∞ multiplier is fit as a function of moderator specific volume, burnup, and soluble boron concentration.

The second K_∞ multiplier incorporates the dependence of K_∞ on fuel temperature. Changing fuel temperature causes a change in resonance absorption. This effect is sensitive only to burnup. Therefore, the second K_∞ multiplier is fit as a function of fuel temperature and burnup.

3.2.1.2 Migration Area

The migration area, M^2, is used by the FLAME3 code as a measure of the leakage from an assembly. As such, M^2 is sensitive only to moderator specific volume, burnup, and enrichment. Therefore, M^2 can be adequately represented by a single table fit as a function of these three parameters.

In addition, the FLAME3 code permits the use of a M^2 multiplier as a normalization factor. The use of M^2 multipliers is discussed in Section 4.1.

3.2.1.3 Input Parameters for Calculating Xenon Concentration

The FLARE neutron source option does not allow the explicit calculation of any material concentrations. However, to accurately represent K_∞ it is necessary to know the xenon concentration at each node in the core. Once the nodal xenon concentrations are found, then K_∞ for each node may be obtained from the appropriate tables.

To find the nodal xenon concentrations, the FLAME3 code solves the differential equations for xenon and iodine based on the assumption of constant power throughout a burnup step (see Section 3.4). This solution requires that several parameters be input to the FLAME3 code in tabular form as functions of the appropriate independent variables. These input parameters are listed below:

$$A = (K_1\Sigma_{f1}\phi_1 + K_2\Sigma_{f2}\phi_2)(1/\phi_2)$$

$$YI = (\gamma_I\Sigma_{f1}\phi_1 + \gamma_I\Sigma_{f2}\phi_2)(1/\phi_2)$$

$$YX = (\gamma_X\Sigma_{f1}\phi_1 + \gamma_X\Sigma_{f2}\phi_2)(1/\phi_2)$$

σ_{a2}^{Xe} = thermal microscopic absorption cross section of xenon,

SIGM = multiplier for σ_{a2}^{Xe}

where: K = energy released per fission

Σ_f = macroscopic fission cross section

ϕ = neutron flux

γ_I = yield per fission of Iodine-135

γ_X = yield per fission of Xenon-135

and subscripts 1 and 2 refer to the fast and thermal energy groups respectively. The parameters are all generated by the NULIF code and are tabulated by FLAFIT for use in the FLAME3 code.

The parameters A, YI, and YX are strongly dependent on burnup and enrichment. However, variations in other independent variables do not significantly influence these parameters. For this reason, A, YI, and YX are fit as a function of burnup and enrichment only.

The thermal microscopic absorption cross section of xenon is dependent upon the neutron energy spectrum in the fuel pellet. The neutron spectrum is, in turn, dependent upon the amounts of absorbing and fissile material in the fuel and the moderation which occurs outside the fuel pellet. Therefore, σ_{a2}^{Xe} is fit as a function of burnup, xenon concentration and enrichment. To account for the spectral effects of the moderator, the multiplier

for σ_{a2}^{Xe}, (SIGM), is fit as a function of soluble boron concentration and moderator specific volume.

3.2.2 Method of Calculating Input Data for the Burnable Poison Rodded Assembly

3.2.2.1 Introduction

The input data for an assembly containing burnable poison (BP) rods are calculated with the Vepco PDQ07 Discrete Model using a 2-D, quarter-assembly representation. Theoretically, these data could be obtained by NULIF supercell calculations (as described in Section 3.2.3 above) in which one of the subcells contains the appropriate amount of BP. However, the fact that the hetergeneous effect of the various subcells are accounted for by applying thermal flux depression factors determined from quarter assembly discrete calculations must be considered. In general, for assemblies containing no BP, these flux depression factors do not change significantly as a function of burnup, so that the flux depression factors calculated at zero burnup are adequate at any stage of depletion. However, this is not the case for subcells containing BP because the BP depletes rapidly with increasing burnup causing the flux depression factors to vary significantly with burnup. Since a large number of quarter-assembly discrete calculations would have to be made to calculate these factors for input to NULIF, it has been decided to use the quarter assembly runs directly to generate K_∞ multipliers to account for BP reactivity effects. These multipliers (in conjunction with the K_∞ data for the non-rodded fuel assembly discussed in Section 3.2.1) are applied to nodes which contain (or have contained) BP rods.

Four K_∞ multipliers are used in the Vepco FLAME Model to represent BP rods. Two multipliers represent the presence of fresh BP in a fuel assembly. The third multiplier accounts for the presence of depleted BP. The fourth K_∞

multiplier is used to represent the reactivity "after-effect" resulting from the depletion of a fuel assembly containing fresh BP rods.

3.2.2.2 K-Infinity Multipliers For Fuel Containing Fresh BP

The presence of fresh BP rods in a fuel assembly changes that assembly's characteristics in two ways. First, a large concentration of non-fissile, neutron absorbing material is added to the assembly. Second, moderator is displaced from the assembly. The reactivity effects associated with these changes depend on initial assembly enrichment, cumulative burnup of the assembly while BP rods are present, soluble boron concentration, and moderator temperature. To represent these effects, two K_∞ multipliers are used.

The first K_∞ multiplier table for BP accounts for the dependence on enrichment, cummulative burnup, and soluble boron concentration. To generate this table, assemblies of various enrichments are depleted at nominal moderator and fuel temperatures with and without BP rods using a quarter assembly representation of the Vepco PDQ07 Discrete Model. At a number of burnup points, recovery cases are performed during which the soluble boron concentration is changed. The values of the first K_∞ multiplier are then obtained by ratioing K_∞ in the rodded state to K_∞ in the non-rodded state. The PICCOLO code is used to tabulate these values as a function of cumulative burnup, initial enrichment, and soluble boron concentration. This procedure is followed to construct separate tables for configurations of 8, 12, 16, and 20 BP rods per assembly.

The second K_∞ multiplier accounts for the variation in the reactivity effect of fresh BP with changes in moderator temperature. Sensitivity calculations have shown that this multiplier is not significantly affected by enrichment or number of BP rods per assembly.[10] Therefore, the second K_∞ multiplier is generated for an assembly of average enrichment (i.e., 2.90 w/o U235) containing

the most commonly used configuration of BP rods (i.e., 12 fresh BP rods per assembly). Again using the Vepco PDQ07 Discrete Model, a 2.90 w/o enriched assembly is first depleted with 12 fresh BP rods present and then depleted without the presence of any BP. At several burnup points during the above two depletions, additional cases are performed in which moderator temperature and soluble boron concentration are varied simultaneously. The values of the second K_∞ multiplier are obtained in two steps. First, for each set of conditions, the value of K_∞ obtained from the depletion case with BP rods is divided by the value of K_∞ obtained from the depletion case without BP rods. Then the ratios determined in the first step are divided by the ratio of K_∞ with BP rods to K_∞ without BP rods obtained for the nominal moderator temperature (i.e., 566°F). The PICCOLO code is then used to tabulate these values in a form acceptable to the FLAME3 code as a function of cumulative burnup, soluble boron concentration, and moderator temperature.

3.2.2.3 K-Infinity Multipliers for Fuel Containing Depleted BP

To account for the presence of depleted BP in a fuel assembly, a third K_∞ multiplier is used. As the BP rods in an assembly are depleted, the boron concentration decreases rapidly. At the end of one cycle of burnup, the boron concentration in the BP rods may be assumed to be zero. When these depleted BP rods are inserted in other assemblies, their principal effects are the displacement of water and absorption of neutrons in stainless steel. Sensitivity calculations have shown that this multiplier is not significantly affected by enrichment.[10] The only configuration of depleted BP rods used in Cycles 1 through 4 of Surry Units 1 and 2 is 12 rods per assembly. Therefore, this multiplier is generated for an assembly of average enrichment (i.e., 2.90 w/o U235) containing 12 depleted BP rods. Using the Vepco PDQ07 Discrete Model, a 2.90 w/o enriched assembly is depleted both with and without 12 depleted BP rods. At several burnup points additional

cases are performed for which moderator temperature and soluble boron concentration are varied simultaneously. The values of the third K_∞ multiplier are obtained by dividing K_∞ with depleted BP by K_∞ without BP. The PICCOLO code is then used to tabulate these values for input to the FLAME3 code as a function of total burnup, moderator temperature, and soluble boron concentration.

3.2.2.4 K-Infinity Multiplier for the "After Effect" of Fresh BP

The presence of fresh BP rods in a fuel assembly during depletion also affects the reactivity in that assembly after the BP rods are removed. This BP "after-effect" arises from the change in isotopics accompanying depletion of the fuel assembly in the harder neutron spectrum resulting from the presence of fresh BP rods. Once the BP rods are removed, the after-effect diminishes with continued depletion of the assembly. To represent this effect, assemblies of various enrichments are depleted in two ways using a quarter assembly representation of the Vepco PDQ07 Discrete Model. First, an assembly is depleted without BP rods. Second, an assembly of the same enrichment containing 12 BP rods is depleted to various burnups. Then, the BP rods are removed, and the assembly is depleted further. The values of the fourth K_∞ multiplier for BP are obtained by dividing K_∞ from the assembly which has had BP by K_∞ of the assembly which has not had BP. The PICCOLO code is used to tabulate these values as a function of cumulative burnup experienced by the assembly with BP rods present, total burnup, and enrichment.

3.2.3 Method of Calculating Input Data for the Control Rodded Assembly

3.2.3.1 Introduction

The input data for assemblies containing control rods are generated in a manner similar to that used to generate the BP data (Section 3.2.2). Again, a quarter-assembly representation of the Vepco PDQ07 Discrete Model is used to perform all the basic calculations, while the PICCOLO code is

used to construct the tables for input to the FLAME3 code.

Four K_∞ multipliers are used in the Vepco FLAME Model to represent control rods. Three multipliers represent the presence of control rods in a fuel assembly. The fourth K_∞ multiplier is used to account for the reactivity "after-effect" resulting from the depletion of a fuel assembly containing control rods.

3.2.3.2 K-Infinity Multipliers for Fuel Containing Control Rods

The presence of control rods in a fuel assembly has much the same effect as the presence of fresh BP in an assembly. First, a large concentration of non-fissile, neutron absorbing material is added to the assembly. Second, moderator is displaced from the assembly. The reactivity effects associated with the presence of control rods depend on initial assembly enrichment, cumulative burnup of the assembly while the rods are present, total assembly burnup, soluble boron concentration, and moderator temperature. To represent these effects, two K_∞ multipliers are used.

The first K_∞ multiplier accounts for the dependence on enrichment, moderator temperature, and soluble boron concentration. To generate the values for this multiplier, calculations are performed for assemblies of various enrichments with and without control rods using the Vepco PDQ07 Discrete Model. These calculations are done at zero burnup and with different values of soluble boron concentration and moderator temperature. The values of the first K_∞ multiplier are obtained by ratioing K_∞ in the rodded condition to K_∞ in the non-rodded condition.

The second K_∞ multiplier accounts for the variation in the reactivity effect of control rods with changes in assembly burnup. The values of the second K_∞ multiplier are generated by depleting assemblies of various enrichments at constant soluble boron concentration and moderator temperature using the Vepco PDQ07 Discrete Model. At various burnup points, separate recovery cases

are performed during which control rods are inserted. To calculate the values of the multiplier, the ratio of K_∞ with the control rods to K_∞ without control rods at each burnup point is divided by the ratio of K_∞ with control rods to K_∞ without control rods at zero burnup.

The third K_∞ multiplier accounts for the dependence on cumulative burnup of fuel while control rods are present. The change in isotopics accompanying depletion of an assembly containing control rods can result in significant reactivity variations while the control rods are still in the assembly. While the input data for BP include this effect in the first K_∞ multiplier for BP (Section 3.2.2.2), a separate multiplier is used to represent this effect for control rods. To generate the values for this multiplier, assemblies of various enrichments are depleted with constant moderator temperature and soluble boron concentration in the following manner:

1) an assembly containing control rods is depleted to various burnups,
2) at these burnups, the control rods are removed and the assembly is depleted further,
3) recovery cases are performed at various burnup points in the non-rodded portion of the depletion for which the control rods are reinserted.

The values of the third K_∞ multiplier for control rods are obtained in two steps. First, for a particular combination of cumulative and total burnup, the value of K_∞ with control rods is divided by the value of K_∞ without control rods. Second, these values are divided by the ratio of K_∞ with and without control rods obtained at zero cumulative and zero total burnup.

3.2.3.3 K-Infinity Multiplier for the "After Effect" of Control Rods

The method by which the fourth K_∞ multiplier for control rods is generated is the same as the method described in Section 3.2.1.4 for the fourth

K_∞ multiplier for BP. First, an assembly is depleted without control rods using the Vepco PDQ07 Discrete Model. Second, an assembly of the same enrichment containing control rods is depleted to various burnups. Then the rods are removed, and the assembly is depleted further. The values of the fourth K_∞ multiplier for control rods are obtained by dividing K_∞ from the assembly which has had control rods by K_∞ of the assembly which has not had control rods present.

3.3 Thermal-Hydraulic Feedback Parameters

Thermal-hydraulic feedback effects are represented in the Vepco FLAME Model in order to more accurately calculate the power distribution. The thermal-hydraulic feedback model incorporated in the FLAME3 code is the same as the feedback model used in the PDQ07 code portion of the Vepco PDQ07 Discrete Model.[7] The input required consists of:

1) Coolant inlet enthalpy,
2) Heated perimeter per unit area of flow,
3) Flow area of the fuel assembly per total cross-sectional area of the assembly,
4) System pressure,
5) Difference between average fuel temperature and moderator temperature as a function of relative power density.

The feedback calculation is performed in the following manner. First, an initial estimate of the fuel and moderator temperatures is made for each coolant channel. Based on this estimate and the function tables supplied, the FLAME3 code calculates the K-infinity and the migration area for each node. These parameters are then used to calculate the power density in each node. This power distribution is used to compute new fuel and moderator temperatures for each channel. In turn, the new fuel and moderator temperatures are used to

calculate new K-infinities and migration areas for another power distribution calculation. This process is continued until the power density for each node in the Nth iteration differs from the power density in the N-1th iteration by less than the specified convergence criterion.

3.4 Xenon Concentration Calculation

The Vepco FLAME Model represents the xenon reactivity effect as a functional dependence of the basic K_∞ on xenon concentration (refer to Section 3.2.1.1). The xenon and iodine concentrations at each node are calculated using the parameters described in Section 3.2.1.3 and the assumption of constant flux and power throughout the duration of a time/burnup step. With the assumption of constant power and flux, the differential equations which describe the dependence of xenon and iodine concentration are solved by integration over the time step interval, Δt.

The nodal iodine concentration, $I_\ell(t)$ (atoms/barn-cm), is calculated with Equation 3.1:

$$I_\ell(t) = \frac{YI_\ell \cdot G1}{\lambda_I} - \left[\frac{YI_\ell \cdot G1}{\lambda_I} - I_\ell(t-\Delta t)\right] \cdot \exp(-\lambda_I \Delta t) \qquad (3.1)$$

where

$$G1 = \left(\frac{S_\ell \cdot P_{core} \cdot 10^{-24}}{A_\ell \cdot V_{core}}\right)\Bigg|_{t=t-\Delta t}$$

A_ℓ, YI_ℓ are given in Section 3.2.1.3,

P_{core} = core power (watts),

V_{core} = core volume (cm^3),

S_ℓ = relative power density at node ℓ,

λ_I = decay constant of Iodine-135.

The nodal xenon concentration, $X_\ell(t)$ (atoms/barn-cm), is calculated with Equation 3.2:

$$X_\ell(t) = \frac{(YI_\ell+YX_\ell)\cdot G1}{G2} - \frac{\lambda_I}{G2-\lambda_I}\cdot\left[\frac{YI_\ell\cdot G1}{\lambda_I} - I_\ell(t-\Delta t)\right]\cdot \exp(-\lambda_I\Delta t)$$
$$- \left\{\frac{(YI_\ell+YX_\ell)\cdot G1}{G2} - X_\ell(t-\Delta t)\right.$$
$$\left. - \frac{\lambda_I}{G2-\lambda_I}\cdot\left[\frac{YI_\ell\cdot G1}{\lambda_I} - I_\ell(t-\Delta t)\right]\right\}\cdot \exp(-G2\cdot\Delta t) \qquad (3.2)$$

where $G2 = \lambda_x + \sigma_{a\ell}^{Xe}(t-\Delta t)\cdot G1$,

$\sigma_{a\ell}^{Xe} = \sigma_{a2\ell}^{Xe}\cdot SIGM_\ell$ = thermal microscopic absorption cross section of Xenon-135 (barns),

λ_x = decay constant of Xenon-135,

YX_ℓ, $\sigma_{a2\ell}^{Xe}$, $SIGM_\ell$ are given in Section 3.2.1.3, and other parameters are as previously defined for Equation 3.1.

SECTION 4 - CALCULATIONAL TECHNIQUES

4.1 Power Distribution Normalization

The FLAME3 code provides two means by which the predicted power distribution may be normalized to the results of either measurements or another calculational model (e.g., Vepco PDQ07 Discrete Model). The two normalization factors which may be used are 1) leakage parameters (radial and/or axial albedoes) and 2) migration area multipliers.

For FLAME3 calculations, all the nodes modeled are inside the core. The presence of the reflector is represented by leakage parameters (albedoes) which may be input for peripheral nodes.

The migration area multiplier is intended to correct a limitation in the FLARE neutron source option. This limitation arises from the inability of the FLARE option to account for spectral effects in assemblies containing burnable poison or control rods. The result of this limitation is that the power may be somewhat underpredicted in these assemblies. The migration area multiplier may also be used to "fine-tune" the radial power distribution of interior located assemblies that do not necessarily contain burnable poison.

4.1.1 Radial Power Distribution

The radial power distribution calculated with the Vepco FLAME Model is normalized to the radial power distribution calculated with the Vepco PDQ07 Discrete Model. This normalization is generally accomplished by using a combination of radial albedoes and migration area multipliers. Radial albedoes are chosen so that the desired in-out power sharing and peripheral powers are given by the FLAME3 code. The migration area multipliers are used to "fine tune" the radial power distribution at interior assembly locations.

The radial power distribution is normalized for two sets of conditions. The first set of conditions consists of cycle depletion calculations where normalization is performed for the all rods out (ARO), hot full power (HFP) condition. The design objective is to maintain less than a 5% difference between the assemblywise radial powers computed by the Vepco FLAME and PDQ07 Discrete Models throughout each cycle. The reason for this 5% limit is to insure that acceptable burnup distributions will be calculated during depletion. For "short" (e.g., annual) cycles in which relatively little fresh BP is used, the normalization factors for beginning of cycle (BOC) generally yield acceptable radial power distributions throughout the cycle. However for "long" cycles (i.e., 18 month cycles) which contain large numbers of fresh fuel assemblies and BP rods, it is necessary to renormalize the in-out power sharing (i.e., change radial albedoes) at approximately the middle of cycle (MOC) to maintain acceptable agreement in radial power distribution.

The second set of conditions at which the radial power distribution is normalized is BOC, HZP with control banks C and D inserted in the core. The primary purpose for this normalization is to find the proper M^2 multiplier for control rodded assemblies. For cases at less than full power and with control rods inserted, the radial albedoes for HFP, ARO provide acceptable peripheral powers so that changing the peripheral albedoes at HZP is usually not required. The acceptance criterion of 5% difference between the Vepco FLAME and PDQ07 Discrete Models is relaxed for rodded cases in which no depletion is required (e.g., HZP and HFP rod worths), because variations in radial power distribution have been demonstrated to have little affect on the axial information calculated with the FLAME model.[11]

4.1.2 Axial Power Distribution

Normalization of the axial power distribution calculated by the FLAME model is required only for zero or part power cases of annual cycles containing little fresh BP. In these cases, a generic value of the axial albedo gives close agreement between measured and calculated axial power distributions for HZP. For part power situations, the axial albedo is taken to be a percentage of the HZP value.

4.2 Differential and Integral Control Rod Worths as a Function of Bank Position

Differential and integral control rod worths are calculated with the Vepco FLAME Model in two steps. First, a series of cases is run with the FLAME3 code in which all reactor parameters are held constant except for the position of the rod bank(s) whose worth is to be determined. For example, if the differential and integral worths of control bank D are required, the following set of cases is analyzed:

1) all rods out

2) D bank inserted in the top node of the appropriate assemblies

3) D bank inserted in the top 2 nodes of the appropriate assemblies

n+1) D bank inserted in the top n nodes of the appropriate assemblies

last) D bank fully inserted into the core.

The change in core reactivity resulting from each movement of the rod bank(s) is a direct measure of the control rod bank(s) differential worth. The second step in the process of calculating bank worths is normalization to results from the Vepco PDQ07 Discrete Model. The discrete model is the production calculational model for determining total integral control rod worths. There-

fore, a normalization factor is applied to the results obtained with the FLAME3 code to assure that the total integral worth predicted by the Vepco FLAME Model is the same as that predicted by the Vepco PDQ07 Discrete Model.

Based on the methodology outlined above, the following equations are used to compute the rod worths:

$$\text{Differential Worth at Node 'i' (pcm/step)} = \frac{k^{i-1} - k^{i}}{k^{i-1} \times k^{i}} \times \frac{10^5}{SPN} \times N \qquad (4.1)$$

$$\text{Integral Worth at Node 'i' (pcm)} = \frac{k^{o} - k^{i}}{k^{o} \times k^{i}} \times 10^5 \times N \qquad (4.2)$$

where k^{o} = eigenvalue given by FLAME3 for the control bank out,

k^{i} = eigenvalue given by FLAME3 for the control bank inserted in the i^{th} node,

SPN = number of steps of control rod movement per node,

N = total integral worth from Vepco PDQ07 Discrete Model divided by total integral worth from Vepco FLAME Model.

SECTION 5 - RESULTS

5.1 Introduction

The purpose of this section is to demonstrate the predictive capability of the Vepco FLAME Model for calculations of axial power distributions, axial offsets, and differential and integral control rod worths. As explained in the previous section, the radial power distribution calculated with the Vepco FLAME Model is normalized to a 2-D (x, y) discrete power distribution calculated with the Vepco PDQ07 Discrete Model prior to initiating axially dependent calculations. Therefore, this section presents 1) typical radial power distribution comparisons between the Vepco FLAME Model (after normalization) and the PDQ07 Discrete Model, and 2) comparisons to measured data taken at the Surry Nuclear Power Stations for axial power distribution, axial offset, and differential and integral rod worths. The specific types of results compared are presented in Table 5-1.

5.2 Radial Power Distribution

As discussed in Section 4.1.1, radial power distributions calculated with the Vepco FLAME Model are normalized to 2-D (x, y) discrete model power distributions calculated at the ARO, HFP condition as a function of burnup. The power distribution comparisons given in Figures 5-1 through 5-4 for Surry 1, Cycle 1 and in Figures 5-5 through 5-8 for Surry 1, Cycle 4 are representative of the agreement obtained between the Vepco FLAME Model (after normalization) and the Vepco PDQ07 Discrete Model.

Normally, it is desirable to maintain the assemblywise agreement in radial power distribution to less than a 5% difference, but this "administrative" limit is usually relaxed if violations only occur infrequently in a small number of fuel assemblies. The reason for this limit is to ensure that the accumulated assemblywise burnup obtained during a cycle depletion will be acceptable. This limit may also be relaxed for power distributions associated

with non-depletion types of calculations (e.g., rod worths), since it has been demonstrated to have little impact based on sensitivity studies. (11)

5.3 Axial Power Distribution

Axial power distribution and axial offset comparisons between the Vepco FLAME Model and measurements are presented in this section for core conditions ranging from beginning-of-cycle (BOC) to end-of-cycle (EOC) at hot zero power (HZP) and hot full power (HFP).

In general, the Vepco Flame Model predictions attempted to simulate the actual core conditions in terms of power level, core burnup, and control rod position. However, for reasons of increased calculational efficiency, the Vepco FLAME Model does not explicitly represent the effect of spacer grids, nor can the control rod position be exactly specified (due to the limitations of the axial mesh spacing). However, the accuracy that is compromised for the increased calculational efficiency is not significant.

Representative axial power distribution comparisons are presented for Surry 1, Cycle 1, Surry 2, Cycle 3, Surry 1, Cycle 4 and Surry 2, Cycle 4. Figures 5-9 and 5-10 give the Surry 1, Cycle 1 core average axial power distribution at BOC, HZP for D-Bank partially inserted and near fully inserted, respectively. The axial power distribution of an individual assembly (B-8) containing a partially inserted control rod (same core conditions as for Figure 5-10) is provided in Figure 5-11. Surry 2, Cycle 3 axial power distribution comparisons are presented in Figures 5-12 and 5-13 at BOC, HZP conditions for ARO and D-bank inserted. Additionally, comparisons at HFP, ARO at approximately BOC, MOC, and EOC conditions are given in Figures 5-14 through 5-16. Similar comparisons for Surry 1 and 2 Cycles 4 are provided in Figures 5-17 through 5-20 and 5-21 through 5-23, respectively. Measured and predicted axial

offset comparisons are also indicated on Figures 5-9 through 5-23, as appropriate.

5.4 Differential And Integral Rod Worths

Results of the Vepco FLAME Model predictions and startup physics measurements for differential and integral control rod bank worths for the first four cycles of Surry Units No. 1 and 2 are presented in this section. It should be noted that Surry 2, Cycle 1 results are not given, since they are essentially identical to Surry 1, Cycle 1.

Figures 5-24 through 5-27 provide the Surry 1, Cycle 1 individual differential and integral bank worths for Banks D through A, respectively. Also worths for Banks D through B moving in 100 step overlap are given in Figure 5-28. For Cycles 2 and 3 of both Surry Units 1 and 2, only banks D and C control rod worths were measured during startup physics testing. These results for Surry 1, Cycle 2 and Surry 2, Cycle 3 are compared to Vepco FLAME Model predictions in Figures 5-29 through 5-32. Measurements taken for Banks D through A during the startup of Surry 1, Cycle 4 are compared with Vepco FLAME Model predictions in Figures 5-33 through 5-36 and in Figure 5-37 for the 100 step overlap mode. Similar comparisons for Surry 2, Cycle 4 are displayed in Figures 5-38 through 5-42.

TABLE 5-1
SUMMARY OF COMPARISONS

Type of Comparison	Reactor Condition At Which Comparision Is Made	Reference To Figure
Radial Power Distribution		
	Unit 1, Cycle 1, HZP, ARO, BOC	5-1
	Unit 1, Cycle 1, HFP, ARO, BOC	5-2
	Unit 1, Cycle 1, HFP, ARO, MOC	5-3
	Unit 1, Cycle 1, HFP, ARO, EOC	5-4
	Unit 1, Cycle 4, HZP, ARO, BOC	5-5
	Unit 1, Cycle 4, HFP, ARO, BOC	5-6
	Unit 1, Cycle 4, HFP, ARO, MOC	5-7
	Unit 1, Cycle 4, HFP, ARO, EOC	5-8
Axial Power Distribution		
	Unit 1, Cycle 1, HZP, D@ 204, 70 HWD/MTU	5-9
	Unit 1, Cycle 1, HZP, D@ 26, 70 MWD/MTU	5-10
	Unit 1, Cycle 1, HZP, D@ 26, 70 MWD/MTU Assembly B-8	5-11
	Unit 2, Cycle 3, HZP, D@ 202, 0 MWD/MTU	5-12
	Unit 2, Cycle 3, HZP, D in, 0 MWD/MTU	5-13
	Unit 2, Cycle 3, HFP, D@ 219, 150 MWD/MTU	5-14
	Unit 2, Cycle 3, HFP, D@ 221, 3920 MWD/MTU	5-15
	Unit 2, Cycle 3, HFP, ARO, 7740 MWD/MTU	5-16
	Unit 1, Cycle 4, HZP, D@ 220, 0 MWD/MTU	5-17
	Unit 1, Cycle 4, HFP, D@ 215, 150 MWD/MTU	5-18
	Unit 1, Cycle 4, HFP, D@ 206, 7715 MWD/MTU	5-19
	Unit 1, Cycle 4, HFP, D@ 220, 12585 MWD/MTU	5-20
	Unit 2, Cycle 4, HZP, ARO, 0 MWD/MTU	5-21
	Unit 2, Cycle 4, HFP, ARO, 204 MWD/MTU	5-22
	Unit 2, Cycle 4, HFP, D@ 210, 6986 MWD/MTU	5-23
Differential and Integral Rod Worths		
	Unit 1, Cycle 1, HZP, BOC, D-Bank	5-24
	Unit 1, Cycle 1, HZP, BOC, C-Bank	5-25
	Unit 1, Cycle 1, HZP, BOC, B-Bank	5-26
	Unit 1, Cycle 1, HZP, BOC, A-Bank	5-27
	Unit 1, Cycle 1, HZP, BOC, B through D in 100 step overlap mode	5-28
	Unit 1, Cycle 2, HZP, BOC, D-Bank	5-29
	Unit 1, Cycle 2, HZP, BOC, C-Bank	5-30
	Unit 2, Cycle 3, HZP, BOC, D-Bank	5-31
	Unit 2, Cycle 3, HZP, BOC, C-Bank	5-32
	Unit 1, Cycle 4, HZP, BOC, D-Bank	5-33
	Unit 1, Cycle 4, HZP, BOC, C-Bank	5-34
	Unit 1, Cycle 4, HZP, BOC, B-Bank	5-35
	Unit 1, Cycle 4, HZP, BOC, A-Bank	5-36

TABLE 5-1
SUMMARY OF COMPARISONS (Continued)

Type of Comparison	Reactor Condition At Which Comparison is Made	Reference To Figures
Differential and Integral Rod Worths (cont.)		
	Unit 1, Cycle 4, HZP, BOC, A through D in 100 step overlap mode	5-37
	Unit 2, Cycle 4, HZP, BOC, D-Bank	5-38
	Unit 2, Cycle 4, HZP, BOC, C-Bank	5-39
	Unit 2, Cycle 4, HZP, BOC, B-Bank	5-40
	Unit 2, Cycle 4, HZP, BOC, A-Bank	5-41
	Unit 2, Cycle 4, HZP, BOC, A through D in 100 step overlap mode	5-42

FIGURE 5-1

RADIAL POWER DISTRIBUTION COMPARISON
FOR SURRY 1, CYCLE 1, HZP, ARO, BOC

	08	09	10	11	12	13	14	15
H	1.158 1.1895 +2.7							
J	1.243 1.2971 +4.4	1.144 1.1708 +2.3						
K	1.134 1.1550 +1.9	1.214 1.2563 +3.5	1.098 1.1098 +1.1					
L	1.197 1.2279 +2.6	1.097 1.1031 +0.6	1.143 1.1640 +1.8	0.998 0.9896 -0.8				
M	1.084 1.0748 -0.8	1.154 1.1630 +0.8	1.019 1.0027 -1.6	0.990 0.9941 +0.4	0.774 0.7630 +1.4			
N	1.144 1.1342 -0.9	1.047 1.0208 -2.5	1.047 1.0525 +0.5	0.943 0.9230 -2.1	0.626 0.6109 -2.4			
P	0.995 0.9809 -1.4	1.103 1.0929 -0.9	0.975 0.9580 -1.7	0.625 0.6108 -2.3				
R	0.872 0.8564 -1.8	0.657 0.6445 -1.9						

PDQ07
FLAME
Δ%

FIGURE 5-2

RADIAL POWER DISTRIBUTION COMPARISON
FOR SURRY 1, CYCLE 1, HFP, ARO, BOC

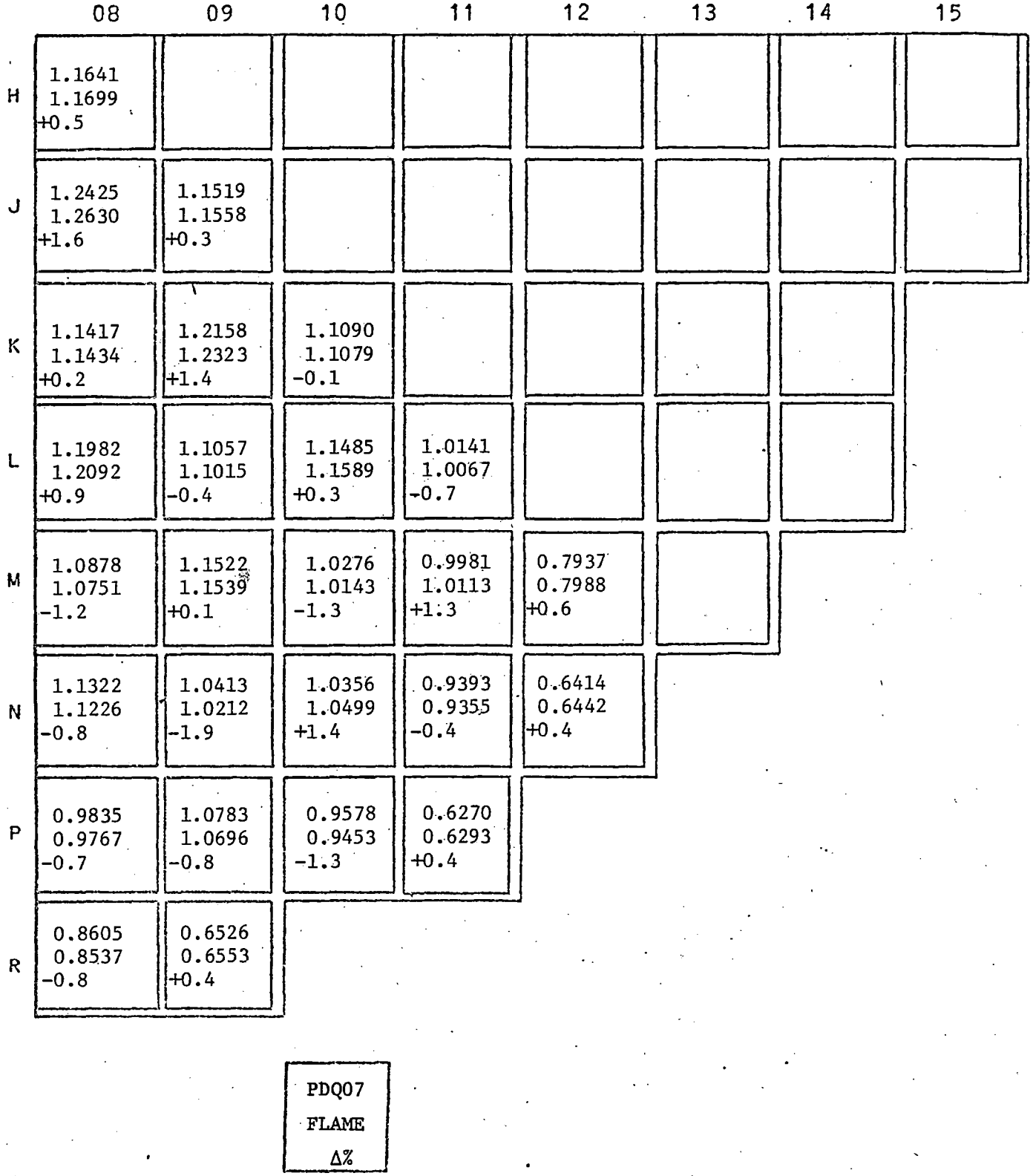

FIGURE 5-3

RADIAL POWER DISTRIBUTION COMPARISON
FOR SURRY 1, CYCLE 1, HFP, ARO, MOC

	08	09	10	11	12	13	14	15
H	1.1290 1.1330 +0.4							
J	1.2249 1.2288 +0.3	1.1273 1.1320 +0.4						
K	1.1248 1.1301 +0.5	1.2186 1.2238 +0.4	1.1155 1.1219 +0.6					
L	1.2095 1.2149 +0.4	1.1115 1.1174 +0.5	1.1901 1.1956 +0.5	1.0646 1.0710 +0.6				
M	1.0920 1.0961 +0.4	1.1773 1.1801 +0.2	1.0639 1.0647 +0.1	1.0772 1.0859 +0.8	0.8549 0.8639 +1.1			
N	1.1295 1.1271 -0.2	1.0332 1.0323 -0.1	1.0649 1.0733 +0.8	0.9825 0.9630 -2.0	0.6601 0.6571 -0.5			
P	0.9288 0.9309 +0.2	1.0140 0.9963 -1.7	0.8825 0.8747 -0.9	0.6152 0.6070 -0.9				
R	0.7427 0.7348 -1.1	0.5884 0.5865 -0.3						

PDQ07
FLAME
Δ %

FIGURE 5-4

RADIAL POWER DISTRIBUTION COMPARISON
FOR SURRY 1, CYCLE 1, HFP, ARO, EOC

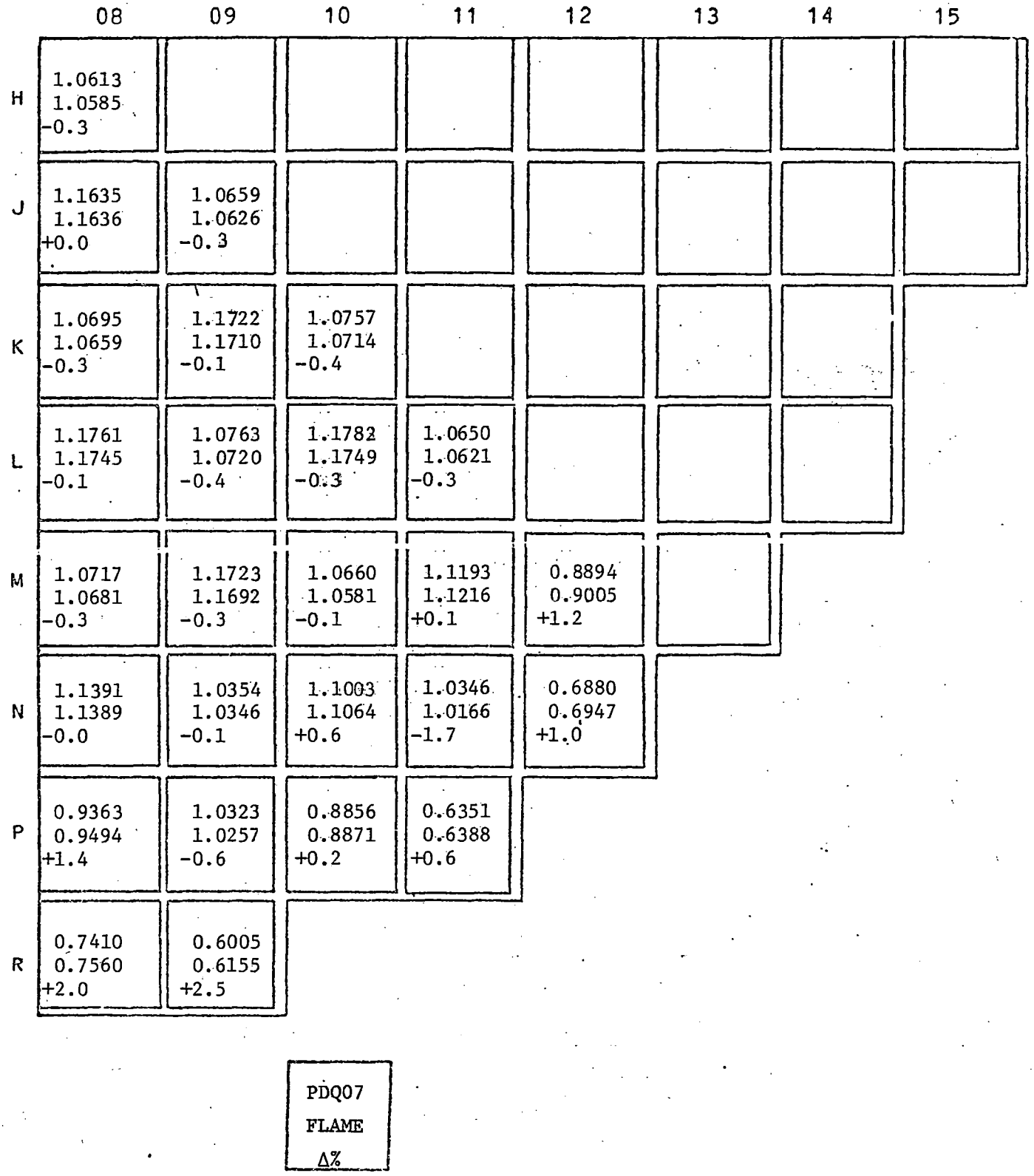

FIGURE 5-5

RADIAL POWER DISTRIBUTION COMPARISON
FOR SURRY 1, CYCLE 4, HZP, ARO, BOC

	08	09	10	11	12	13	14	15
H	0.783 0.7635 -2.5							
J	1.039 1.0722 +3.2	1.088 1.1422 +5.0						
K	0.907 0.8911 -1.8	1.028 1.0454 +1.7	1.096 1.0651 -2.8					
L	1.036 1.0229 -1.3	1.101 1.1211 +1.8	1.083 1.0873 +0.4	1.157 1.1509 -0.5				
M	1.113 1.0890 -2.2	1.078 1.0606 -1.6	1.153 1.1539 +0.1	1.108 1.1145 +0.6	1.029 1.0391 +1.0			
N	0.954 0.9242 -3.1	1.208 1.1702 -3.1	1.078 1.0577 -1.9	1.030 1.0339 +0.4	0.689 0.6967 +1.0			
P	1.075 1.0302 -4.2	1.091 1.1194 +2.6	0.967 0.9837 +1.7	0.634 0.6421 +1.3				
R	0.810 0.8057 -0.5	0.627 0.6268 -0.0						

PDQ07
FLAME
Δ%

FIGURE 5-6

RADIAL POWER DISTRIBUTION COMPARISON
FOR SURRY 1, CYCLE 4, HFP, ARO, BOC

	08	09	10	11	12	13	14	15
H	0.820 0.8139 -0.7							
J	1.067 1.0962 +2.7	1.108 1.1489 +3.7						
K	0.930 0.9300 0.0	1.040 1.0616 +2.1	1.097 1.0737 -2.1					
L	1.037 1.0347 -0.2	1.093 1.1097 +1.5	1.071 1.0785 +0.7	1.132 1.1194 -1.1				
M	1.103 1.0886 -1.3	1.061 1.0478 -1.2	1.130 1.1246 -0.5	1.085 1.0837 -0.1	1.018 1.0197 +0.2			
N	0.954 0.9419 -1.3	1.190 1.1470 -3.6	1.068 1.0494 -1.7	1.027 1.0242 -0.3	0.701 0.7132 +1.7			
P	1.082 1.0394 -3.9	1.093 1.1087 +1.4	0.976 0.9839 +0.8	0.652 0.6656 +2.1				
R	0.837 0.8379 +0.1	0.653 0.6604 +1.1						

PDQ07
FLAME
Δ%

FIGURE 5-7

RADIAL POWER DISTRIBUTION COMPARISON
FOR SURRY 1, CYCLE 4, HFP, ARO, MOC

	08	09	10	11	12	13	14	15
H	0.937 0.9228 -1.5							
J	1.233 1.1850 -2.9	1.198 1.2102 +1.0						
K	1.057 1.0261 -2.9	1.238 1.1947 -3.5	1.175 1.1356 -3.4					
L	1.212 1.1649 -3.9	1.212 1.2233 +0.9	1.202 1.1796 -1.9	1.117 1.1374 +1.8				
M	1.085 1.0793 -0.5	1.103 1.1046 +0.1	1.106 1.1332 +2.5	1.067 1.0890 +2.1	0.938 0.9728 +3.7			
N	0.877 0.8779 +0.1	1.069 1.0868 +1.7	1.070 1.0641 -0.6	1.001 1.0087 +0.8	0.662 0.6742 +1.8			
P	0.913 0.9004 -1.4	0.979 0.9940 +1.5	0.868 0.8812 +1.5	0.613 0.6169 +0.6				
R	0.701 0.7012 +0.0	0.567 0.5640 -0.5						

PDQ07
FLAME
Δ%

FIGURE 5-8

RADIAL POWER DISTRIBUTION COMPARISON
FOR SURRY 1, CYCLE 4, HFP, ARO, EOC

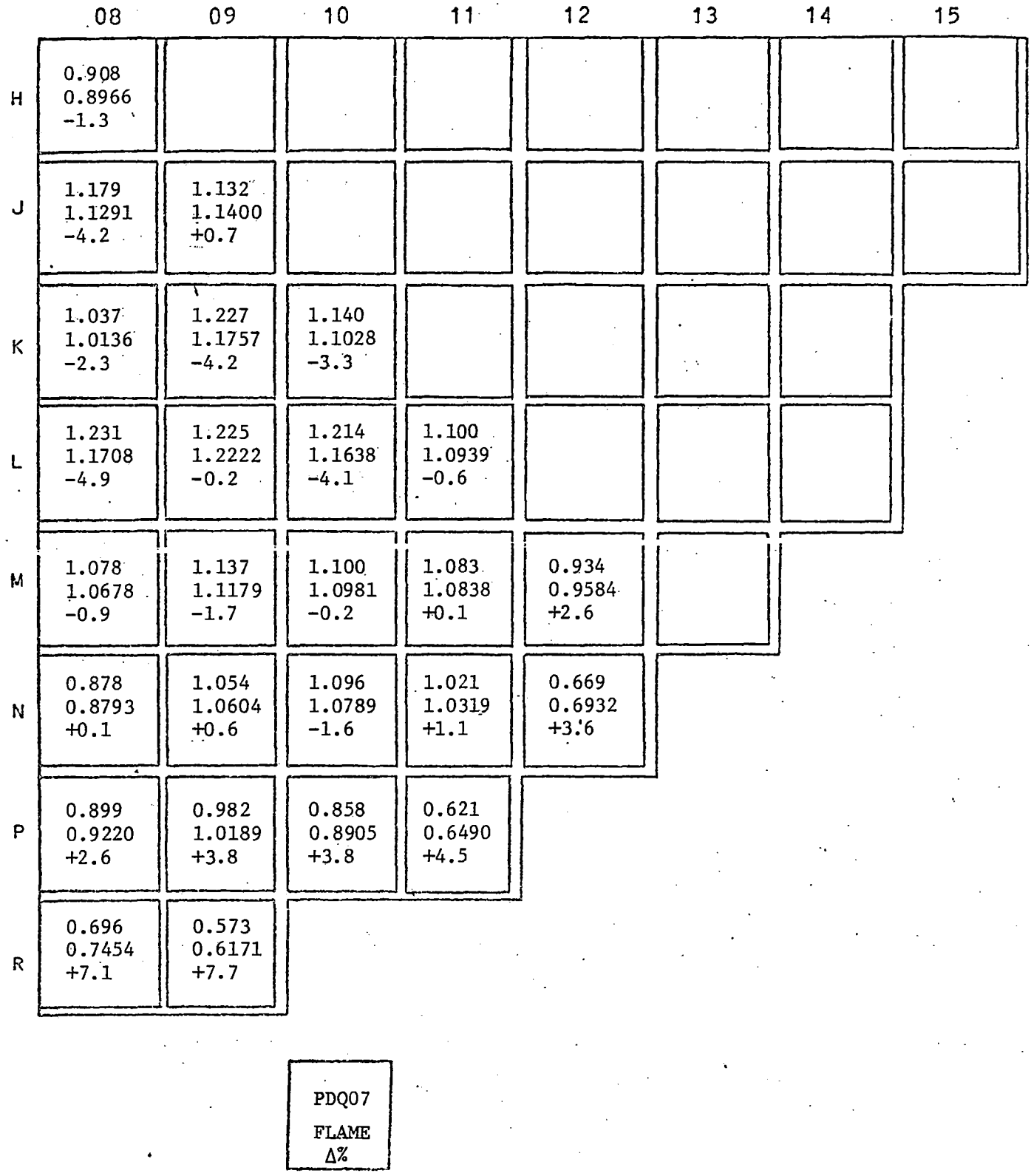

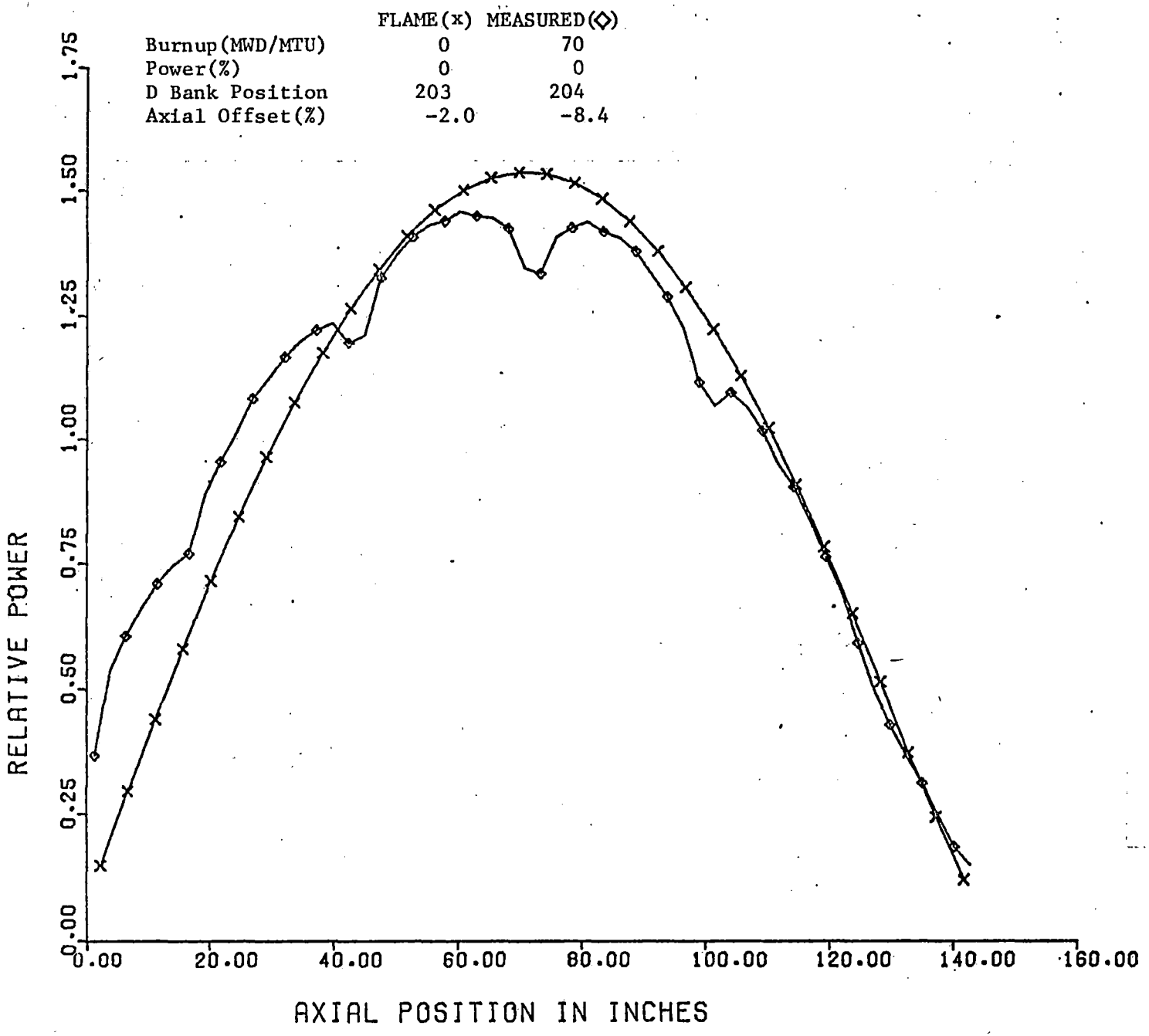

Figure 5-9

Core Average Axial Power Distribution Comparison
for Surry 1, Cycle 1, BOC,
HZP, ARO

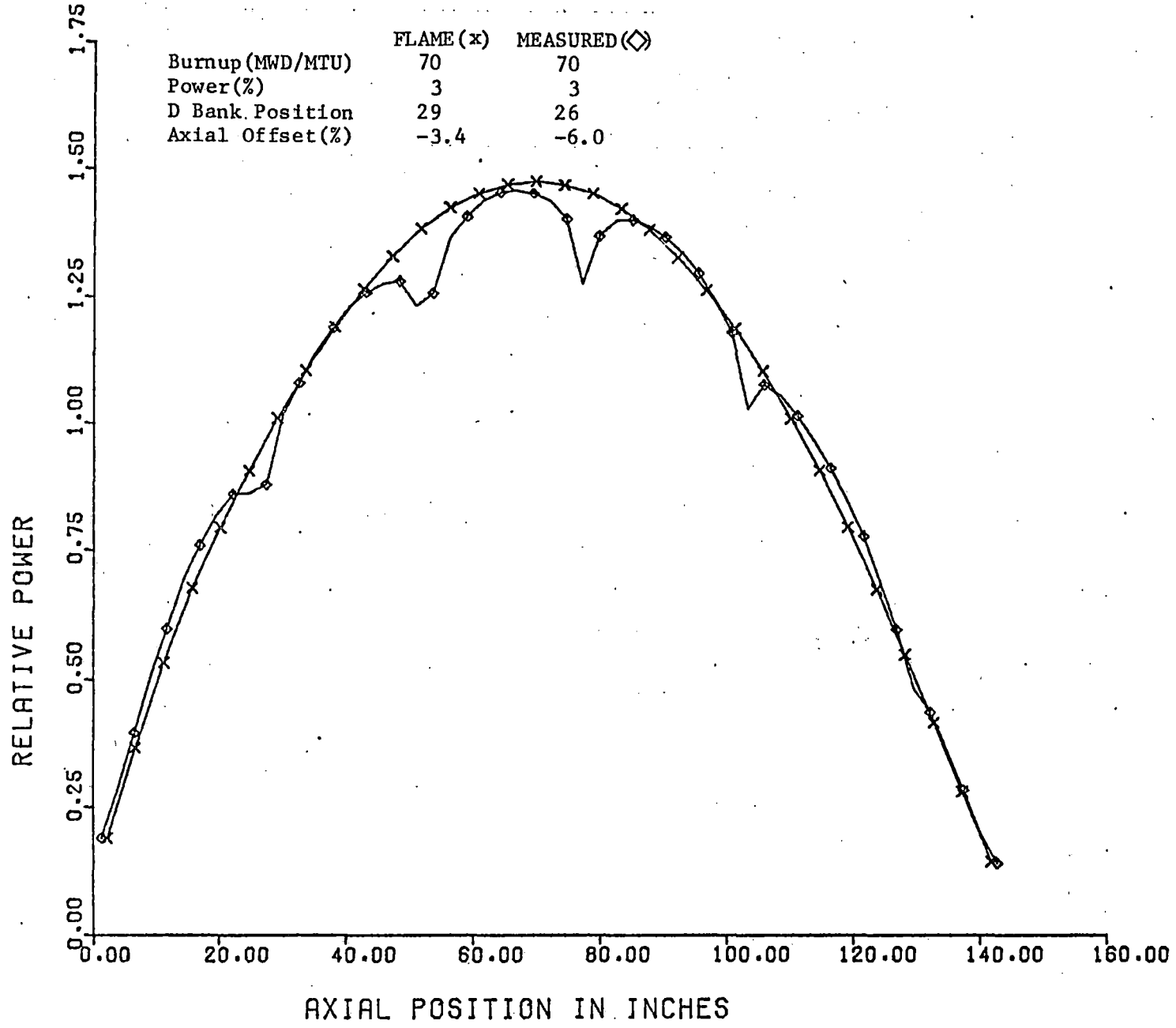

FIGURE 5-10

Core Average Axial Power Distribution Comparison
for Surry 1, Cycle 1, BOC,
HZP, D Bank In

FIGURE 5-11

Assembly B-8 Axial Power Distribution Comparison
Surry 1, Cycle 1, BOC,
HZP, D Bank In

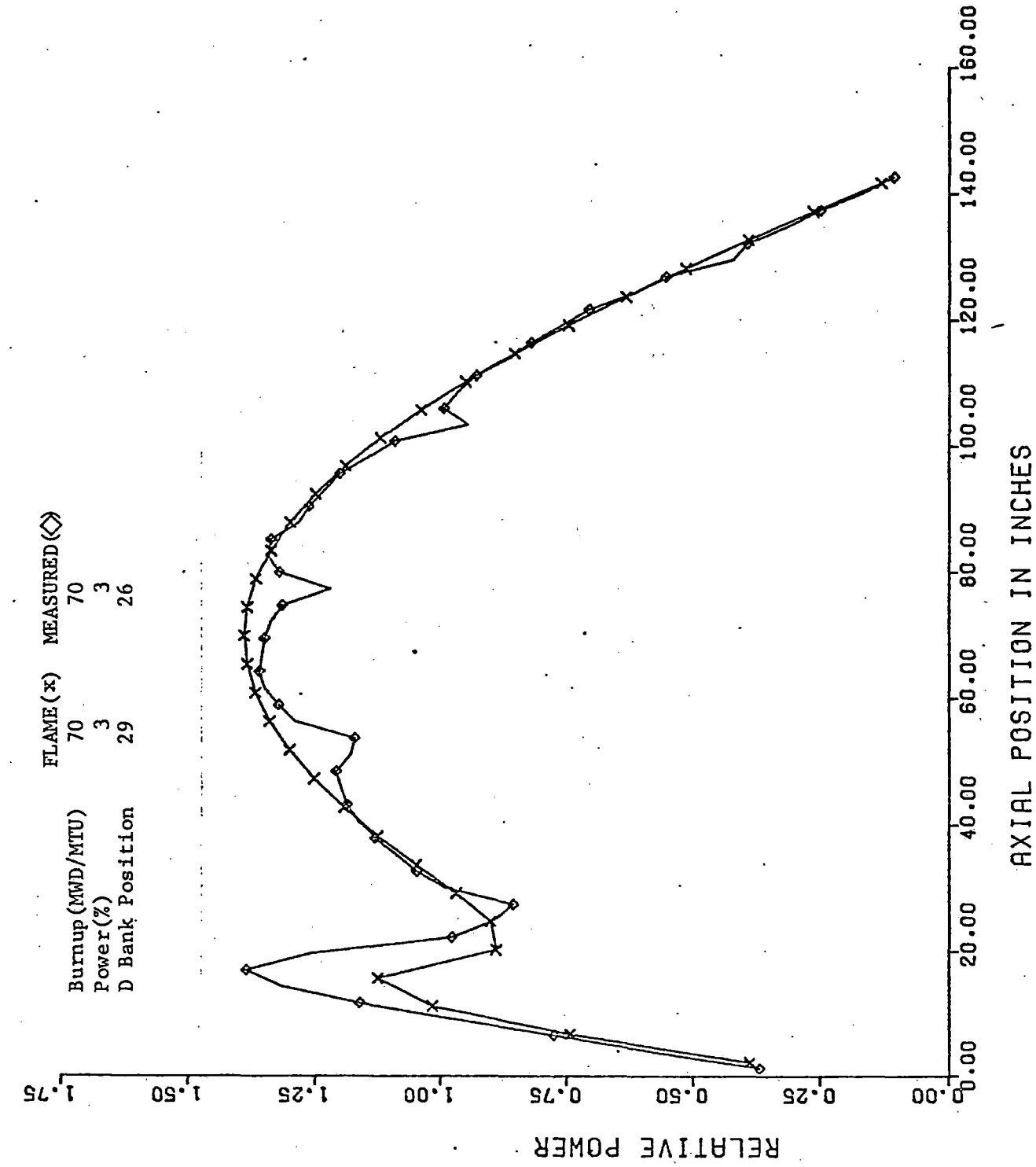

FIGURE 5-12

Core Average Axial Power Distribution Comparison
Surry 2, Cycle 3, BOC,
HZP, ARO

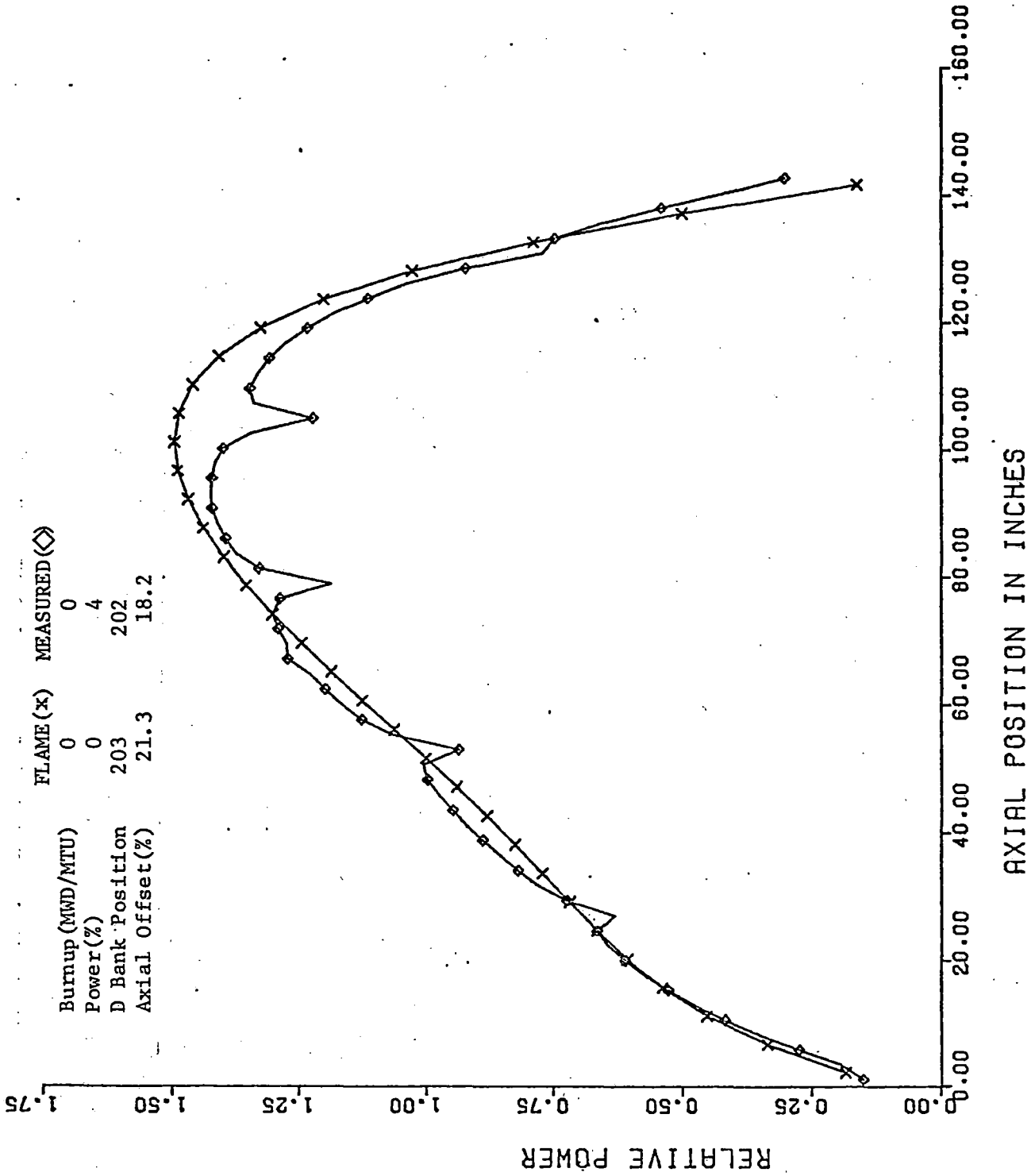

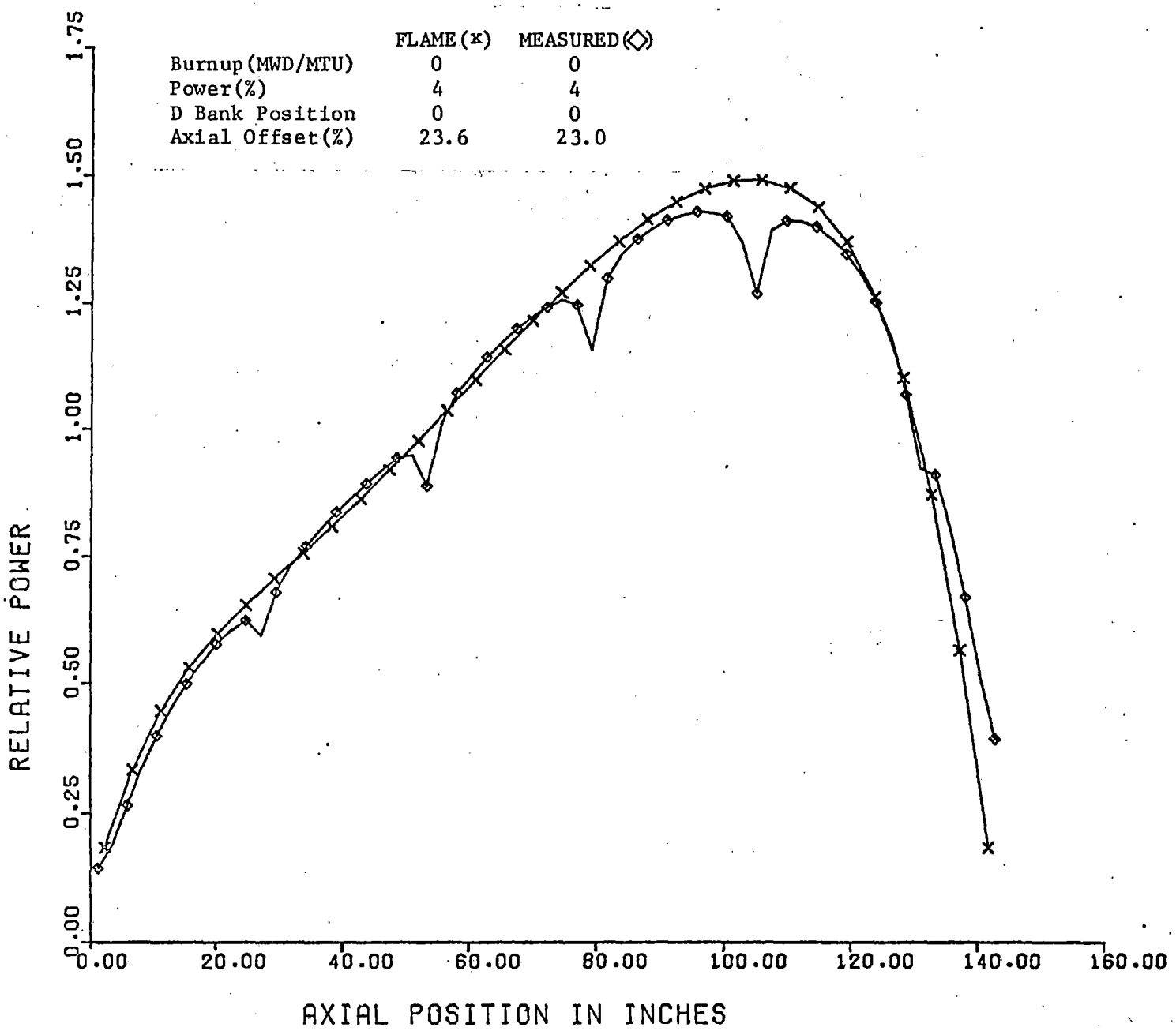

FIGURE 5-13

Core Average Axial Power Distribution Comparison
Surry 2, Cycle 3, BOC,
HZP, D Bank In

FIGURE 5-14

Core Average Axial Power Distribution Comparison
Surry 2, Cycle 3, BOC,
HFP, ARO

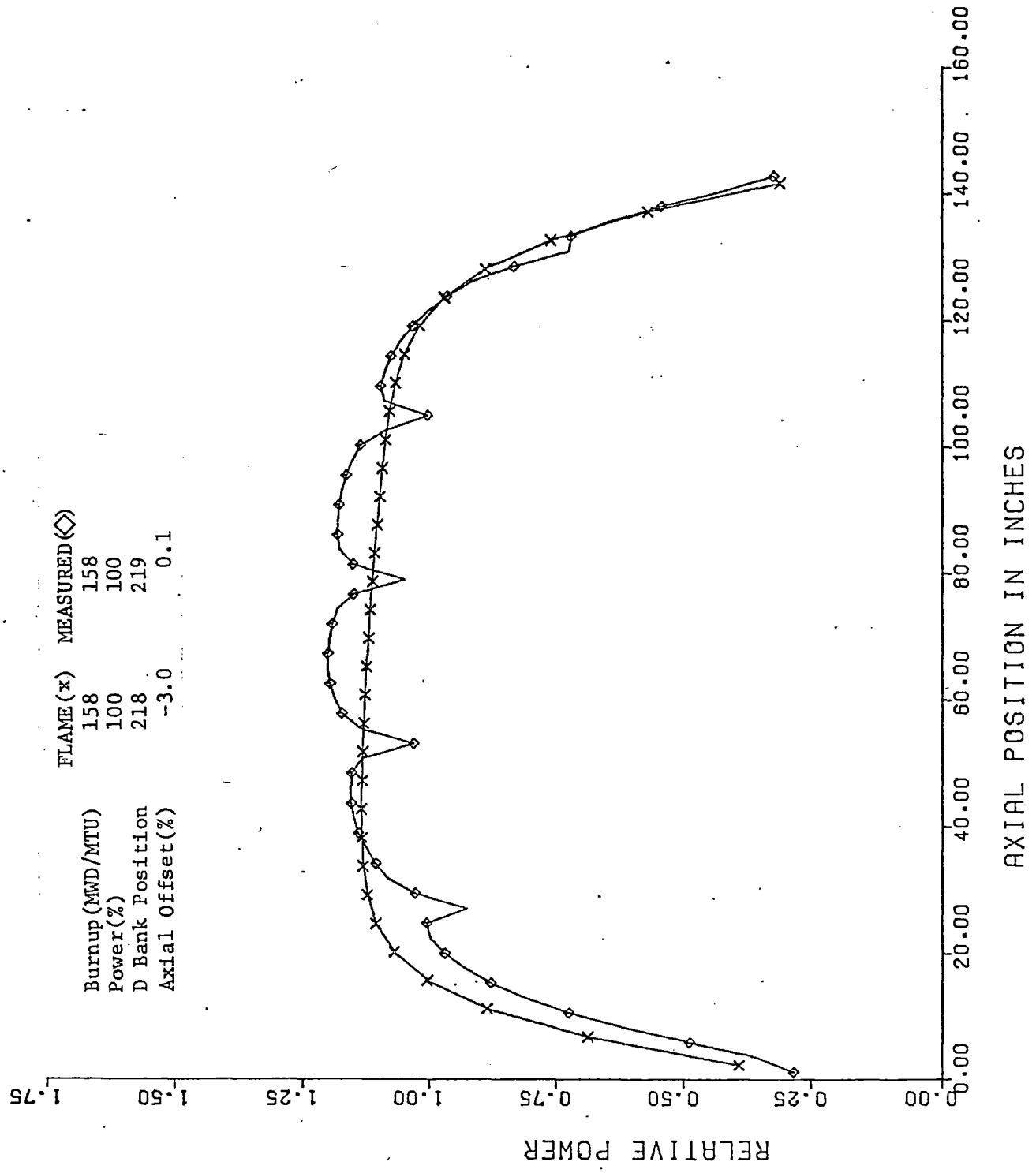

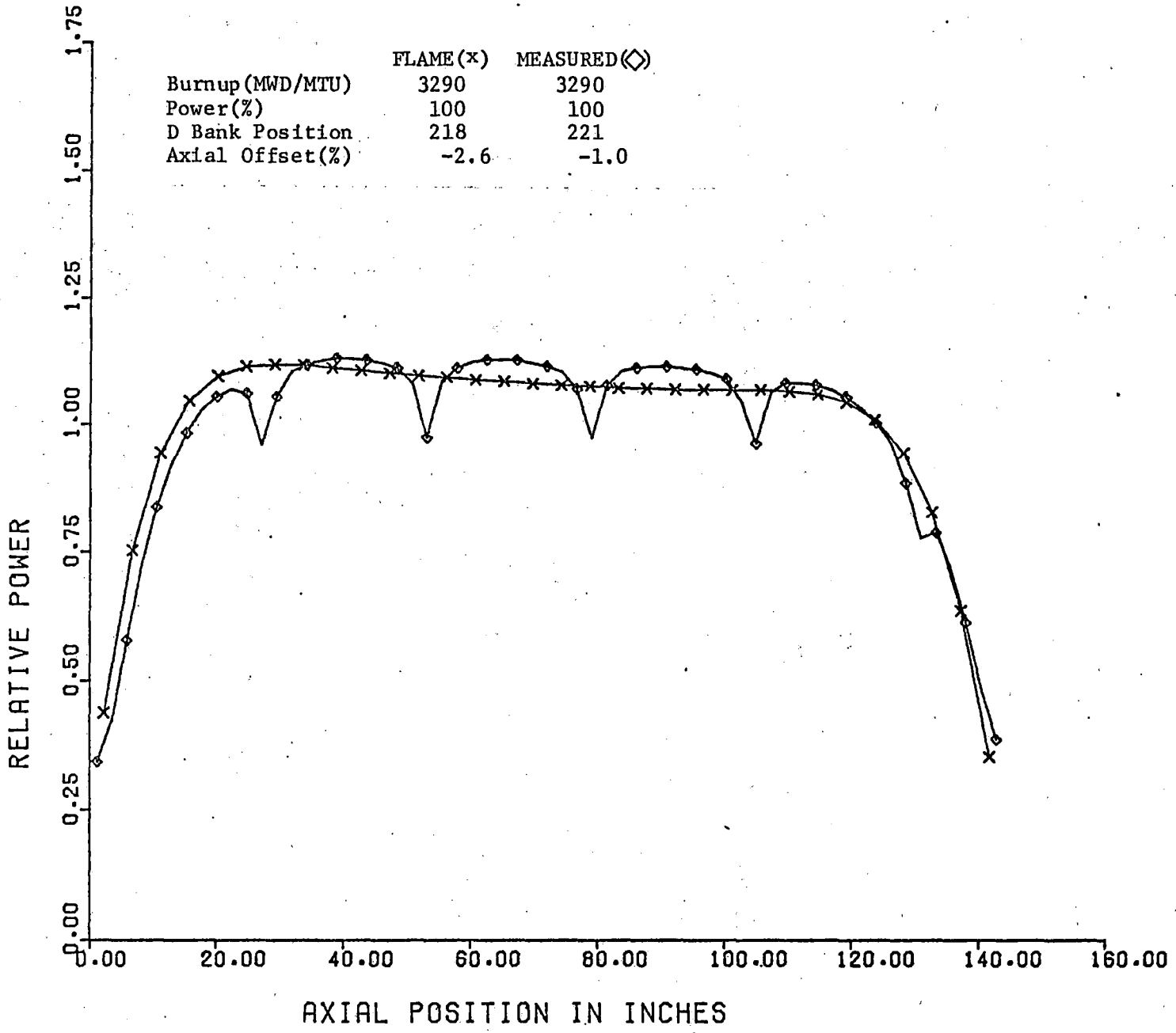

FIGURE 5-15

Core Average Axial Power Distribution Comparison
for Surry 2, Cycle 3, MOC,
HFP, ARO

FIGURE 5-16

Core Average Axial Power Distribution Comparison
for Surry 2, Cycle 3, EOC,
HFP, ARO

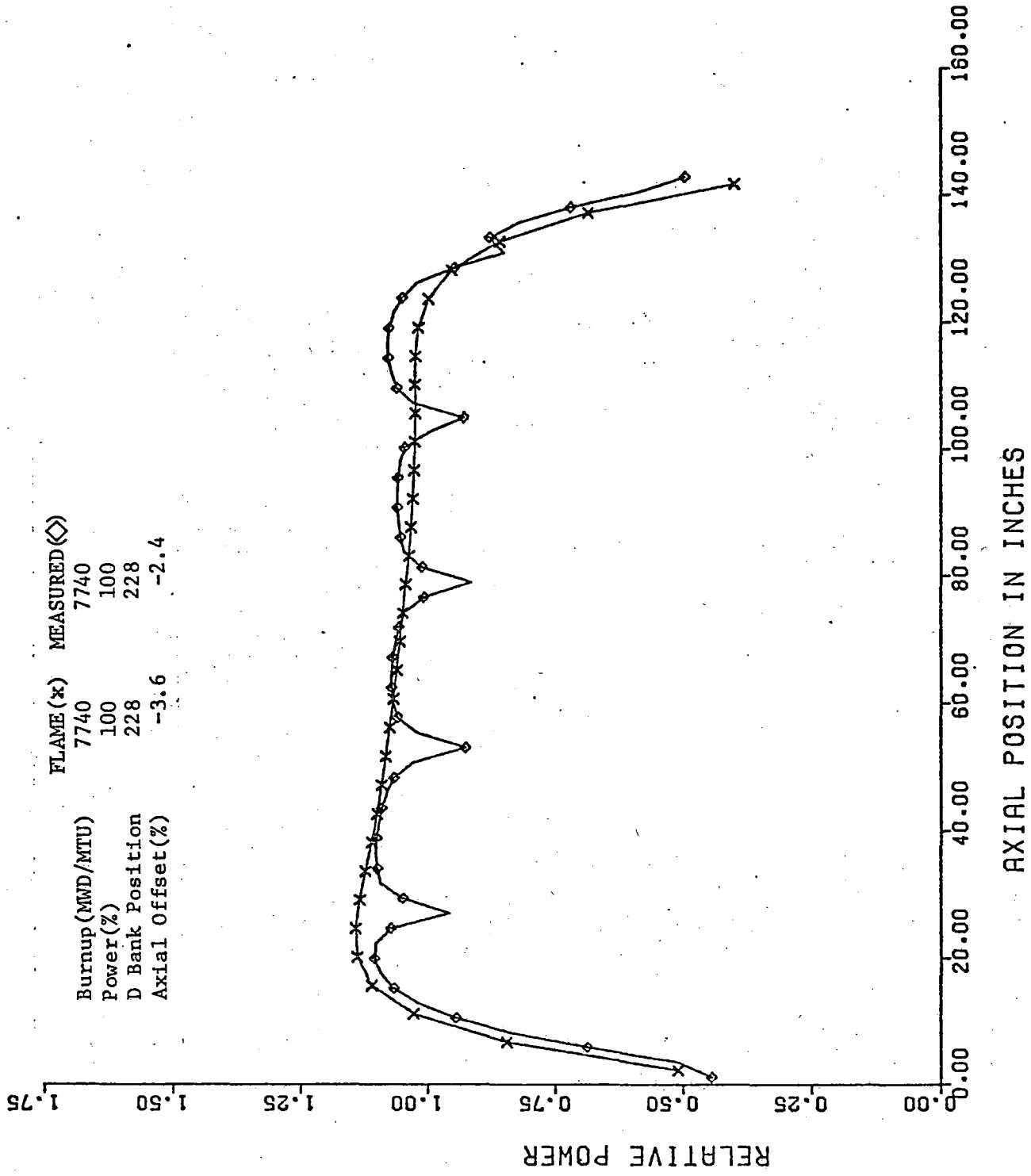

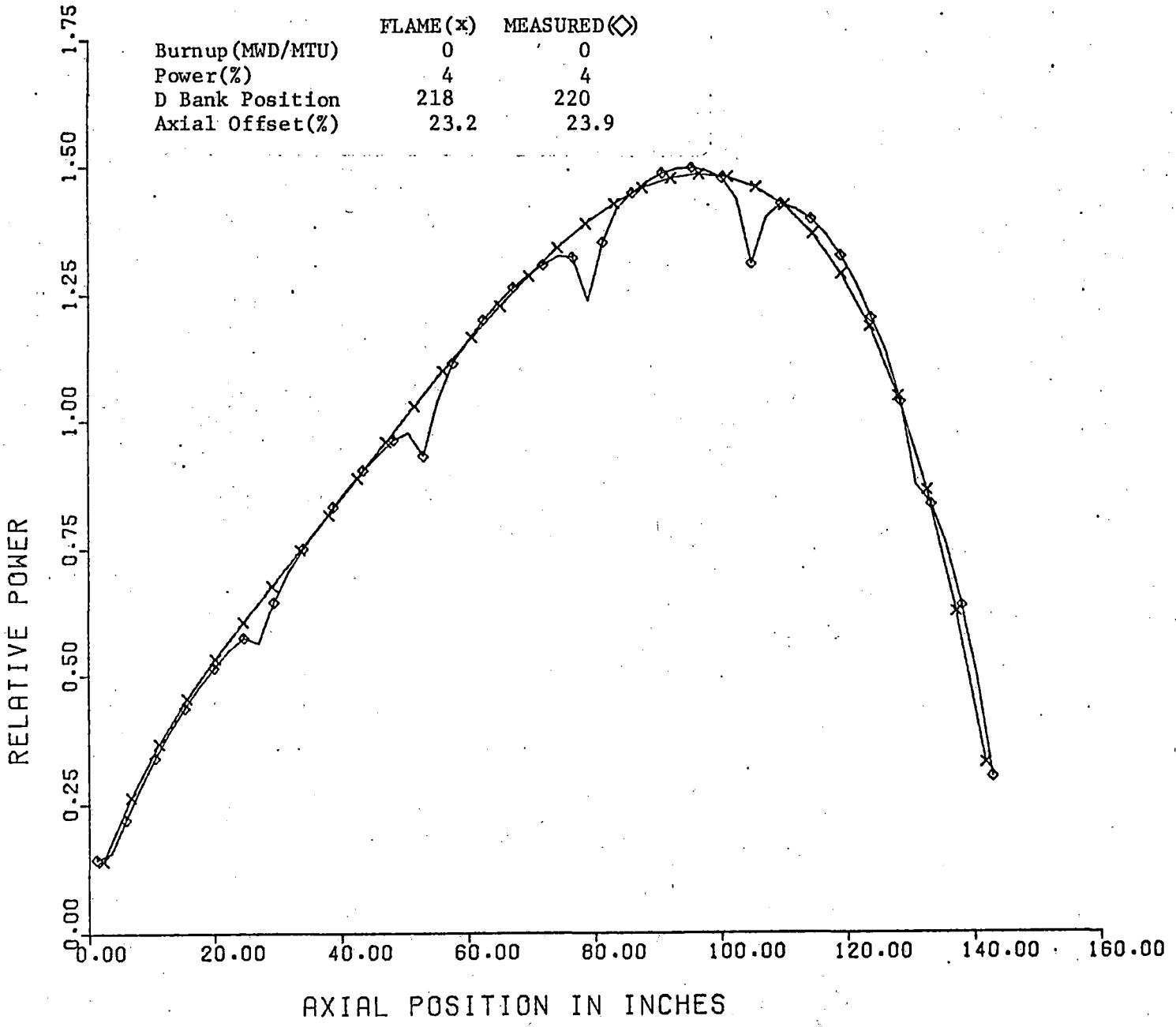

Core Average Axial Power Distribution Comparison
Surry 1, Cycle 4, BOC,
HZP, ARO

FIGURE 5-17

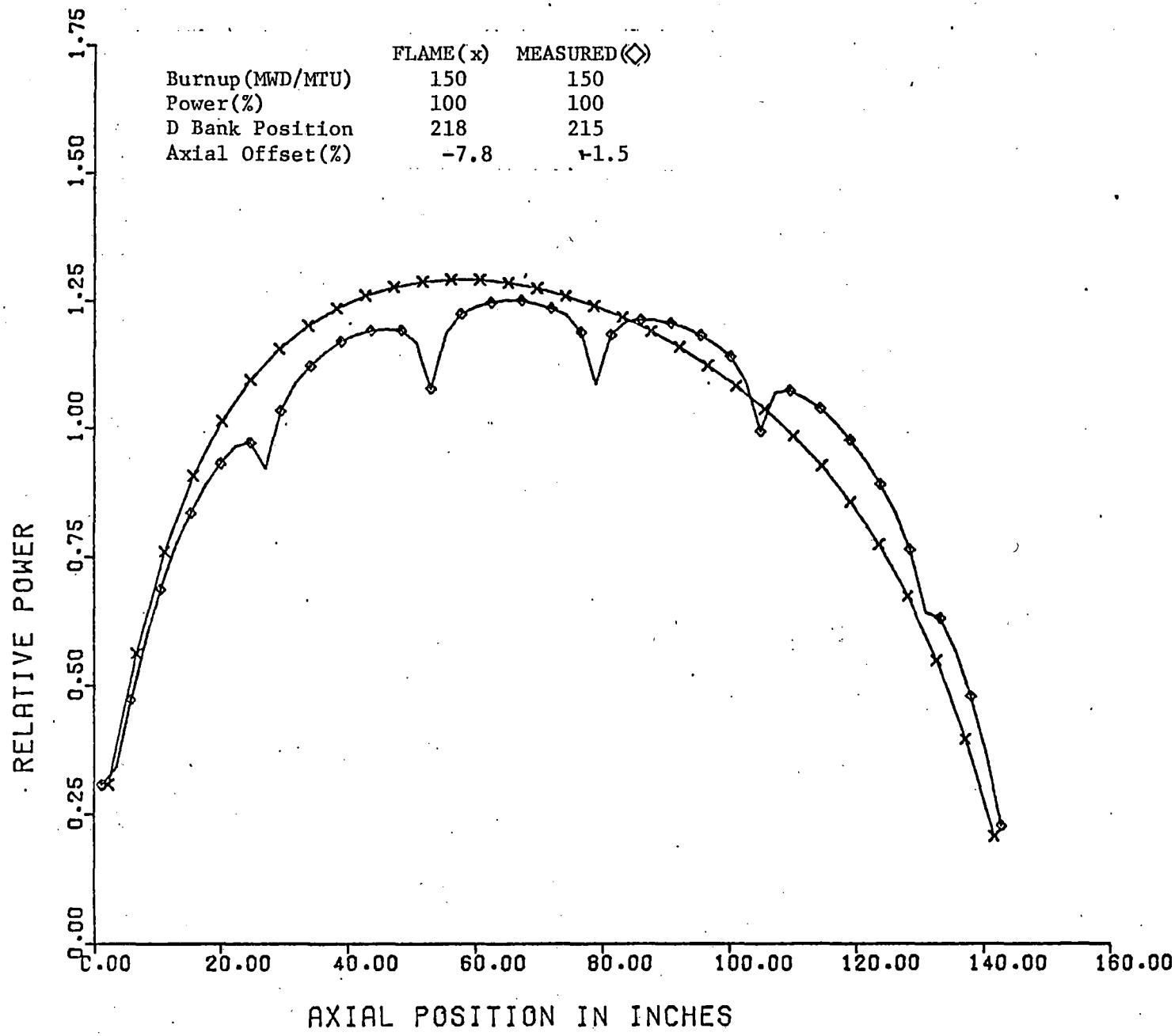

FIGURE 5-18

Core Average Axial Power Distribution Comparison for Surry 1, Cycle 4, BOC, HFP, ARO

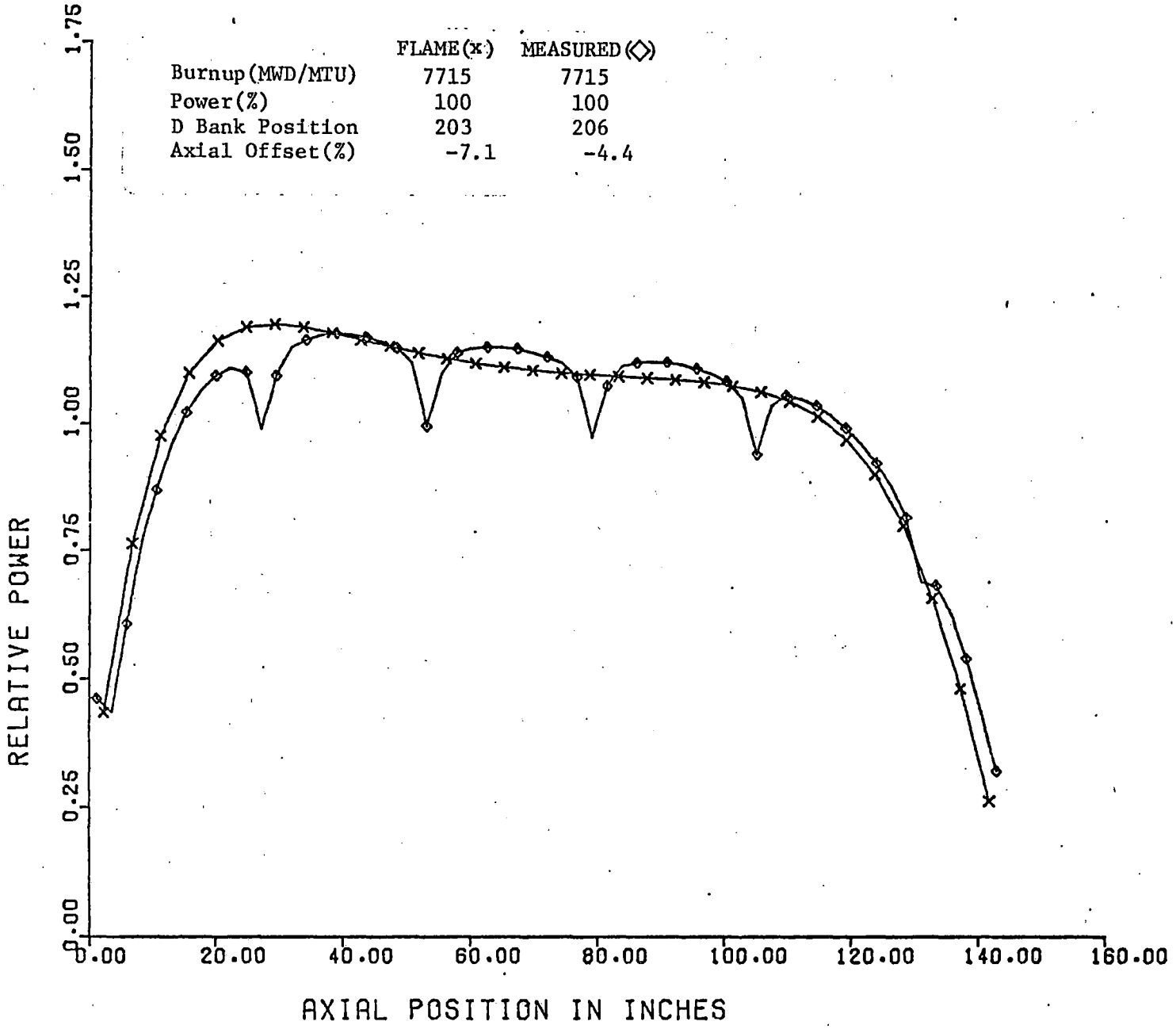

FIGURE 5-19

Core Average Axial Power Distribution Comparison
for Surry 1, Cycle 4, MOC,
HFP, ARO

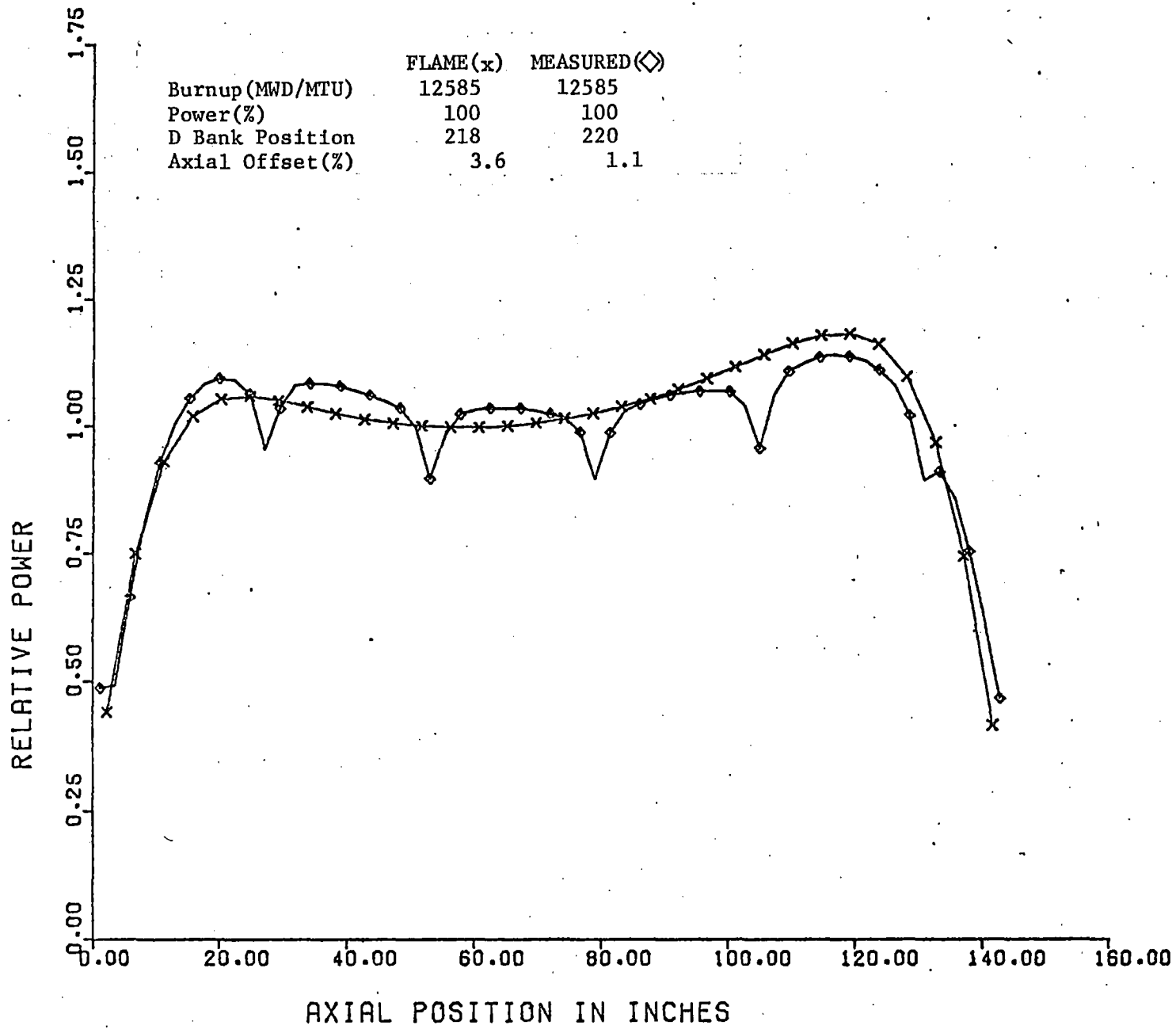

Core Average Axial Power Distribution Comparison
for Surry 1, Cycle 4, EOC,
HFP, ARO

FIGURE 5-20

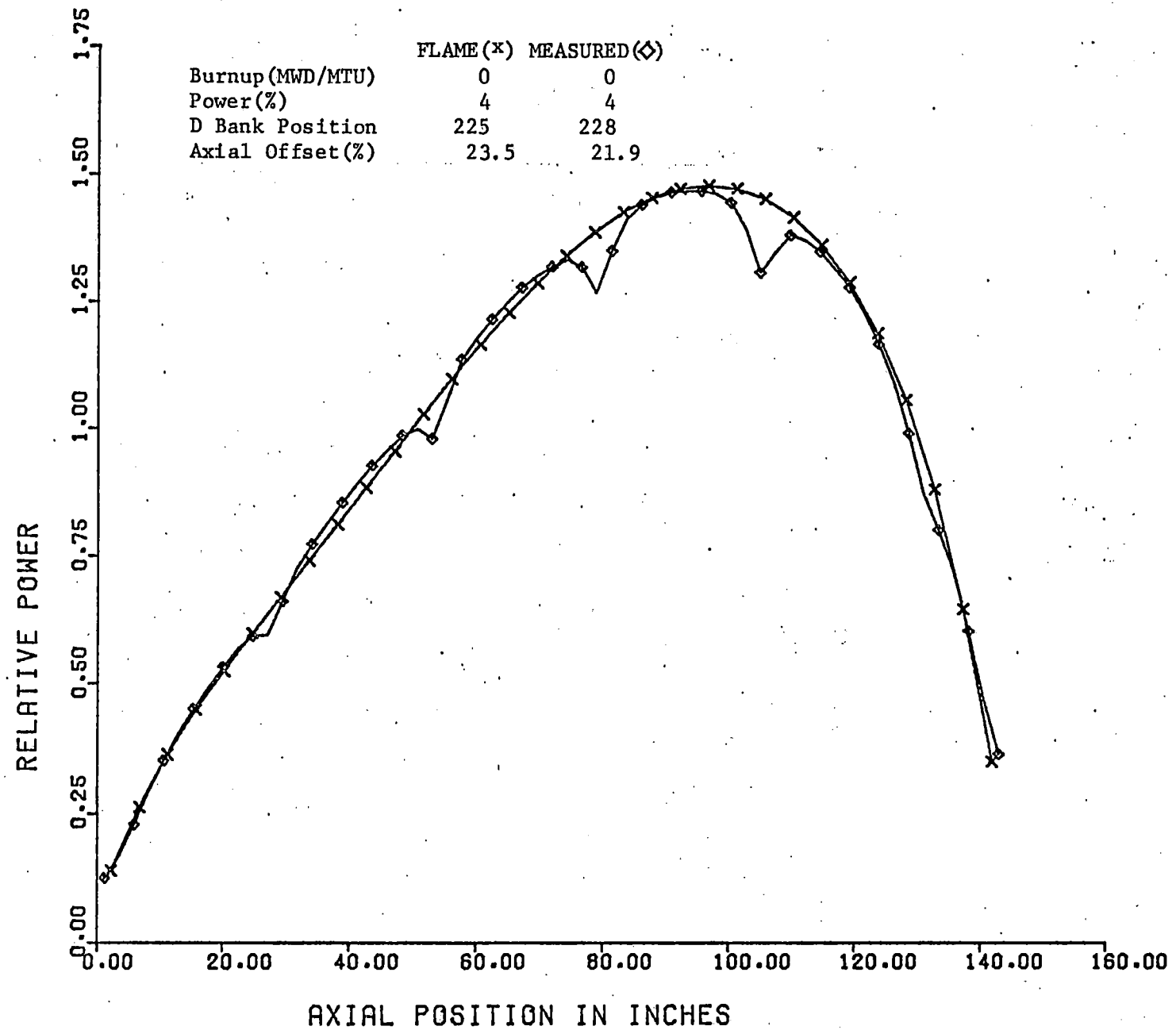

FIGURE 5-21

Core Average Axial Power Distribution Comparison
for Surry 2, Cycle 4, BOC,
HZP, ARO

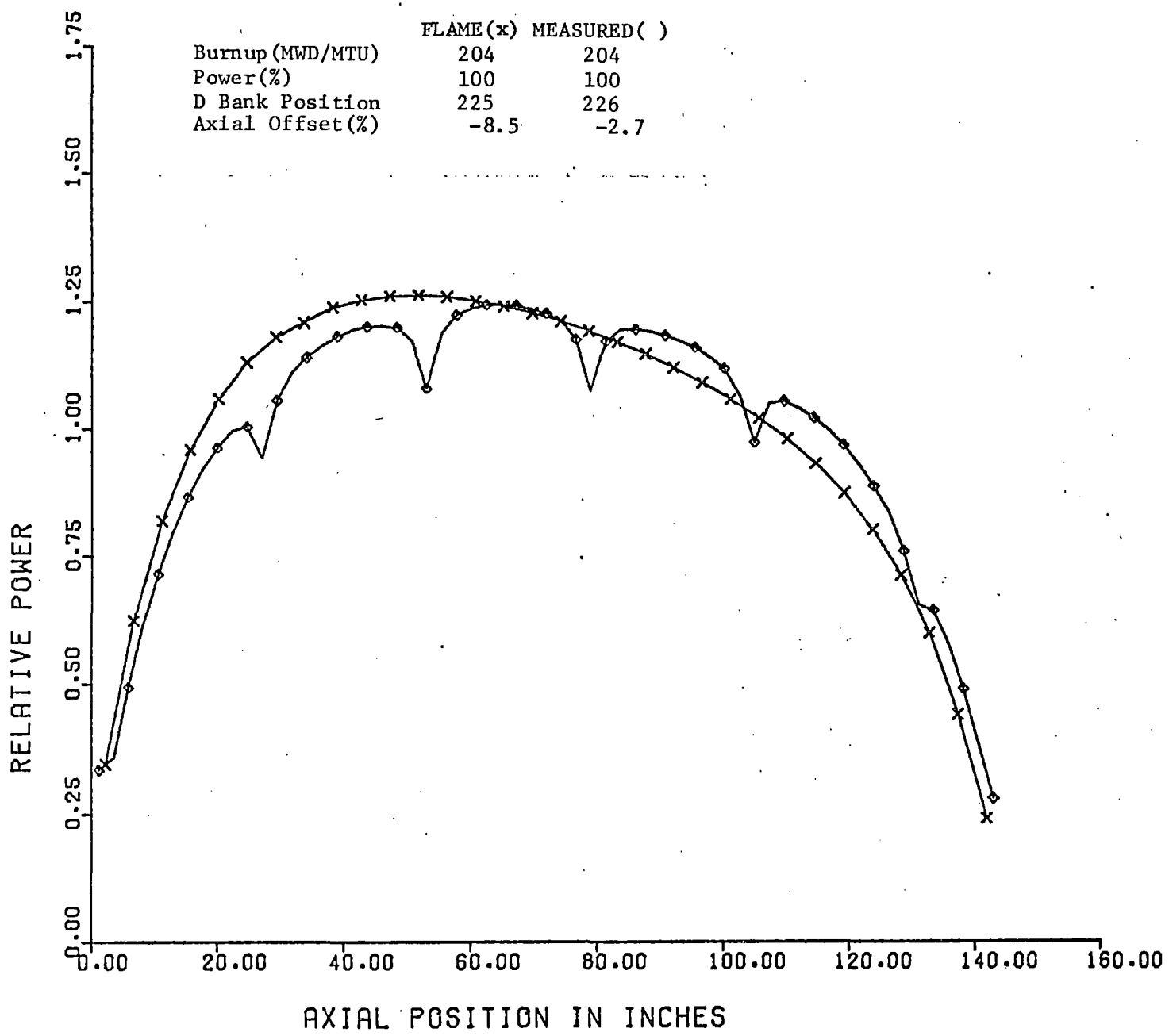

FIGURE 5-22

Core Average Axial Power Distribution Comparison
for Surry 2, Cycle 4, BOC,
HFP, ARO

FIGURE 5-23

Core Average Axial Power Distribution Comparison
for Surry 2, Cycle 4, MOC,
HFP, ARO

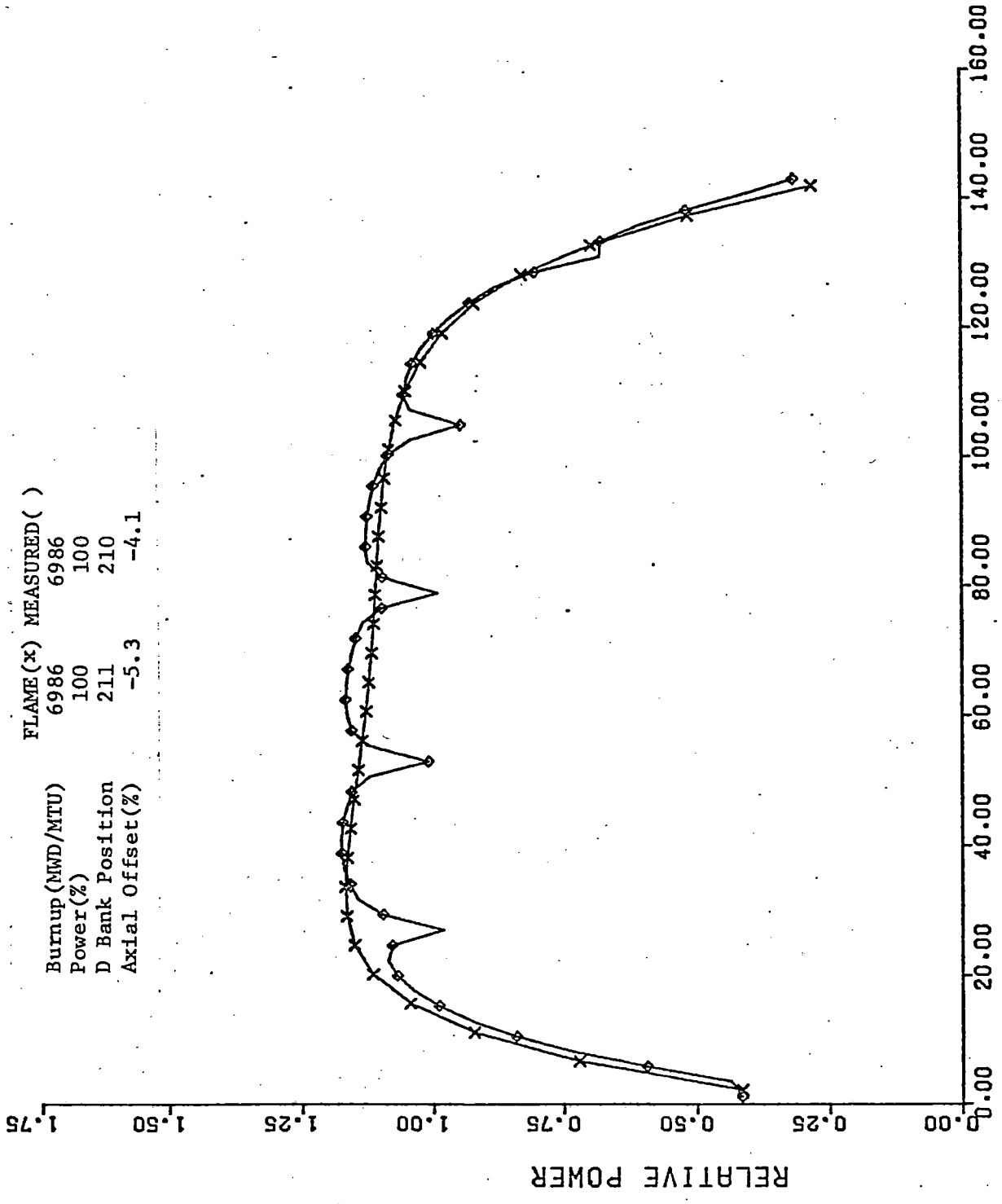

FIGURE 5-24

Control Rod Worth Comparison
for Surry 1, Cycle 1, BOC,
HZP, D Bank

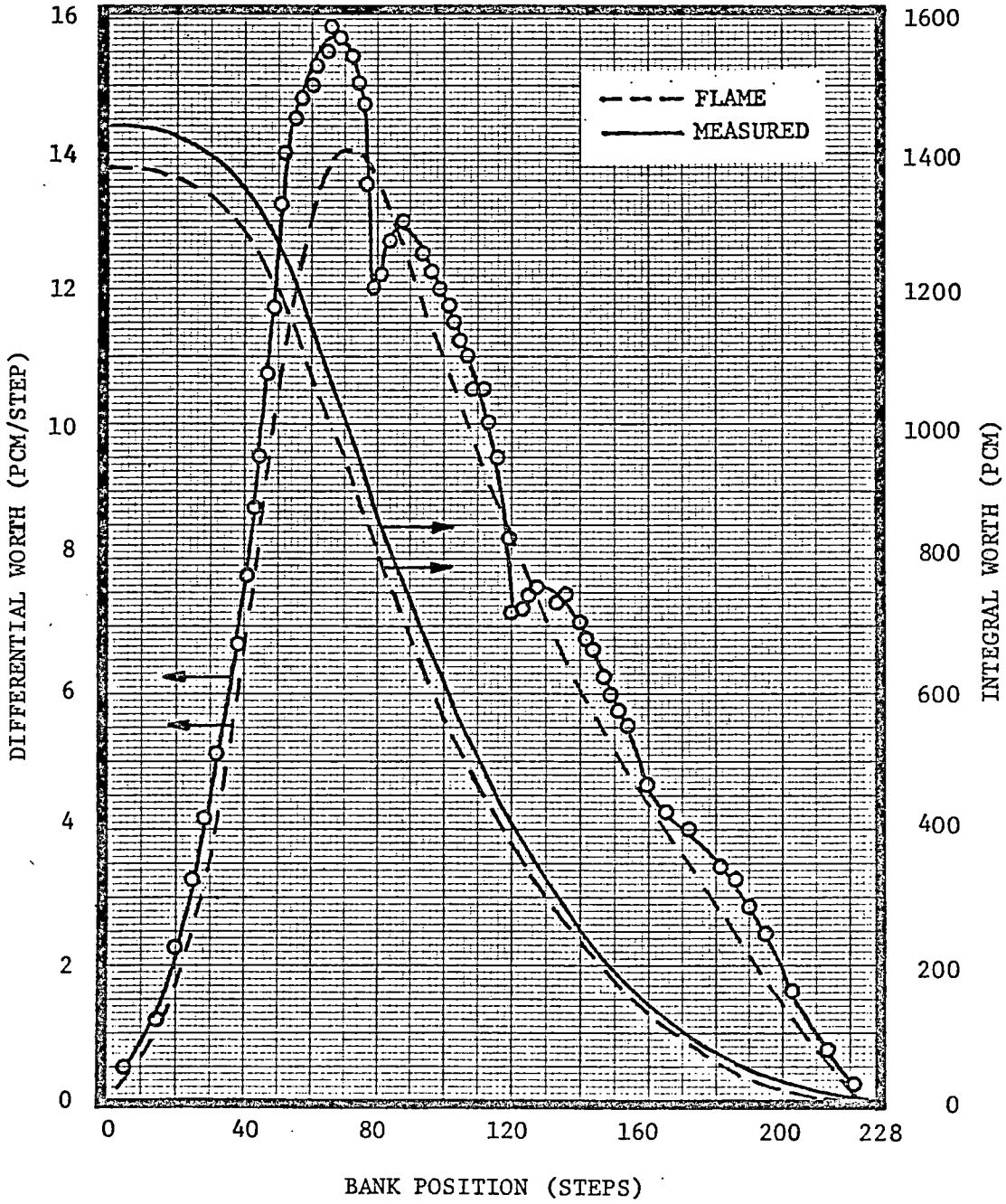

FIGURE 5-25

Control Rod Worth Comparison
for Surry 1, Cycle 1, BOC,
HZP, C Bank

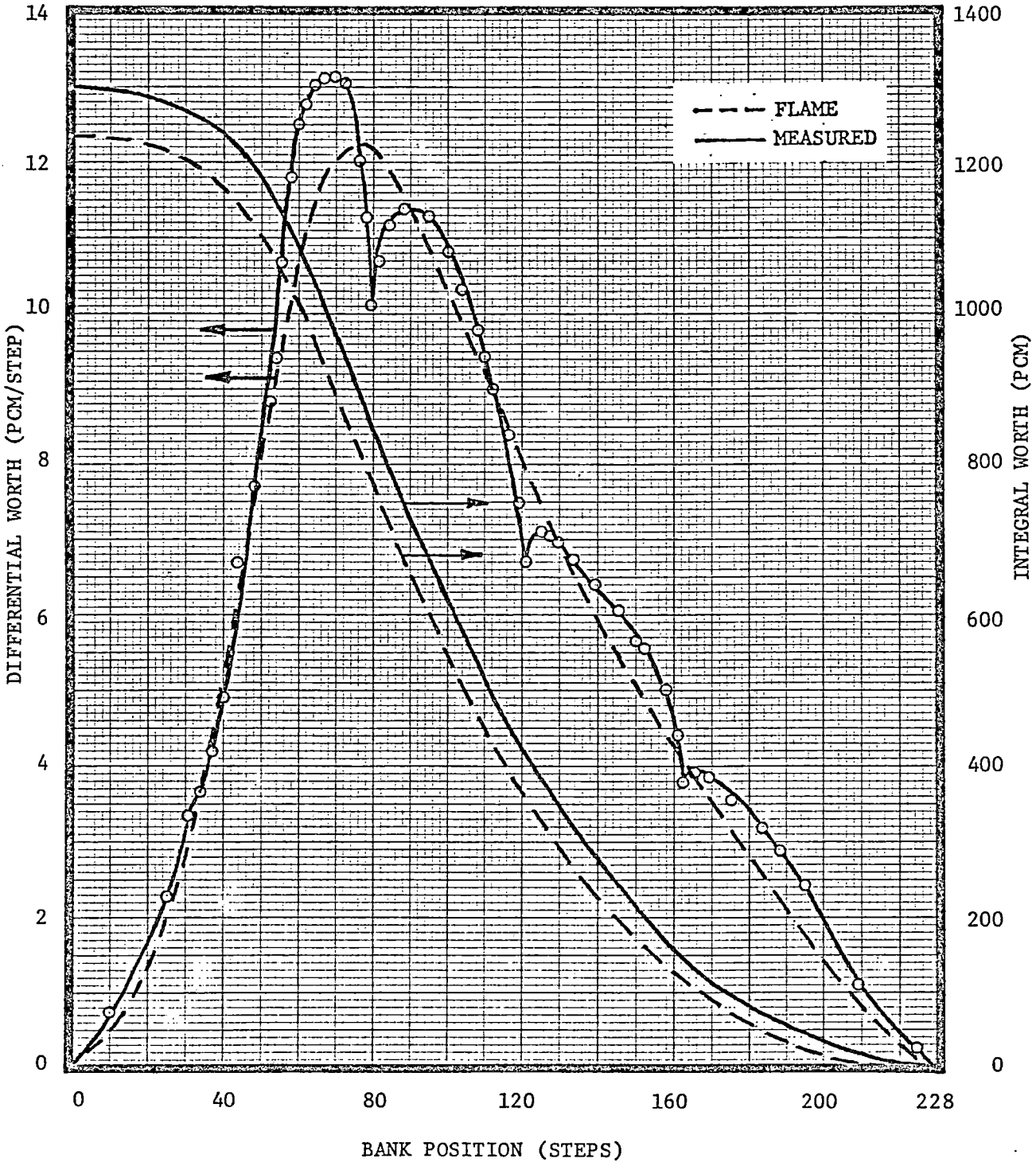

FIGURE 5-26

Control Rod Worth Comparison
for Surry 1, Cycle 1, BOC,
HZP, B Bank

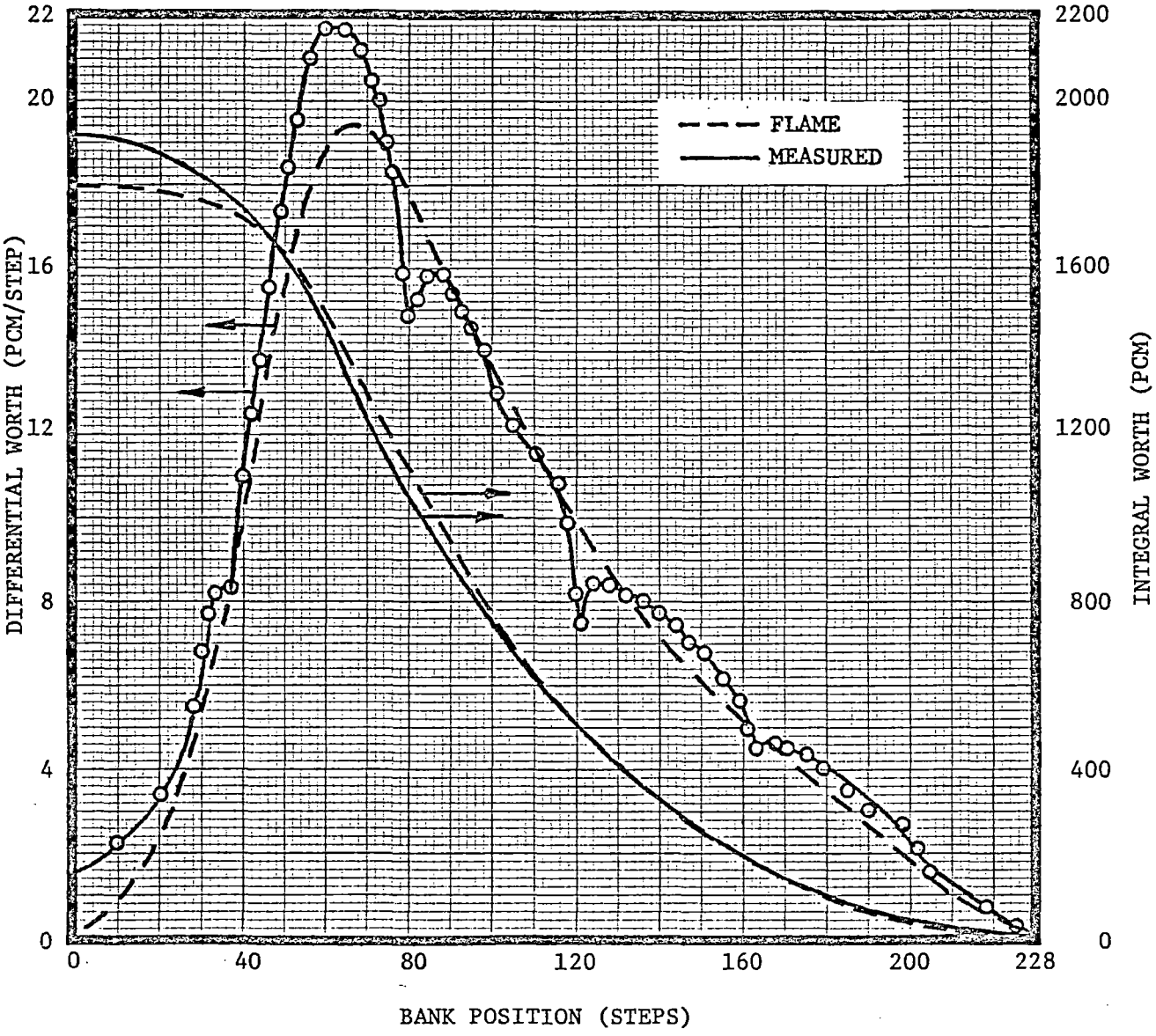

FIGURE 5-27

Control Rod Worth Comparison
for Surry 1, Cycle 1, BOC,
HZP, A Bank

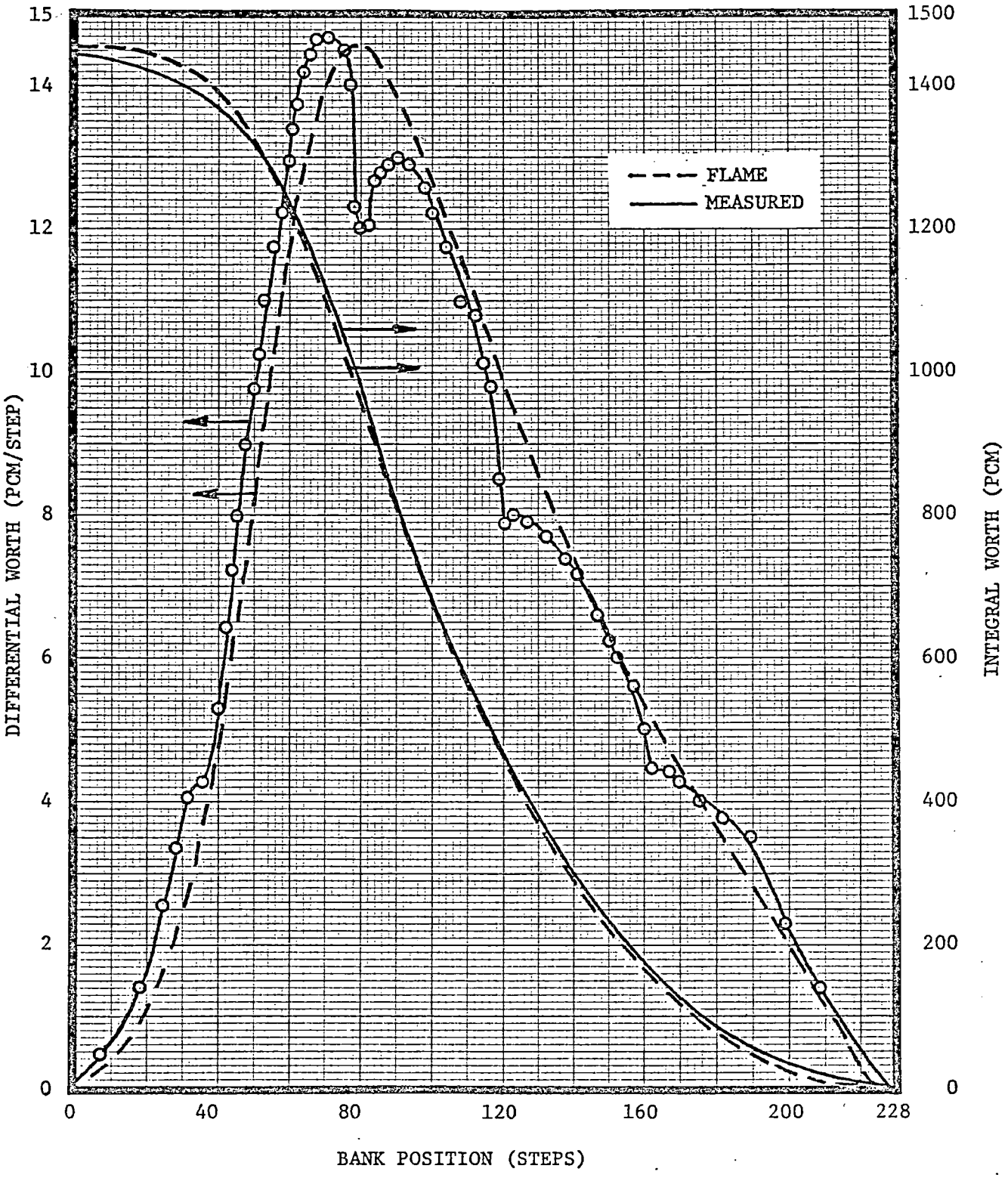

Figure 5-28
Control Rod Worth Comparison
for Surry 1, Cycle 1, BOC,
HZP, Banks B - D moving in
100 Step Overlap

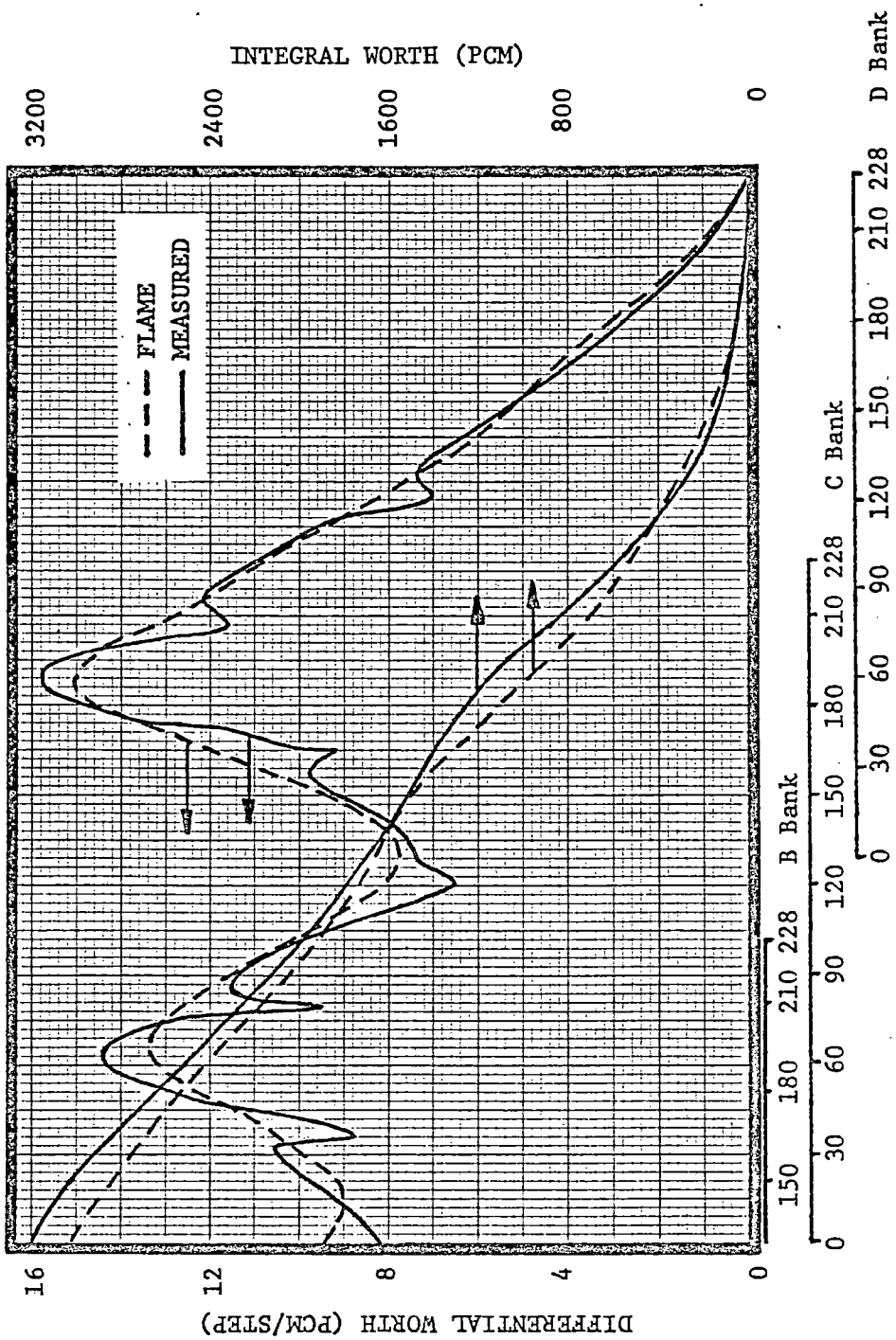

FIGURE 5-29

Control Rod Worth Comparison
for Surry 1, Cycle 2, BOC,
HZP, D Bank

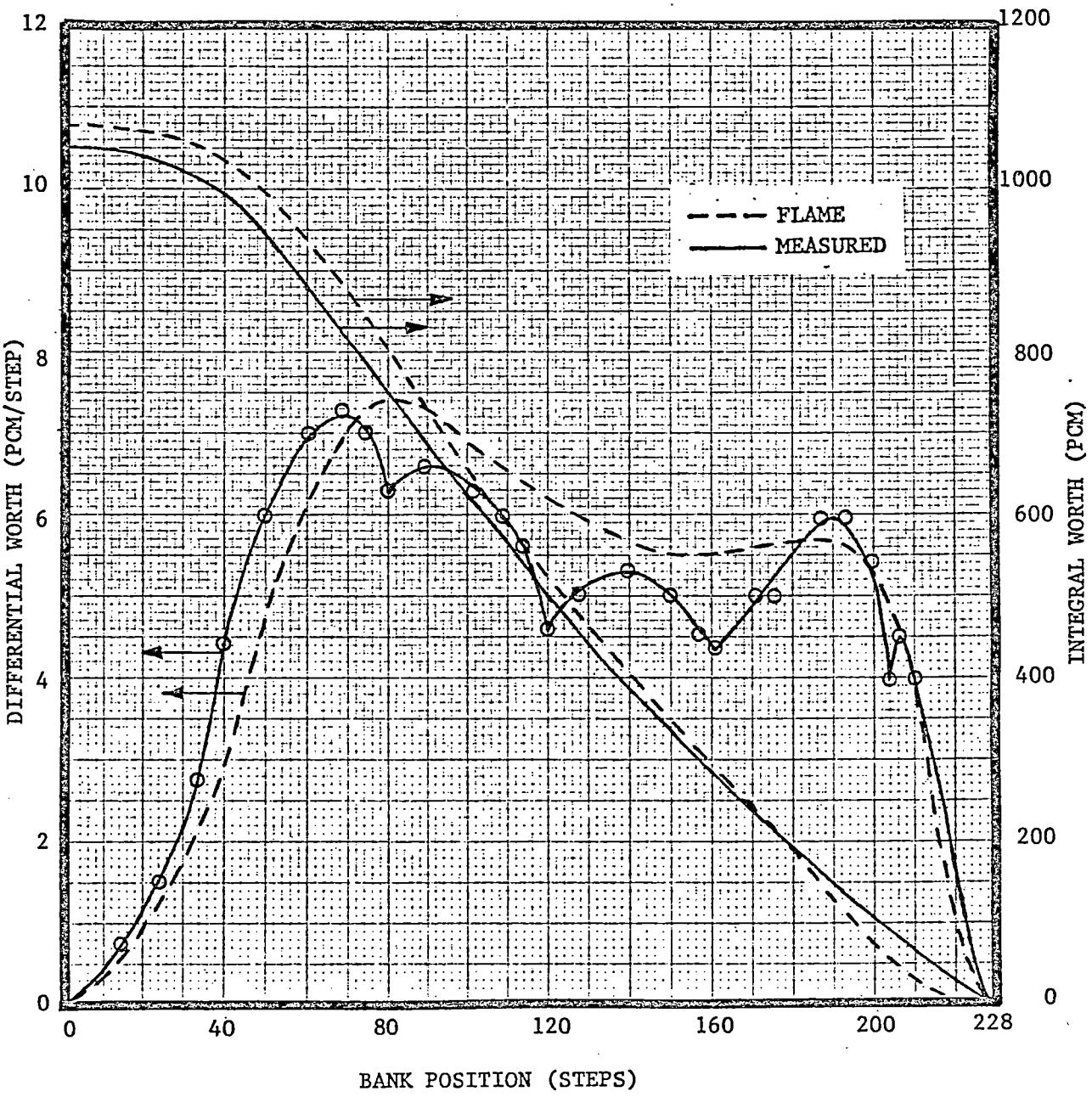

FIGURE 5-30

Control Rod Worth Comparison
for Surry 1, Cycle 2, BOC,
HZP, C Bank

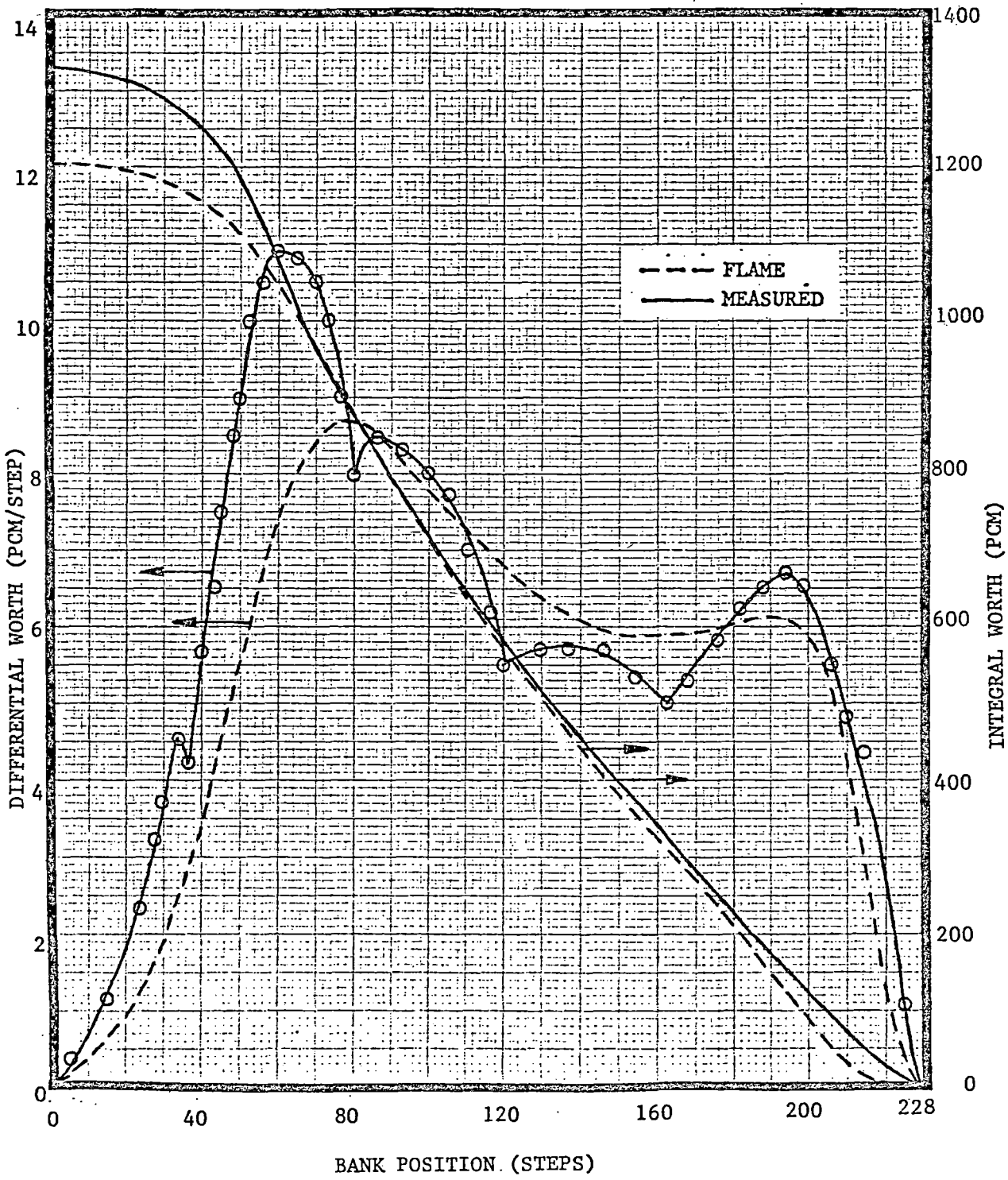

FIGURE 5-31

Control Rod Worth Comparison
for Surry 2, Cycle 3, BOC,
HZP, D Bank

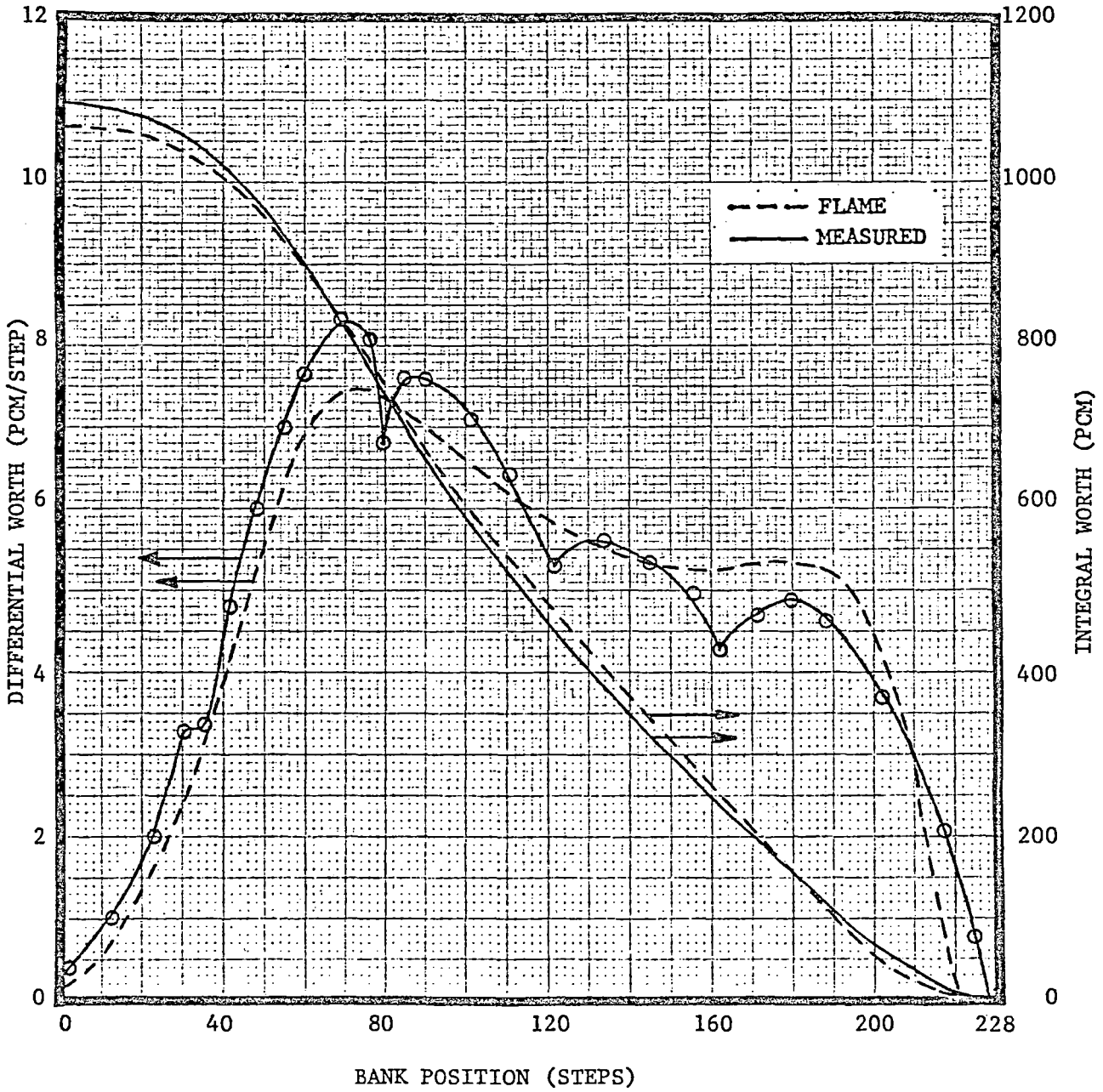

FIGURE 5-32

Control Rod Worth Comparison
for Surry 2, Cycle 3, BOC,
HZP, C Bank

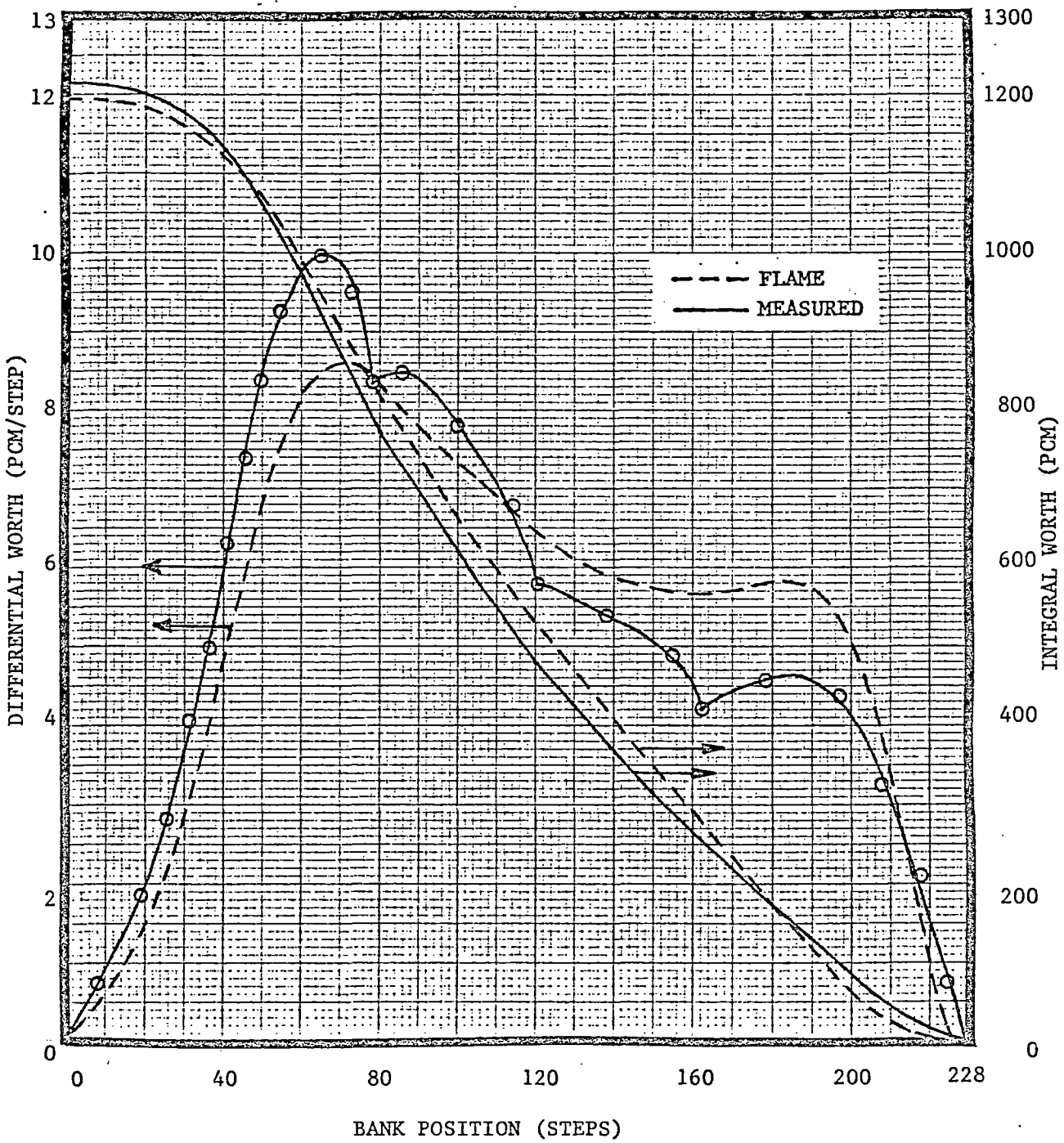

Figure 5-33
Control Rod Worth Comparison
for Surry 1, Cycle 4, BOC,
HZP, D Bank

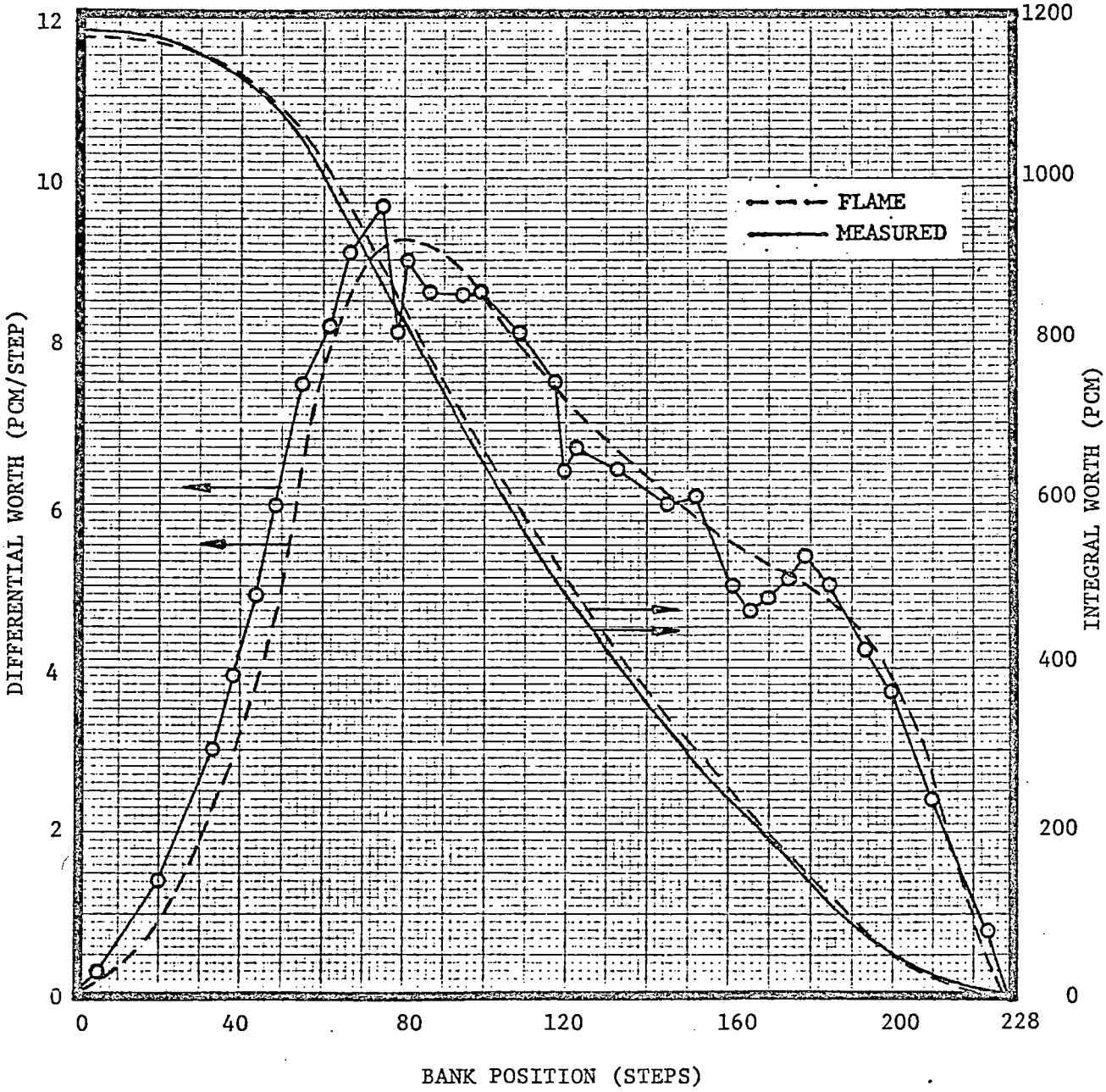

Figure 5-34
Control Rod Worth Comparison
for Surry 1, Cycle 4, BOC,
HZP, C Bank

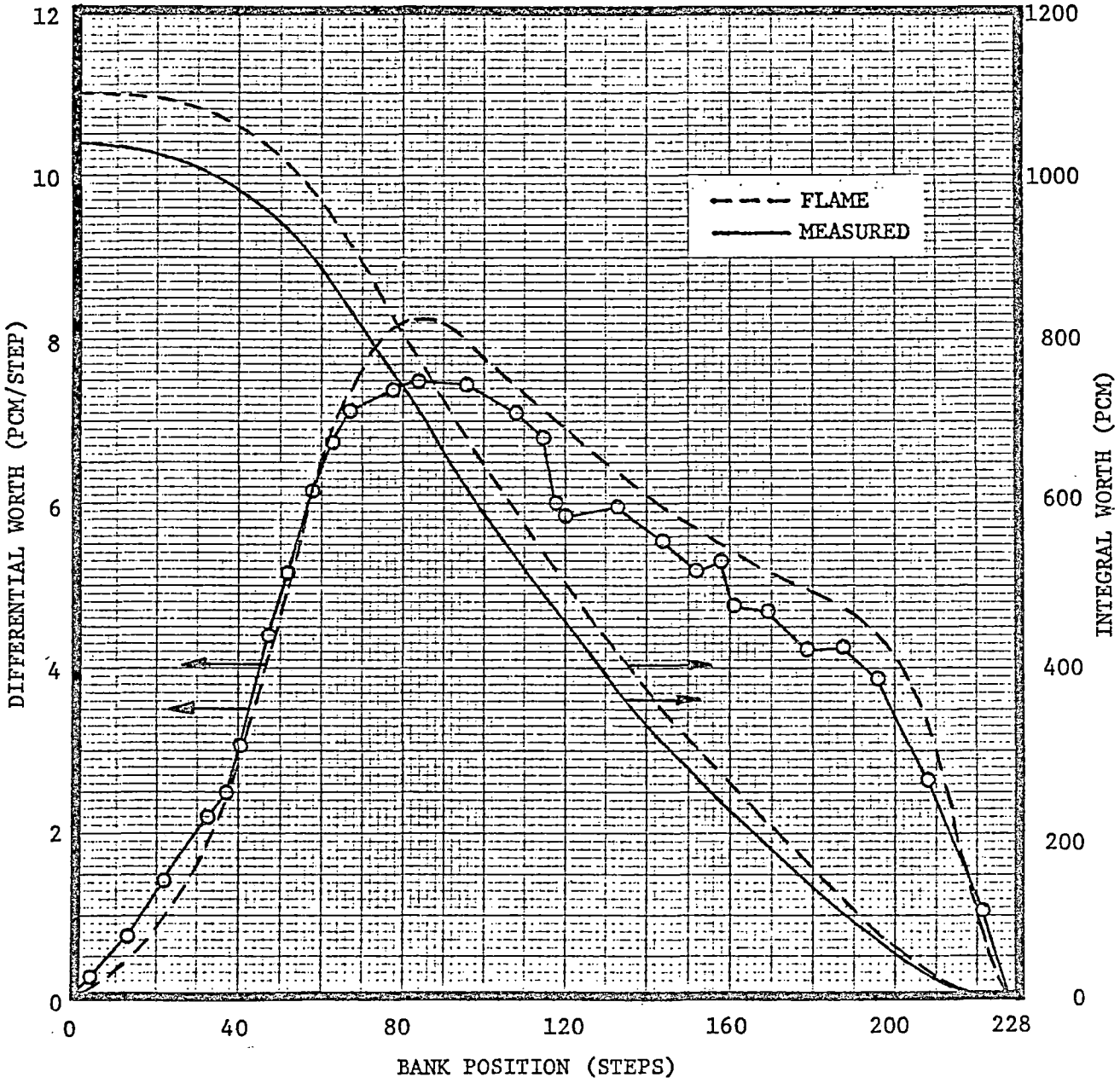

Figure 5-35
Control Rod Worth Comparison
for Surry 1, Cycle 4, BOC,
HZP, B Bank

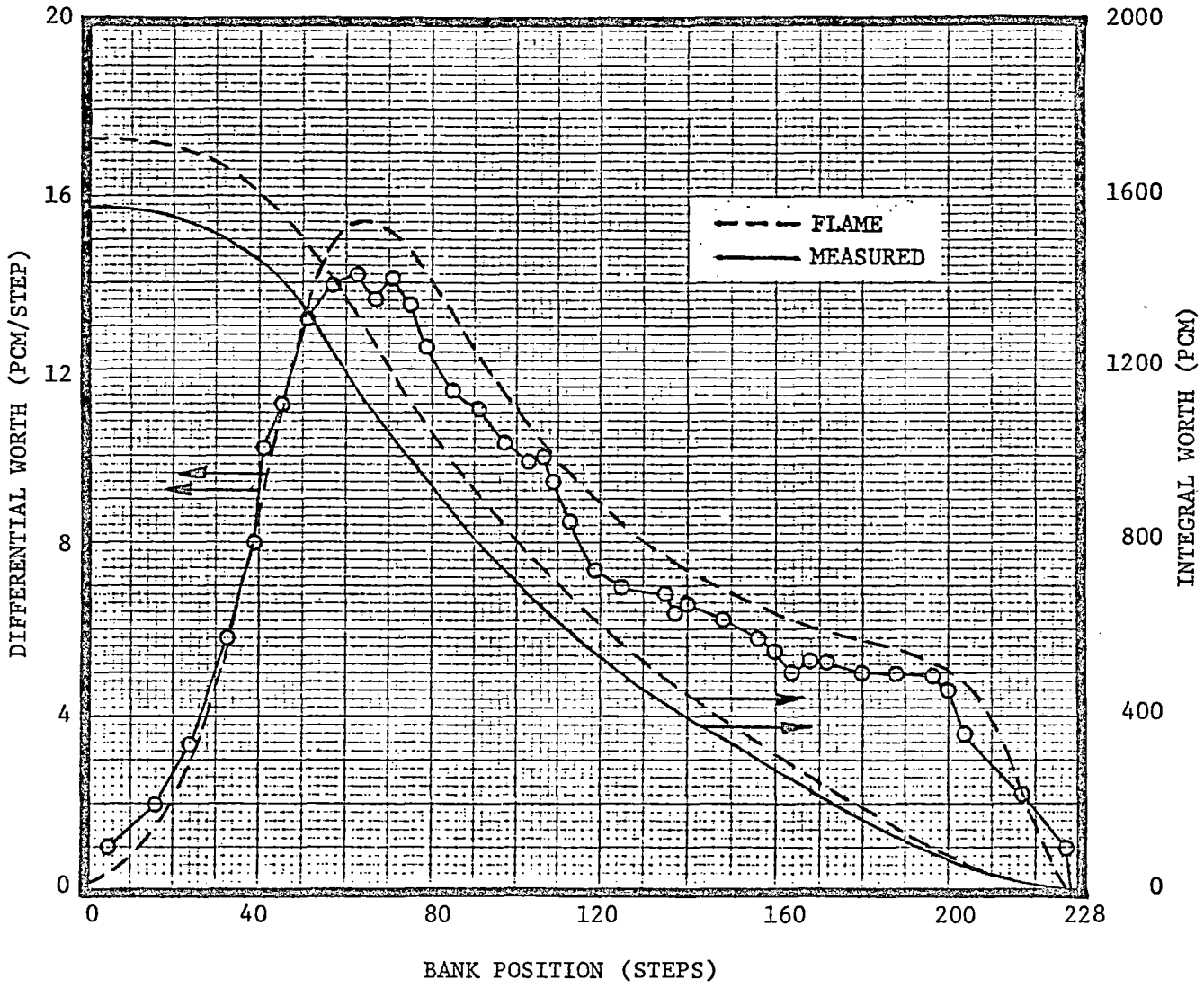

Figure 5-36
Control Rod Worth Comparison
for Surry 1, Cycle 4, BOC,
HZP, A Bank

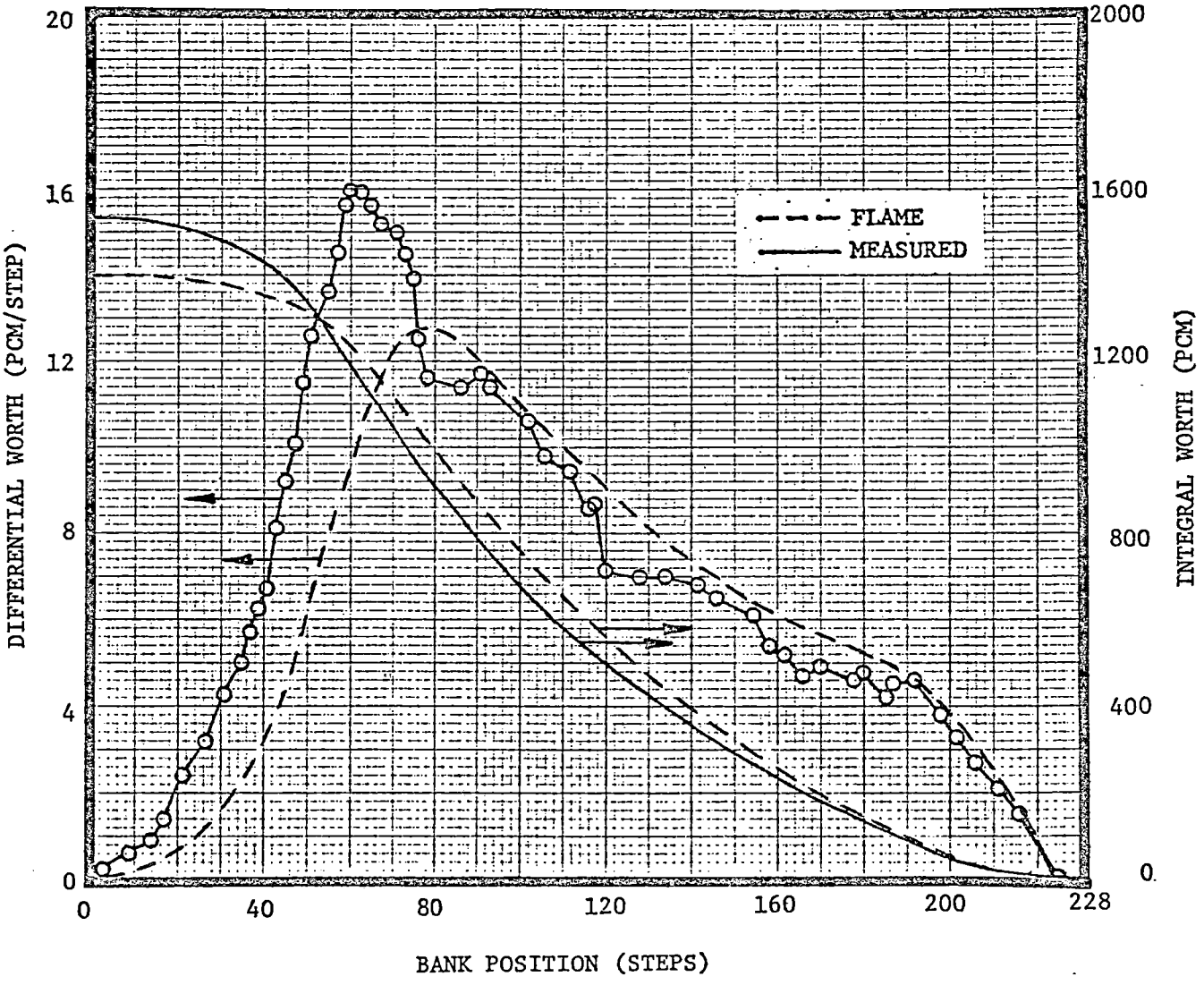

Figure 5-37
Control Rod Worth Comparison
for Surry 1, Cycle 4, BOC,
HZP, Banks A - D moving in
100 Step Overlap

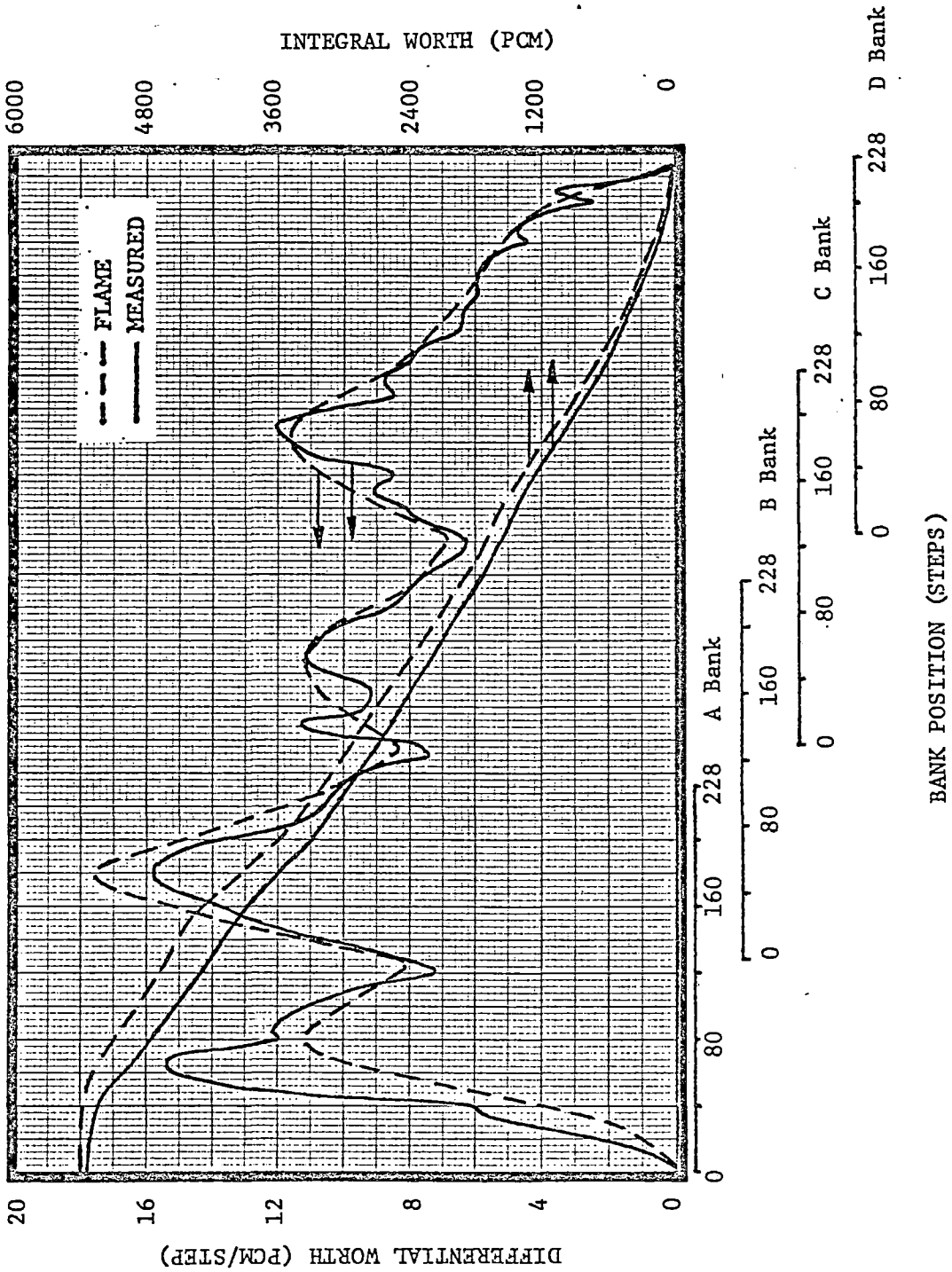

Figure 5-38
Control Rod Worth Comparison
for Surry 2, Cycle 4, BOC,
HZP, D Bank

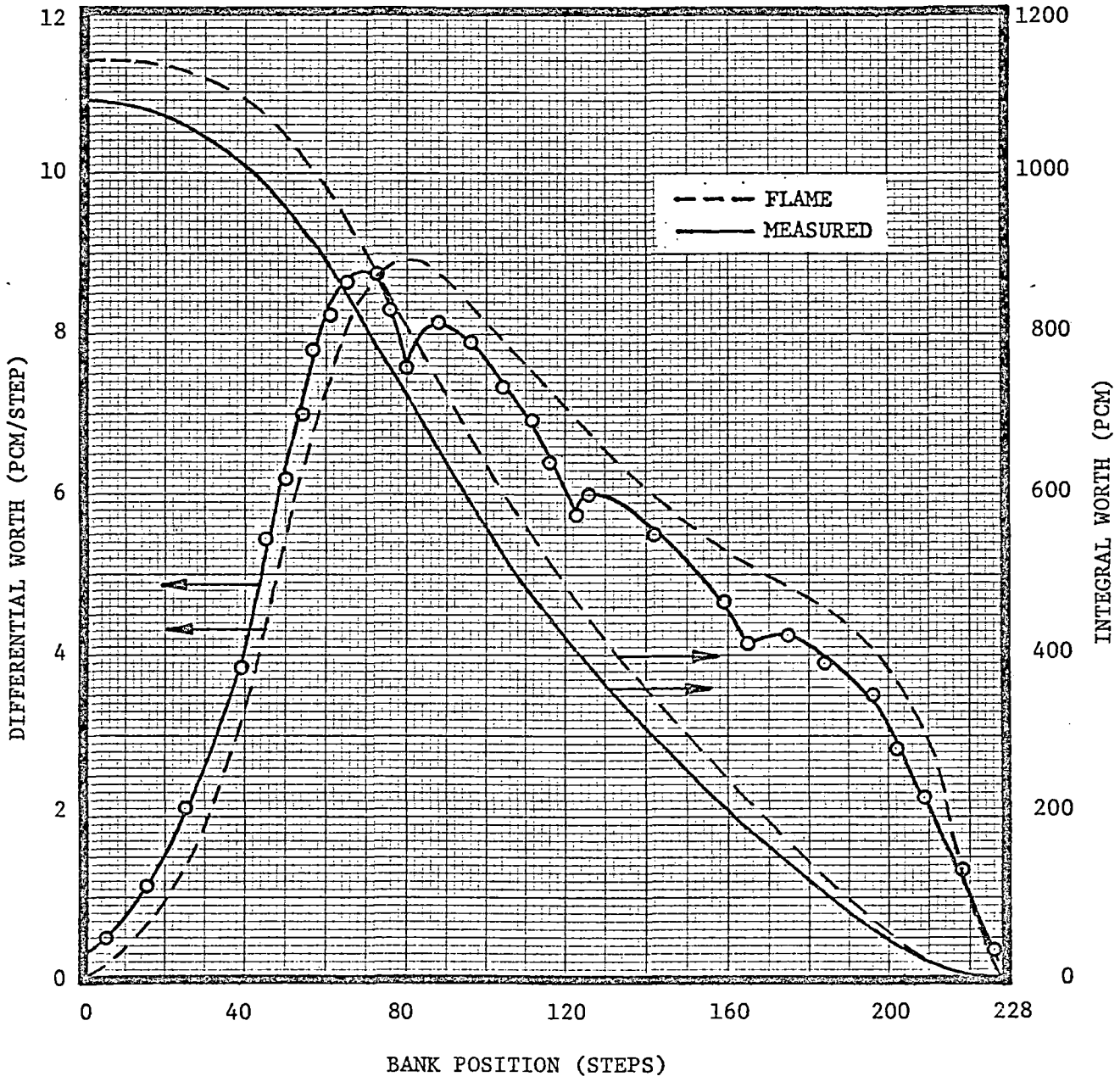

Figure 5-39
Control Rod Worth Comparison
for Surry 2, Cycle 4, BOC,
HZP, C Bank

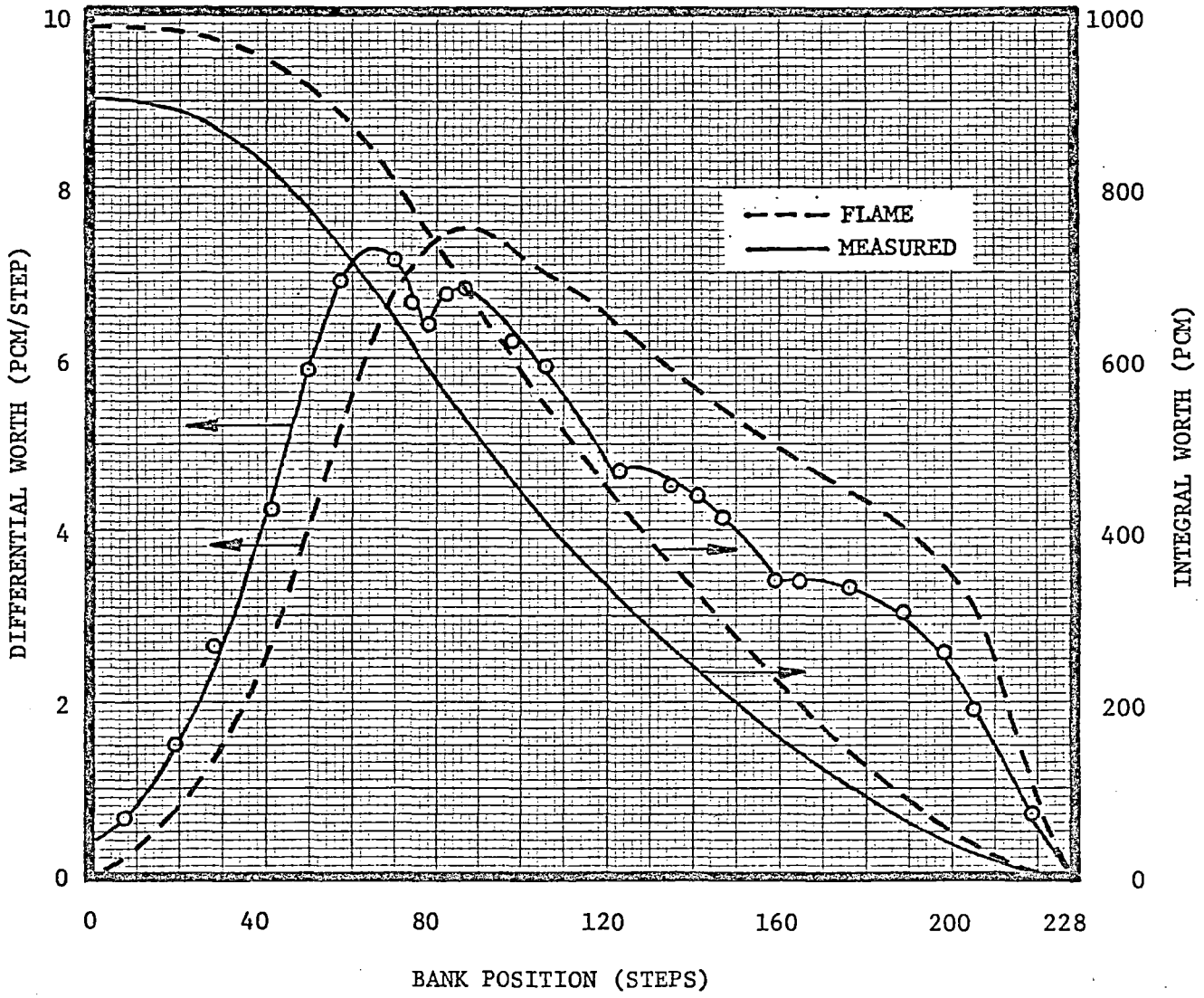

Figure 5-40
Control Rod Worth Comparison
for Surry 2, Cycle 4, BOC,
HZP, B Bank

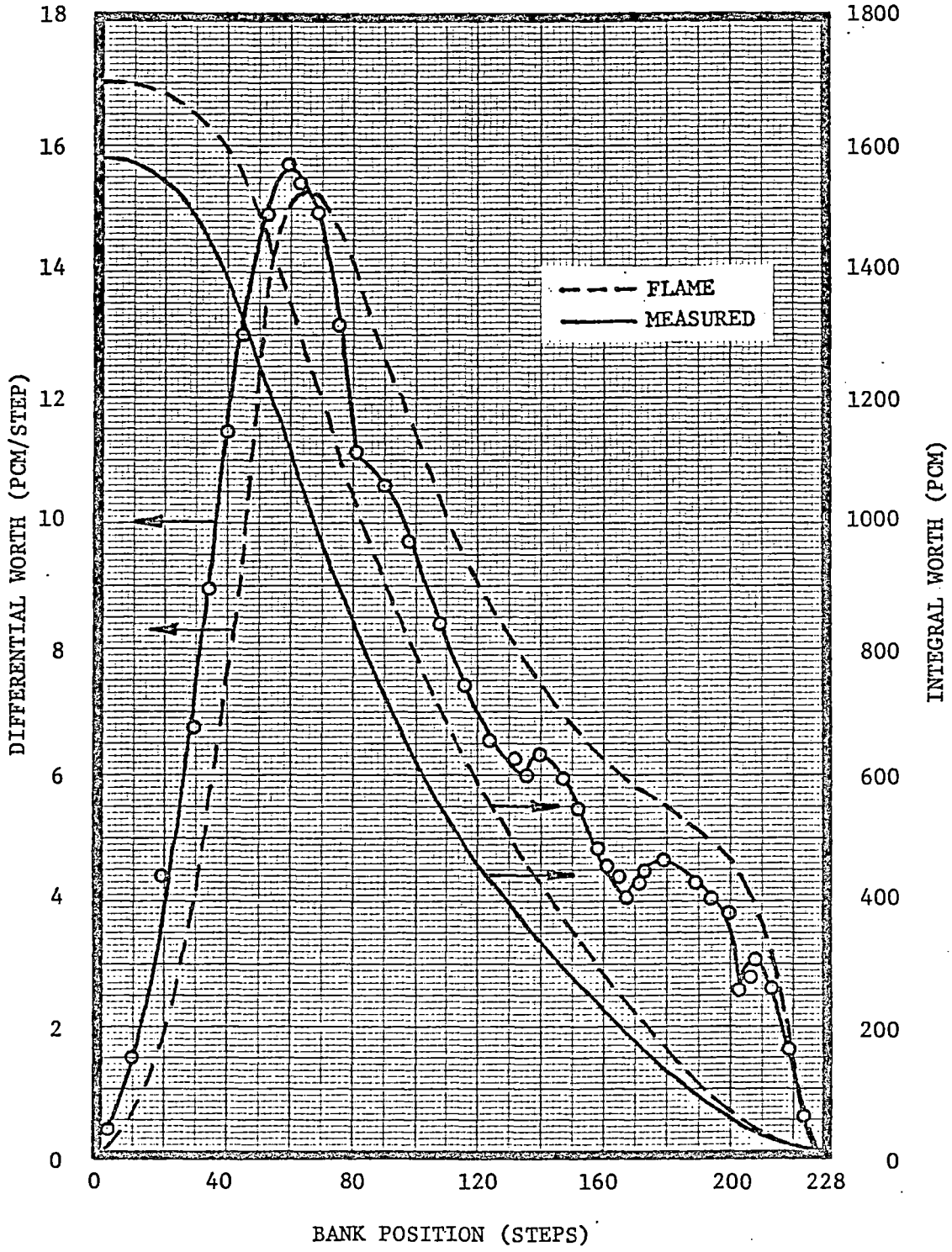

Figure 5-41
Control Rod Worth Comparison
for Surry 2, Cycle 4, BOC,
HZP, A Bank

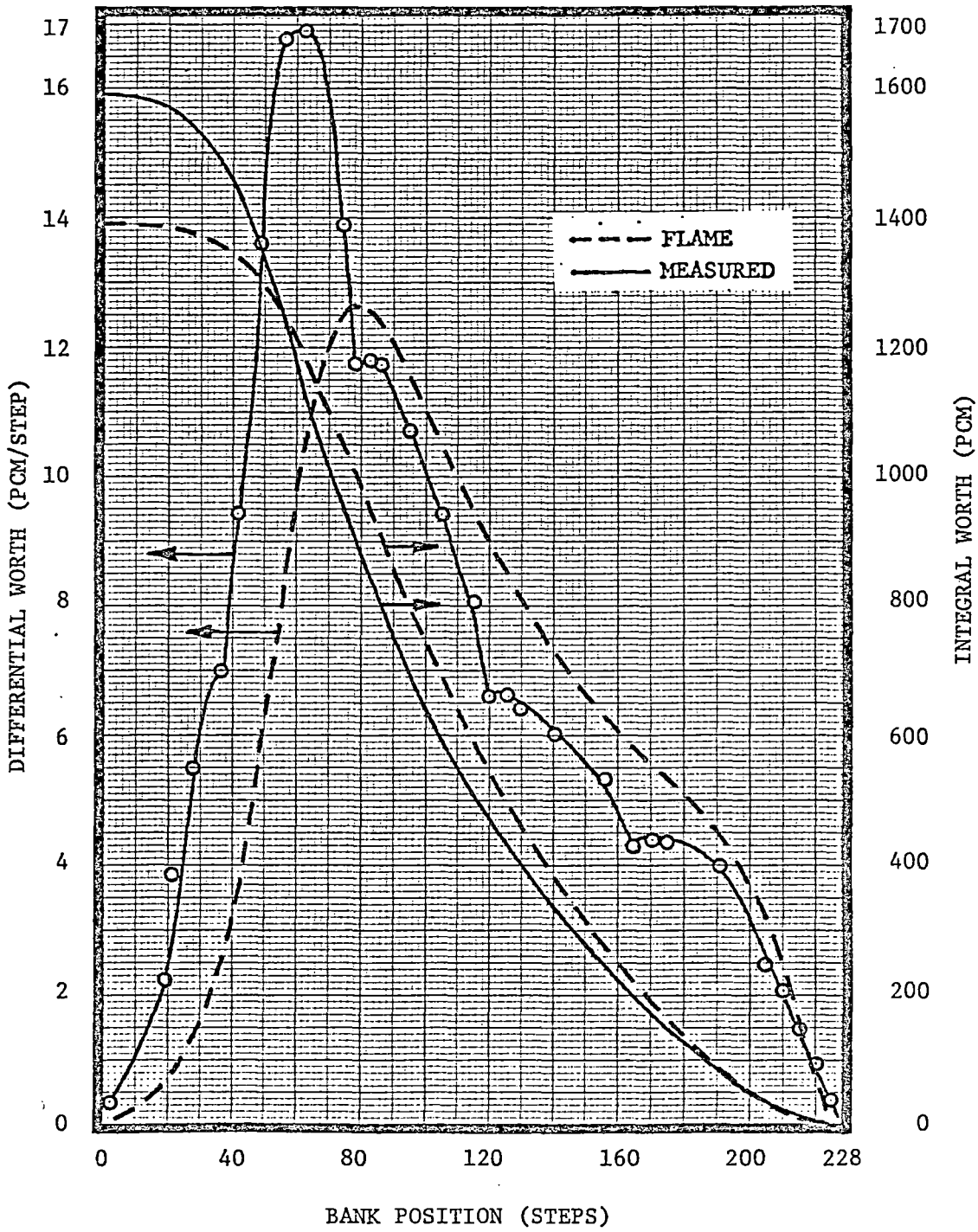

Figure 5-42

Control Rod Worth Comparison for Surry 2, Cycle 4, BOC, HZP, Banks A - D moving in 100 Step Overlap

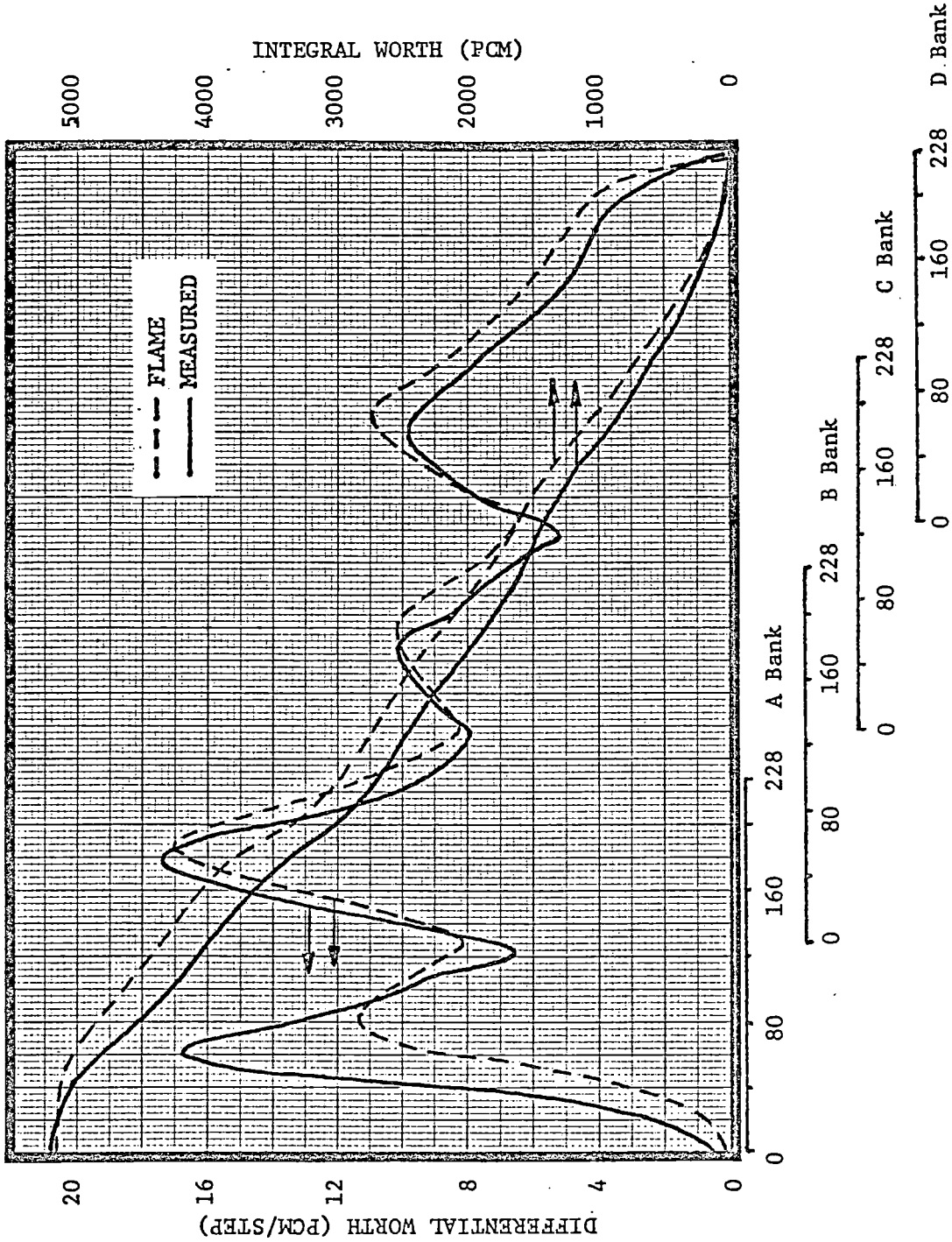

Section 6 - Summary and Conclusions

The Vepco FLAME Model is operational at Vepco for the purpose of performing three-dimensional reactor physics analyses and supporting the evaluation of core performance. The model consists of the FLAME3 code with the NULIF, PDQ07, FLAFIT, EDITQAR, PICCOLO, and FLMSHUFL codes being used to provide either input or data manipulation. The accuracy of the Vepco FLAME Model has been established through extensive comparision of calculations with measurements from the Surry Units No. 1 and 2 over eight cycles of operation. The results of these comparisions indicate that the Vepco FLAME Model (which includes normalization to the Vepco PDQ07 Discrete Model) provides the capability to predict axial peaking factors and axial power distributions as well as differential and integral control rod worths. The comparisions also indicate an acceptable capability to predict axial offset trends as a function of changing reactor core conditions.

Verification, as well as improvements to the Vepco FLAME Model, will continue to be made as more experience is obtained through the application of the model to the units at the Surry and North Anna Nuclear Power Stations.

SECTION 7 - REFERENCES

1. W. A. Wittkopf, et. al., "NULIF - Neutron Spectrum Generator, Few Group Constant Calculator, and Fuel Depletion Code," BAW-10115, June 1976 (Babcock and Wilcox).

2. H. H. Hassan, et. al., "Babcock and Wilcox Version of PDQ07 - User's Manual," BAW-10117P, December 1975 (Babcock and Wilcox).

3. C. W. Mays and M. Furtney, "FLAME3 - A Three-Dimensional Nodal Code for Calculating Core Reactivity and Power Distributions," BAW-10124A, August 1976 (Babcock and Wilcox).

4. Private correspondence from the Babcock and Wilcox Company to the Virginia Electric and Power Company dated February 3, 1971, and October 6, 1971.

5. C. B. Franklin, "EDITQAR and PICCOLO - Auxiliary Fortran Computer Codes for Use with FLAME3," NFE Technical Report No. 27, April 1977 (Virginia Electric and Power Co.).

6. W. C. Beck, "FLMSHUFL - An Auxiliary Fortran Computer Code for Use with FLAME3," NFE Technical Report No. 55, October 1977 (Virginia Electric and Power Co.).

7. M. L. Smith, "The PDQ07 Discrete Model," VEP-FRD-19, July 1976 (Virginia Electric and Power Co.).

8. Final Safety Analysis Report - Surry Power Station Units 1 and 2, Virginia Electric and Power Company, December 1969.

9. D. L. Delp, et. al., "FLARE - A Three-Dimensional Boiling Water Reactor Simulator," GEAP-4598, July 1964 (General Electric).

10. C. B. Franklin, "Sensitivity Study of K-Infinity Multipliers for Depleted BP for the FLAME Model," NFE Calculational Note PM-4, July 1978 (Virginia Electric and Power Co.).

11. W. C. Beck, "Sensitivity of Control Rod Worth Shapes to Variation in Radial Power Distribution," NFE Calculational Note PM-3, July 1978 (Virginia Electric and Power Co.).